UNIVERSITÀ DEGLI STUDI DI MILANO

Scuola di Dottorato in Scienze Biologiche e Molecolari

XXVII Ciclo

Focal Adhesion Kinase involvement in modulating the proliferation of tumor cells.

SDD: MED16, BIO/11

Katia Rea

PhD Thesis

Scientific tutor: Dr. Antonella Tomassetti

Thesis performed at Fondazione IRCCS Istituto Nazionale per lo Studio e la Cura dei Tumori di Milano, Dipartimento di Oncologia Sperimentale e Medicina Molecolare, Unita' di Terapie Molecolari

Academic year: 2013-2014

CONTENTS

Focal Adhesion Kinase involvement in modulating the proliferation of tumor cells.

PART I

Summary

The focal adhesion kinase (FAK) is well characterized non-receptor tyrosine kinase, although it undergoes also to phosphorylation on serine residues whose role is not fully understood. FAK is ubiquitously expressed and plays a crucial role as integrator of signaling from either integrins or Receptor Tyrosine Kinases (RTKs) and has been linked to cell transformation and progression in many solid tumors. Among those, the Epithelial Ovarian Cancer (EOC) has a different behaviour during progression: it rarely metastasizes to distant sites but disseminate within the peritoneal cavity.

Our attention was focused on the characterization of the role of FAK in different type of tumor cells and in particular on the phosphorylation (P) on the serine 732 of FAK (P-FAKSer732). We found that P-FAKSer732 was present at variable levels in cancer cell lines but its activation was independent from integrin engagement and from the kinase activity of FAK. P-FAKSer732 was not localized at the focal adhesion site during migration but it was accumulated in dividing cells, co-localizing with the tubulin of the spindle during mitosis and regulating microtubule (MT) polymerization and mitotic spindle formation. CDK5 was identified as the specific kinase responsible for FAK serine phosphorylation whose activation was induced by EGF stimulation of the EGFR/ERK signalling. Thus, we have identified for the first time the axis EGFR/MEK/ERK/CDK5/P-FAKSer732 as a novel pathway leading to mitosis of tumor cells.

We next aimed to identify the mechanism governing the crosstalk between adhesion molecules and RTKs thus leading to proliferation, migration and invasion of tumor cells. I focused my analysis on EOC which is the main cancer histotype studied in our laboratory. We therefore investigated in EOC cells a possible role of E-cadherin (cadh) to contribute to the novel signalling pathway

described above. Indeed, we found that E-cadh was the adhesion molecule necessary for the formation of the EOC multi-cellular aggregates (MCAs) present in the ascites. The E-cadh and CDK5 resulted to be necessary to the generation of FAKSer732 and this protein complex was necessary for the EGF-mediated EGFR activation likely due to the stabilization of EGFR protein on the cell membrane. In line with these results, E-cadh expressing EOC cells were more susceptible to the CDK5 inhibitor, roscovitine. These data demonstrated a pivotal role of E-cadh in contributing to the proliferation of EOC MCAs.

To clarify the processes responsible for the switch from a proliferative to a more invasive phenotype of EOC MCAs necessary for tumor dissemination, we were studied another RTK, Axl whose expression has been already reported to be associated to a more invasive phenotype. We found that the stimulation of Axl by its ligand Gas6 required the engagement of β3-integrin with components of the extra-cellular matrix (ECM). The crosstalk between Gas6/Axl and the integrin signallings was independent by FAK but required the contribution of p130Cas, a scaffold protein involved in the transmission of the ECM-integrin signalling, for adhesion, migration and invasion of EOC cells. Indeed, the lack of p130Cas decreased the level of Gas6-dependent Axl activation and inhibited Gas6-induced EOC cells adhesion, migration and invasion. In 56 out of 72 EOC biopsies, Axl and p130Cas were significantly co-expressed indicating of a collaborative signaling between Axl and p130Cas also *in vivo*. We have identified an Axl signalling which requires a p130Cas-mediated crosstalk with integrins for the dissemination of EOCs. Altogether, our investigation allowed the definition of two novel adhesion-dependent signalling pathways which drive the proliferation and the invasion of EOC cells, respectively. The inhibition of these pathways will likely affect EOC MCA growth as well as the invasion of EOC solid primary and secondary lesions.

Introduction

1. The Focal Adhesion Kinase

Focal adhesions (FAs) are sites where cells contact the extracellular matrix (ECM). The interaction between cells and ECM is possible through specific transmembrane proteins, the integrins, and various cytoskeletal scaffold and signaling protein that connect the ECM to the actin cytoskeleton. FAs are highly dynamic structures that grow or shrink due to the turnover of their component proteins (2). The main protein involved in the control of the FAs turnover is the Focal Adhesion Kinase (FAK).

Since its discovery, FAK has been emerging as an important player in both normal development and cancer.

1.1 FAK structure

FAK is a non-receptor tyrosine kinase discovered in the 90' by two converging line of research: as a 120 kDa protein localized at the FAs and tyrosine-phosphorylated upon integrins clustering and src activation (3, 4). FAK is expressed in most tissues and its sequence is highly conserved across species. It is composed by a N-terminal FERM (erythrocyte band four.1-ezrin-radixin-moesin) domain; a 40 amino acid linker domain; a central tyrosine kinase domain; a C-terminal domain which is responsible for the FAK targeting at the FA (FAT domain); and a prolin rich region localized between the kinase and the C-terminal domain (Fig.1). The FERM domain, the FAT domain and the proline rich region are docking site for other molecules that belong to the FAK signaling. The FERM domain docks also with catalytic domain to auto-inhibit the kinase activity (5).

FAK activation occurs upon integrin engagement with the ECM through an ordered sequence of events, starting from the auto-phosphorylation of FAK on

tyrosine 397 (Tyr397), achieved by the interaction between the FERM domain with activators such integrin β cytoplasmic domain or growth factor receptors (RTKs). The full catalytic activation is achieved by binding of src to the phosphorylated FAKTyr397 leading to the subsequent phosphorylation of FAK on Tyr576 and Tyr577. Those phosphorylation events are followed by the recruitment of FAK-binding proteins. In the N-terminal linker region, phosphorylation of Tyr397 appears to be important for the recruitment of other SH2-containing proteins, including the 85 kDa subunit of phosphoinositide 3-kinase (PI3K), phospholipase C (PLC)-γ and the Grb2-SOS complex (6-8). The C-terminal domain harbors multiple protein-protein interactions sites. In addition to the paxillin-binding site in the FAT domains, the proline-rich region is recognized by the SH3 domain of p130Cas, a multi-functional adaptor protein (9). FAK-induced phosphorylation of p130Cas leads to membrane ruffling, lamellipodium formation and actin reorganization. The C-terminal region of FAK contains also several serine residues but their role is poorly understood.

1.2 Serine phosphorylation of FAK

Beside the Tyr phosphorylation, FAK is also phosphorylated on serine (Ser) residues but just little is known about their function and the role of the Ser phosphorylation of FAK has never been studied in cancer. Five major serine phosphorylation sites are located in the C-terminal domain of FAK corresponding to serine residues 722, 732, 840, 843 and 910 (10, 11). The Ser phosphorylation of FAK seems to play an important role during mitosis. The cell rounding up at the early stages of mitosis is achieved by the tyrosine de-phosphorylation of FAK which inhibit FAK/src interaction, and Ser phosphorylation of FAK which inhibit FAK/p130Cas interaction. The phosphorylation of FAK on Ser residues inhibits also its interaction with β-

integrin (12). The phosphorylation on Ser722, which is induced by GSK3-β was identified as the responsible for the inhibition of the kinase activity of FAK (13), and for the distruption of the interaction with the scaffold protein p130Cas (10). The Ser-phosphorylated FAK allows the detachment of cells from the substrate and the rounding up necessary for mitosis. At the end of mitosis, the cell spreading is achieved by the dephosphorylation of FAK on Ser722 by PP1 (13).

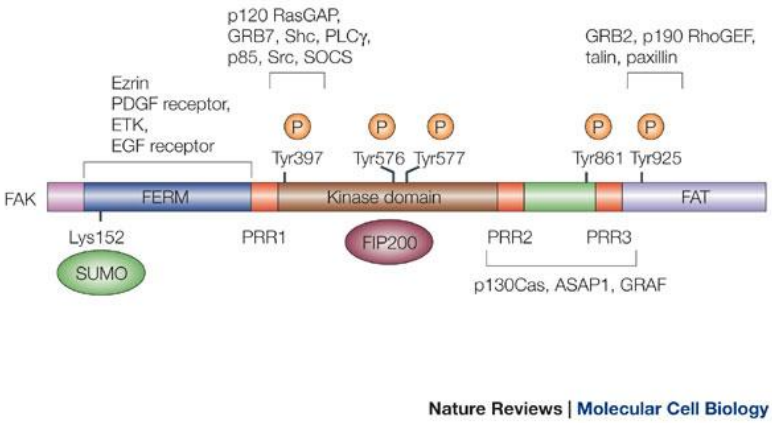

Fig.1 FAK structure (5).

RTKs ligands, such as PDGF, FGF and EGF, induce the phosphorylation of FAK on Ser910 by ERK (14). The phosporylation of FAK on Ser910 is coupled with a reduced binding to paxillin and with the release of FAK from the FAs.

In migrating neurons, phosphorylation of FAKSer732 (P-FAKSer732) by CDK5 regulates MT stability thus pulling the proximal region of the nucleus into the leading process, likely in the direction of the centrosome (11, 15). In endothelial cells (EC), VEGF-induced activation of the Rho-dependent kinase (ROCK) leads to phosphorylation of FAKSer732 that is crucial for the phosphorylation of FAKTyr407 promoting cell migration (16). A new function for FAK has been shown in the regulation of centrosome functions in a Ser732

phosphorylation-dependent manner during mitosis. Deletion of FAK in primary ECs causes increases in centrosome numbers, multipolar and disorganized spindles In this case the kinase responsible for P-FAKSer732 was CDK5 (17). In pancreatic β-cells, the CDK5/P-FAKSer732 signaling is associated with cell survival via the activation of the PI3K/Akt pathway (18).

1.3 FAK function in normal cells

FAK expression is required in several tissues for normal development and solves a pivotal role during embryogenesis: FAK gene knockout in mice resulted in an embryonic lethal phenotype. FAK sequence is conserved among the species and is expressed in many cells where it is involved in proliferation, survival and migration.

1.3.1 FAK regulation of cell proliferation and survival

FAK regulates cell proliferation. In NIH3T3 fibroblasts over-expression of wild-type FAK promotes cell proliferation inducing the exit from the G1 phase. FAK promotion of cell cycle progression in NIH3T3 cells requires integrin engagement and ERK activity (19). It has been shown that FAK induces the expression of the KLF8 transcription factor and promotes cyclin D1 transcription through the binding of KLF8 to the GT box in the cyclin D1 promoter. FAK favors cell survival through the degradation of p53. This function is solved by the nuclear enriched FAK. The N-terminal region of FAK, the FERM domain, can be modified by the addiction of the small ubiquitin-related modifier (SUMO) at lysine-152 (20). This SUMOylated FAK is localized at the nucleus where it binds to Mdm2 and p53 enhancing the Mdm2-dependent p53 ubiquitination (21). The nuclear FAK is also able to control the expression of specific genes, for example the genes that encode mesenchymal markers in the TGF-β-induced Epithelial to Mesenchymal Transition (EMT)

(22). Another FAK-dependent mechanism of cell survival was shown in epithelial and endothelial cells and involves the activation of the PI3K/Akt pathway. The phosphorylation of FAK on Tyr397 creates a potential binding site for the SH2 domains of the p85 subunit of PI3K (23). Phosphorylation of the PI3K subunit, p85, by FAK may activate the p110 catalytic subunit and the PI3K/Akt signaling pathway leading to cell survival. In fibroblasts, FAK mediates the β1 integrin/PI3K/Akt survival signal in collagen matrices. Thus integrin-ECM ligation may activate FAK and promote an adhesion-dependent survival signaling through the FAK/PI3K/Akt axis (24).

1.3.2 FAK regulation of cell migration

Cell migration is a dynamic and multistep process bringing to rapid changes in the dynamics of actin filaments, together with the rapid assembly and disassembly of the FAs. In this contest, FAK could be activated by both integrins and RTKs and acts as a mediator of the signaling that leads to the actin cytoskeleton remodeling and cell migration.

Upon integrin engagement with the ECM, FAK is recruited to the site of FAs and is autophosphorylated on Tyr397 which creates a high-affinity SH2 binding site for cellular src. Consequently, src phosphorylates additional tyrosines of FAK which in turn, causes maximal FAK kinase activity and phosphorylation of p130Cas by the FAK/src complex. Migration requires change in the actin cytoskeleton such as membrane ruffling. Tyrosine phosphorylated p130Cas associates with several SH2-containing proteins including Crk. The Cas/Crk complex formation plays a key role in regulating membrane ruffling and cell migration through DOCK180 and Rac. Paxillin is another adaptor molecule which has been linked to the FAK signaling. Paxillin is also a major substrate of FAK/src kinase complex and its phosphorylation at Tyr31 and Tyr118 residues could function to recruit Crk in a similar manner as p130Cas (5).

Recently, it has been reported that inhibiting FAK/paxillin interactions led to a complete loss of FAK localization at FAs together with reduced phosphorylation of FAK and FAK targets such as paxillin and p130Cas. In turn this resulted in altered FA dynamics and inhibition of cell adhesion, migration and invasion (25). FAK is also able to interact directly with small GTPase proteins such as Rho, Rac, Cdc42 or can also stimulate their activation or inactivation via the association with both, Guanine Exchange Factors (GEFs) and GTPase activating proteins (GAPs) which in general, GEFs activate, while GAPs inactivate RhoGTPases (26). For example, FAK regulates RhoA activation by the phosphorylation and activation of p190RhoGEF (27). FAK can also phosphorylate N-WASP, a Cdc42 downstream effector, inducing its cytoplasmic localization and activation of the Arp2/3 complex for actin polymerization at the leading edge of migrating cells (28). FAK interaction with PI3K could stimulate cell migration through its downstream effector Rac, which is a key regulator of cortical actin and lamellipodia in cell migration (5). Cell migration requires also the disassembly of FAs. Phopshorylation of FAK on Tyr925 by src has been linked with FAK loss from focal adhesions and FAs disassembly (5).

1.3.3 FAK, microtubules and mitosis.

Cell migration is a very complex process. To migrate directionally, cells need to assemble and disassemble their FAs. The FA life cycle involves the formation of integrin-mediated nascent adhesions at leading edge, which either rapidly turn over. Actomyosin-mediated pulling forces allow a subset of these nascent FAs to grow and mature, and provide forward traction forces. At the rear of the cell, FAs also have to release and disassemble (29). An interesting link between FAK and microtubules (MTs) has emerged since MTs play an important role in controlling FA turnover.

MTs are rigid hollow rods highly dynamic characterized by dynamic instability, in which individual microtubules alternate between cycles of growth and shrinkage. They are involved in cell movement, cell shape, intracellular transport, and mitosis.

A reciprocal regulation exists between FAs and MTs. For example, in migrating goldfish fibroblasts, MTs targeting to FAs induces FA disassembly demonstrating that MTs may control FA turnover (30). MTs at FAs go through growth-to-shortening transitions five times more frequently respect to other sites in the cytoplasm, and this also involves paxillin (31).

The MTs growth-to-shortening transitions is named catastrophe. It could be dependent on the availability of free tubulin or be induced by polymerization of the MTs against an obstacle. Usually also the presence of catastrophic factors, as stathmin, are necessary. Thus, it has been proposed that the density of the plaques at the FAs could exert two effects: it is not accessible to free tubulin and is a physical obstacle. Paxillin, in this contest, could act as scaffold protein for catastrophic factors leading to MT depolymerization (31). Paxillin is phosphorylated by FAK, therefore is not weird that FAK could exert a role in MT catastrophe at the adhesion site.

In fibroblasts, integrin-mediated activation of FAK at the leading edge is required for MT stabilization by the Rho-mDia signaling pathway (32). On the other hand, FAK phosphorylation on Tyr925 and the subsequent recruitment of Grb2 and dynamin into a complex with FAK are required for MT-induced disassembly of FAs (33).

The most important changes in cell shape happen during mitosis. The mitosis and the formation of the mitotic spindle, the MT composed-structure necessary for chromosome segregation into the two daughter cells, involve deep reorganization of the component of the cytoskeleton with the destroy of the actin framework and FA disassembly with subsequent cell rounding up (34).

During mitosis, the integrin signaling is necessarily inactivated by the serine phosphorylation and tyrosine dephosphorylation of protein of the FAs, such as FAK, p130Cas and paxillin (12).

In ECs, deletion of FAK causes an increased in centrosome numbers and mitotic spindles defects during mitosis. Transfection with FAK mutated on different phosphorylation sites, demonstrated that P-FAKSer732 is involved in mitotic spindle regulation and present at the centrosome co-localized with γ-tubulin. Indeed, P-FAKSer732 was found associated with the MTs motor protein dynein (17).

1.4 FAK in malignant cells

As reported above, FAK is known to have a pivotal role in the regulation of cell adhesion, motility, proliferation, and survival in normal cells. Deregulation of FAK, usually correlated with an increased protein expression, has been implicated in cancer.

1.4.1 FAK in proliferation of tumor cells

Over-expression of FAK has been linked with tumor proliferation. Recently, in breast cancer, it has been found that FAK signaling can occur in the nucleolus where it protects nucleostemin, a nucleolar-localized protein which modulates cell cycle progression, inducing tumor growth (35). NISCH which encodes the imidazoline receptor Nischarin, inhibits FAK-induced tumor growth and metastasis in ovarian cancer, and it is usually inactivated by hypermethylation (36). FAK and insulin-like growth factor receptor-1 (IGF-1R) directly interact with each other and thereby activate crucial signaling pathways that benefit cancer cells. Inhibition of FAK and IGF-1R function has been shown to significantly decrease cancer cell proliferation and to increase sensitivity to chemotherapy and radiation treatment in melanoma (37). In transgenic mouse

model of ErbB2-expressing breast cancer, the inactivation of FAK reduced the proliferative potential of ErbB2 mammary tumour cells but is dispensable for ErbB2 mammary tumour induction *in vivo*. FAK-null ErbB2 tumours still expressed the FAK-related Pyk2 kinase that could substitute FAK in cancer progression (38).The integrin β1/FAK axis is necessary for the initial proliferation of micrometastatic cancer cells disseminated in the lung. Infact, proliferation of these cells is reduced upon FAK knock-down (39). In glioblastoma cells, FAK-induced cyclin D1 expression depends on the phosphorylation of FAK on Tyr397 and requires ERK in a integrin-independent way (40).

Cell detachment from ECM leads to a specific programmed cell death named anoikis. An increased expression of FAK or an uncontrolled function has been reported to be involved in the escape from anoikis and the anchorage-independent growth observed in cancer. In fact, FAK suppresses anoikis in pancreatic adenocarcinoma cells (41). In ovarian cancer, it has been reported that tumor cells exposed to either norepinephrine or epinephrine exhibit lower levels of anoikis due to activated FAK (42).

1.4.2 FAK in migration and invasion of tumor cells

The process of metastasis formation is a key step in cancer progression and requires the capability of tumor cells to migrate and invade by the degradation of the ECM through the expression and the activation of the metalloproteases (MMPs). In v-src transformed cells, FAK induced src-mediated phosphorylation of endophilin A2 decreased its interaction with dynamin, which is important in the endocytosis of the cell surface matrix metalloprotease MT1-MMP (43). The accumulation of MT1-MMP at the cell membrane leads to invasion. The association of FAK with p130Cas also promotes the expression of MMP2 and MMP9 via Cas-Crk-Dock180 signaling cascade and activation of

Rac1 and JNK as well as their secretion into microenvironment of cancer cells. In different cancer cell lines, it was shown that MT1-MMP dependent degradation of ECM at the sites of FA requires the formation of a FAK/p130Cas/MT1complex. The distruption of the FAK/p130Cas/MT1 complex significantly impairs FA-mediated degradation and tumor cell invasion but doesn't affect invadopodia formation (44).

In liver cancer cell migration and invasion is induced by FAK/AKT-mediated MMP-2 and MMP-9 production and activation (45).

Several reports correlate FAK activity with the EMT that is a hallmark of cancer.

In colon cancer cells, expression of FAK mutants that cannot be phosphorylated by src induced the disruption of E-cadherin (cadh)-based cell contacts.

FAK is an important regulator of ECs, neutrophil, platelet, macrophage and fibroblast signalling in the tumour microenvironment. In ECs, FAK controls vascular permeability and tumour intravasation and extravasation leading to metastasis. FAK activity affects macrophages and fibroblasts recruitment to the tumour site. FAK promotes spreading, adhesion and survival of stromal cells, with concomitant regulation of ECM synthesis or remodelling to promote tumour progression (reviewed in (46)).

2. RTKs

Growth factors and their receptors are the core components of signal transduction pathways. The majority of growth factor receptors are composed of extracellular, transmembrane, and cytoplasmic tyrosine kinase domains. RTKs are a large family of transmembrane proteins with heterogeneous extracellular regions and common highly conserved intracellular tyrosine kinase domain. The binding of extracellular ligands triggers receptor dimerization and activation of the receptor's kinase activity leading to the recruitment, phosphorylation, and activation of multiple downstream signaling proteins, which ultimately change the physiology of the cell. RTKs are divided into 20 families by amino acid sequence identity within the kinase domain and structural similarities within their extracellular regions. In normal cells, RTK activity is strictly regulated; but dysregulation or constitutive activation of RTKs has been found in a wide range of cancers. The deregulated activation occurs by gain-of-function mutation, gene rearrangement, gene amplification, over-expression or abnormal autocrine, endocrine or paracrine stimulation of both receptor and ligand (47). Since RTKs have been implicated in many aspects of the malignant phenotype, they are emerging as promising therapeutic targets. Among them, we studied two RTKs which are usually deregulated in cancer: The EGFR which belongs to the ErbB family and the Axl receptor which belongs to the TAM family

2.1 The EGFR receptor

The Epidermal Growth Factor Receptor (EGFR) is a transmembrane glycoprotein receptor that belongs to ErbB family. ErbB family comprises four members named: erbB1/EGFR/HER1, ErbB2/HER2/Neu, ErbB3/HER3 and ErbB4/HER4. They share a common structure that consists of an extracellular N-terminal ligand binding domain with a dimerization arm, a trans-membrane

domain and a C-terminal domain with a tyrosine kinase activity. ErbB receptors binds different ligands: EGF (epidermal growth factor), betacellulin (BTC), heparin binding EGF-like growth factor (HB-EGF), transforming growth factor-α (TGF-α), amphiregulin (AR), epiregulin (EPR), epigen (EPG) and neuregulins (NRG) (48). EGFR could bind different of these ligands: EGF, TGF-α, AR, BTC and EPR. EGFR ligands can induce the homodimerization of EGFR with HER1 and the heterodimerization with other member of the family: HER2, HER3 and HER4 (49). The extracellular domains of the EGFR are subdivided and numbered as I-IV. Several deletion mutations occur in the EGFR such as EGFRvI (AAΔ1–541), EGFRvIII (AAΔ6–273), EGFRvII (AAΔ521–603), EGFRvIV (AAΔ959–1053) and EGFRvV (AAΔ959–1186). Additionally, several point mutations occur in TK domain of EGFR (Fig.2).

Once EGFR have bound one of its ligands, the receptor dimerizes, and the tyrosine kinase domain of one receptor is able to induce the phosphorylation of specific tyrosine residues placed on the other receptor. These events are necessary to create a scaffold platform to recruit different effectors and docking proteins (50). The platform constituted by effectors and docking proteins associated to the activated receptor is able to recruits downstream signaling molecules thus causing the activation of different signaling cascades such as the Ras/Raf/mitogen-activated protein kinase pathway. This is a critically important route that regulates cell proliferation and survival through the MAPK extracellular signal-regulated kinases 1 and 2. Activated MAPKs are imported into the nucleus where they phosphorylate specific transcription factors involved in cell proliferation. EGFR activation is linked also to the PI3K/Akt pathway. This pathway is involved in cell growth, apoptosis resistance, invasion, and migration. EGFR interacts also with the src kinase pathways. src activates a series of substrates, including FAK, PI3K, and STAT proteins (51).

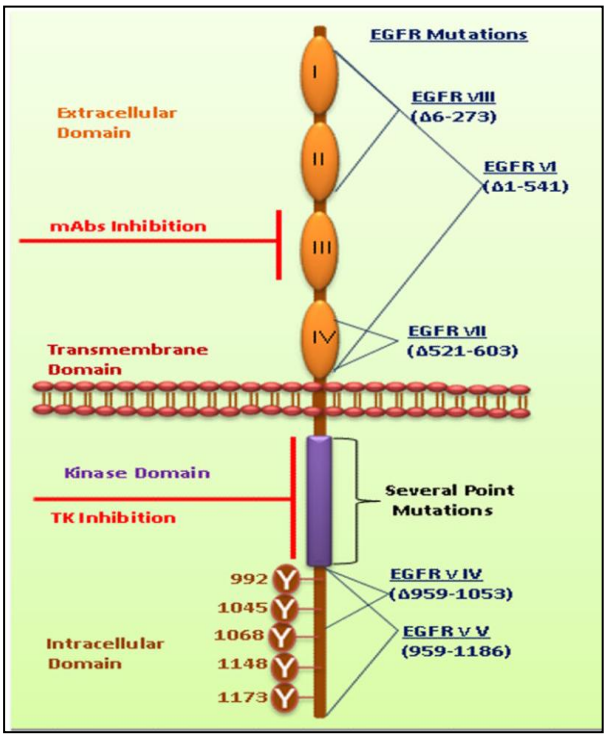

Fig. 2. The structure of EGFR (49).

2.1.1. EGFR in cancer

EGFR is a key factor in epithelial malignancies, and its activity enhances tumor growth, invasion, and metastasis. In cancer, EGFR is often perpetually stimulated because of the sustained production of EGFR ligands in the tumor microenvironment or as a result of a mutation in EGFR itself that locks the receptor in a state of continual activation or for gene amplification that results in protein overexpression. Though its altered activity has been studied primarily in development and growth of non-small cell lung cancer (NSCLC), many other tumors, including head and neck, ovary, cervix, bladder, esophagus, stomach, brain, endometrium, colon, breast, and liver are also known to exhibit deregulation of EGFR.

Gene amplification of EGFR has been demonstrated to occur in different tumor types and it is usually associated with EGFR protein overexpression. In

glioblastoma multiforme (GBM), EGFR gene amplification has been found in 37% to 58% of the tumors. Interestingly, a significant fraction of GBM (33%) with EGFR amplification showed multiple types of EGFR mutations. The most frequent variant of EGFR is the EGFRvIII, which accounts for more than 50% of the genomic alteration of EGFR observed in GBM. The EGFRvIII mutant receptor contains an in-frame deletion of exons 2-7 from the extracellular region that results in a truncated isoform of the receptor which unable to bind any ligands but, at the same time, the receptor is constitutively activated. Expression of EGFRvIII has been also described to occur in carcinomas such as breast and lung cancers (52).

EGFR deregulation in cancer also occurs from point mutation in the tyrosine kinase (TK) domain. Most of this mutation has been identified in lung cancer and correlated with a better response to TK inhibitors (53). In ovarian cancer, EGFR expression and activation could contribute to aggressiveness of EOC cells through the promotion of cell proliferation, invasion, angiogenesis and escape from apoptosis (54). EGFR was found amplified in about 4-22 % of ovarian cancer patients (55) and in about 4% of EOC cases activating mutations in the catalytic domain of EGFR were found (56).

2.2 The Axl receptor

Axl, also called Ark and Ufo, belongs to the TAM family which comprises also Tyro-3 (also called Sky) and Mer. The primary ligand for TAM receptors is growth arrest-specific 6 (Gas6), a fairly large (75 kDa) vitamin K–dependent protein known to activate downstream signalings (57).

Axl is ubiquitously expressed and has been detected in a wide variety of organs and cells, including the hippocampus and cerebellum, monocytes, macrophages, platelets, ECs, heart, skeletal muscle, liver, kidney, and testis (58).

The N-terminal region of Axl undergoes to partial or complete glycosylation and the protein reaches the molecular weight of 120-140 kDa, respectively.

The extracellular component of the Axl receptor contains two Ig-like domains followed by two FNIII domains. Between the FNIII domains and the C-terminal region of Axl there is a proteolytic cleavage site, yielding an 80 kDa soluble form of Axl (sAxl) which only comprises the extracellular domains of the full-length protein (Fig. 3). The generation of sAxl involves the activity of disintegrin-like metalloproteinase 10 (ADAM10). A dynamic equilibrium between sAxl and Gas6 levels in biological fluids may have an important regulatory role and affect Gas6 function. The intracellular C-terminal region displays the highest level of conservation and comprises catalytic domains responsible for the kinase activity, which catalyses receptor autophosphorylation and tyrosine phosphorylation. The interaction between Axl and Gas6 leads to the dimerization of Gas6/Axl complexes which results in autophosphorylation of tyrosine residues on the intracellular tyrosine kinase domain of Axl (59).

Gas6/Axl signaling promotes growth, survival, and proliferation of numerous cell types by activation of two main signalling pathways: PI3K and RAS/RAF/MAPK/ERK1/2 signalling pathways. The Gas6/Axl/PI3K/Akt pathway protects cells from apoptosis via multiple mechanisms. Akt inhibits the pro-apoptotic role of the caspase 3 and phosphorylates NF-κB which increases the expression of the anti-apoptotic proteins Bcl-2 and Bcl-xL (60). In some cell types, Axl activates ERK and contributes to proliferation. Axl has been linked also to the modulation of the cell shapes and migration. Activation of p38 and phosphorylation of HSP25 (heat-shock protein 25), a regulator of actin remodelling, is downstream of Axl.

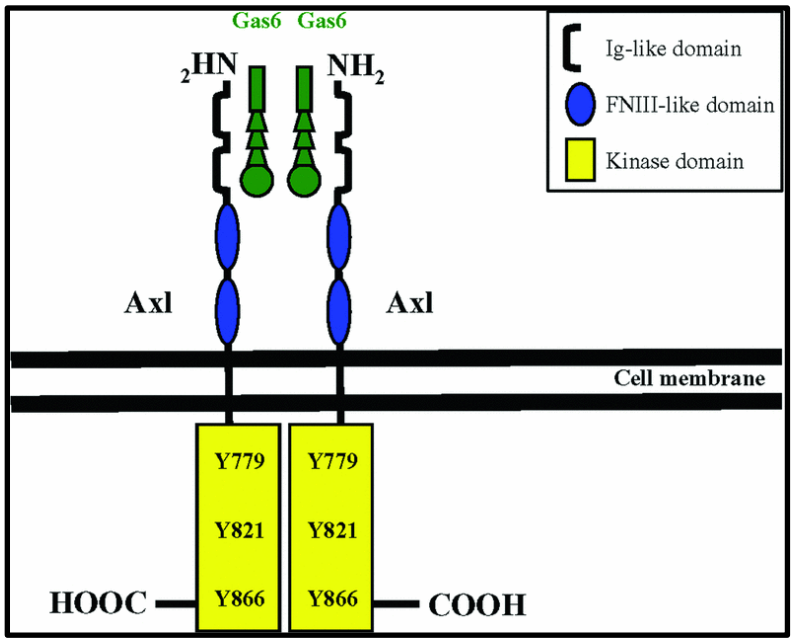

Fig. 3. Axl structure (59).

The Axl-Nck2 (NCK adaptor protein 2) recruits Axl to a ternary complex composed by the particularly interesting new cysteine-histidine–rich protein (PINCH) and integrin-linked kinase (ILK), which are proteins necessary to FAs formation and migration (61).The Gas6/Axl pathway can inhibit other growth factor signals. Activation of the tyrosine phosphatase SHP-2 is responsible for Gas6/Axl-mediated VEGFR2 inhibition (62). Axl pathway increases the expression of suppressors of pro-inflammatory signals, SOCS1 and SOCS3, suppressing the inflammatory response (63). Taken together, Axl-dependent signalling is responsible for cell survival, migration and growth. Aberrant functions of the Gas6/Axl pathway are linked to cancer.

2.2.1 Axl in cancer

RTKs, including Axl, have been implicated in the pathophysiology of many cancers. Up-regulation of Axl has been reported in a variety of cancers including breast, gastric, prostate, ovarian, lung and other (58).

Overexpression of Axl was shown to correlate with poorer prognosis, as well as increased invasiveness and xenograft growth of human cancers. Axl was further shown to be a downstream effector of the EMT program, which is an enhancer of invasive mobility of malignant cells (64).

Axl is over-expressed and activated in several drug-resistant cancer cell lines, suggesting that Axl may play a role in chemotherapy-resistant cancers. Increased Axl levels have been linked with Imatinib-resistant gastrointestinal stromal tumors, Nilotinib-resistant chronic myeloid leukemia cells, BMS-754087(IKB kinase inhibitor)-resistant Rhabdomyosarcoma, Lapatinib-resistant HER-2 positive breast tumor cells and resistance to cisplatin in ovarian and esophageal adenocarcinoma (65). In melanoma, Axl-positive cells possessed a greater *in vitro* invasive potential compared with Axl-negative ones. Motility, invasivity, and ability to heal a wound or to migrate across an endothelial barrier were inhibited *in vitro* by Axl knockdown (66). In ovarian cancer, Axl and Gas6 overexpression was found in 90 cases, regardless of histopathological type or clinical stage of ovarian cancers (67) and the therapeutic blockade of Axl reduced the migratory and invasive capability of tumor cells *in vitro* and *in vivo* tumor xenografts (68). High levels of Axl mRNA were also reported in a cisplatin-resistant ovarian carcinoma cell line obtained by exposure to increasing concentrations of cisplatin. (69)

Although Axl is consistently associated with resistance to chemotherapy and metastasis in cancer cells, the pathway downstream of Axl activation remain poorly defined. The emerging role of Axl in cancer holds potential for cancer treatment and therefore represents an important direction for future research.

3. Crosstalk between adhesion molecules and RTKs in cancer.

Tumorigenesis is a multistep process and reflects genetic alterations that drive the progressive transformation of normal human cells into highly malignant

derivatives. Nonetheless there are many types of cancer characterized by dfferent genetic aberrations and the activation of different signalling pathway, all cancer cells share some common hallmarks: self-sufficiency in growth signals, insensitivity to antigrowth signals, escape from apoptosis, sustained angiogenesis, tissue invasion and metastasis. In particular, migration, invasion and metastasis formation of tumor cells are responsible for most cancer-related mortality. Understanding how tumor cells acquire a migratory phenotype to become invasive and metastatic is crucial to develope effective strategies to block tumor progression. The first step in tumor cell invasion is the dissolution of cell-cell adhesions in favour of cell-matrix adhesions that support cell migration. Cells migrate in response to extracellular cues such as growth factors, which bind their RTKs at the cell surface. RTK activation initiates signalling cascades that contribute to the destabilization of cell-cell adhesions and promote migration by influencing the reorganization of the actin cytoskeleton often cooperating with integrins (70).

3.1 Cadherins

Cadherins are single pass transmembrane proteins that play crucial roles in normal development and in tissue homeostasis. They form Ca^{2+}-dependent homophilic interaction for proper cell-cell adhesion. The main cadherin-based cell-cell adhesion structure is the Adherent Junctions (AJ). AJs are dynamic structures that physically connect neighboring epithelial cells, coupling intercellular adhesive contacts to the cytoskeleton. Infact, the intracellular domain of cadherins contains binding sites for the catenins p120 and β-catenin. p120 catenin links cadherin to microtubules and is also important to prevent cadherin endocytosis and degradation. β-catenin binds α-catenin, which in turn binds actin and several actin-associated proteins, including α-actinin, vinculin, and formin-1(71).

Change in the expression or localization of cadherins have been regularly associated with cancer. It has been suggested that cadherins and RTKs cross-signal each other in a way that the activation of one receptor leads to the activation or inactivation of the other receptor mediated pathway. It has been shown that RTKs activation leads to loss of cell-cell contacts by destabilizing cadherin-mediated adhesions. However, formation of cadherin-mediated adhesions inhibits RTK activity by decreased ligand binding, tyrosine phosphorylation and receptor mobility. In addition, the interaction might also result in co-internalization of cadherins and RTKs after ligand stimulation (72). The best characterized cadherin in tumors is E-cadh. Loss of E-cadh expression, reported in many types of tumors, is usually associated with a worst prognosis. Infact, loss of E-cadh leads to a more mesenchymal invasive and metastatic phenotype (73).

It has been demonstrated that there is a bi-directional regulation of RTKs and E-cadh For example, E-cadh was found to interact through its extracellular domain with EGFR thereby decreasing receptor mobility and ligand-affinity. On the contrary, low density cells showed a positive E-cadh- regulation on the EGF/EGFR signalling (74).

EGFR activation has been linked with down-regulation of E-cadh-mediated cell-cell adhesion which results in increased tumor cell migration. This effect can be achieved by three different ways:

1) Distruption of the E-cadh/catenin complexes,
2) E-cadh endocytosis,
3) Down-regulation of E-cadh expression.

The presence of E-cadh has been shown to be important for the sensitivity to EGFR inhibitors for cancer therapy (75), thus studies into the mechanism of RTK/cadherin crosstalk in tumour cells could provide approaches for controlling invasiveness and resistance to current therapies.

3.2 Integrins

Integrins are αβ heterodimeric transmembrane proteins implicated in numerous physiological processes including adhesion to the extracellular matrix, proliferation, survival, migration and differentiation. Integrins control signaling pathway that are usually deregulated in tumors, therefore they have a profound influence in cancer progression and numerous studies suggest that the cooperation between integrins and RTKs exists and exerts a central role in cancer progression regulating invasion, proliferation and survival (76).

Considering that neither α or β subunit possess catalytic activity, it is possible that multiple mechanisms may regulate crosstalk between integrins and RTKs.

Three main type of Integrins/RTKs interaction has been identified:

1. Integrins can physically bind to RTKs.
2. Integrins clustering can enhance signaling pathway that are activated also upon ligand-dependent RTKs activation.
3. Integrins and RTKs reciprocally control their surface expression.

α6β4 integrin directly associates with the ERBB2 receptor in breast cancer and enhances tumor formation and invasion (77).

In pancreatic cancer, the iper-activation of EGFR leads to cancer metastasis but this process is dependent on the presence of αvβ5 integrin. On the other side, αvβ5 requires EGFR-mediated src activation to induce cell migration (78).

In breast cancer cells, HGF binding to MET increases anchorage-independent growth by inducing the phosphorylation of β4 integrin resulting in the activation of src and ERK (79).

The examples reported above are just a little portion of the increasing evidences regarding the central role of the integrins/RTKs crosstalk in cancer. The interaction between RTKs and integrins has made the last appealing as therapeutic targets for tumors that are responsive to particular growth factors.

4. The Epithelial Ovarian Cancer (EOC)

EOC is the fifth leading cause of cancer death in women and is the most lethal gynaecological malignancy. The EOC is usually diagnosed when the tumor is already disseminated outside from the ovary because of the absence of specific clinical symptoms and marker for an earlier diagnosis. The plasma levels of the ovarian tumor antigen CA125 (Mucin16) is used for the follow up of the disease, but unfortunately it has not a sufficient specificity and sensitivity for population screening (80). The gold standard treatment for EOC is primary surgery, followed by adjuvant platinum-based chemotherapy with or without paclitaxel. Surgical debulking is an important prognostic factor and it is widely accepted that the volume of residual disease after primary surgery influences overall survival (OS). Despite an initial good response to the chemotherapy, recurrence is common and fatal. Therefore, research in the EOC field is devoted to achieve a better prevention, detection and screening methods.

4.1 EOC classification

EOC are heterogeneous neoplasms that are divided in: Type I and Type II on the basis of their molecular and clinopathologic features (Fig. 4). Type I tumors comprise low grade serous carcinomas (LGSCs), low-grade endometrioid, clear cell and mucinous carcinomas. They originate from precursor lesions, endometriosis such as borderline tumors. The borderline tumors, identified as low malignant potential (LMP), comprise a group of tumors characterized by cellular proliferation and nuclear atypia but without stromal invasion (81). Type I tumors are usually confined to one ovary, are indolents and with a good prognosis.

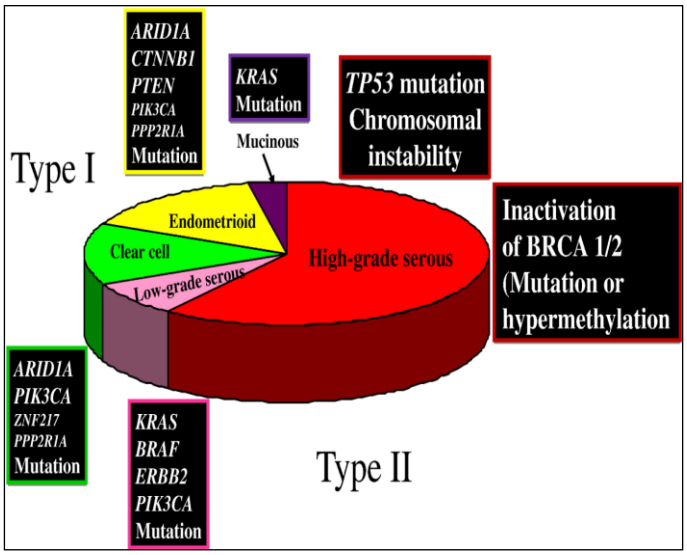

Fig.4. The histologic types of EOC and its associated genetic alterations (82).

They constitute only 25% of EOCs with a 5 year survival of about 55%. Type I tumors are associated with frequent KRAS, BRAF, CTNNB, PTEN and PI3Ca genetic alterations, with rare mutations in TP53 gene. Type II tumors comprise high grade endometrioid and serous carcinomas (HGSCs) that are tumors with high cellular proliferation, frequent TP53 mutations (>90%) and genetic defects as mutations and inactivations in BRCA1 and BRCA2 genes. Type II tumors represent approximately 75% of all EOCs with a five year survival of about 30% (82).

.

4.2. Pattern of spread of EOC

The main characteristic of the EOC progression is that they rarely metastatize to distant sites but disseminate within the peritoneal cavity. Small clusters of cancer cells shed from the primary turmor, persist as free floating cells or multi-cellular aggregates (MCAs) in the ascite and attach on the abdominal peritoneum or omentum (1) (Fig. 5). Tumor cells interact with mesothelial cells, placed in the inner surface of the peritoneal cavity giving secondary lesions to adiacent pelvic organs (83).

EOC originates from the ovarian surface epithelium (OSE) which invaginates into the underlying stroma resulting in inclusion cysts that eventually undergo malignant transformation (82). OSE cell integrity, unlike the other epithelia, is maintained by cell-cell adhesion through neural cadherins (N-cadh) expression; however E-cadh is expressed in the clefts and inclusion cysts (1). EOC normally displays both epithelial and mesenchymal characteristics retaining a high degree of plasticity, expressing vimentin together with cytokeratins 8 and 18 (84). It was demonstrated that in EOC, E-cadh localization is maintained at cell-cell contacts during tumor progression and some advanced EOCs concomitantly express both E- and N-cadh (85). MCAs of the ascites present E-cadh at the cell-cell contact. (86). In addition, while E-cadh expression is

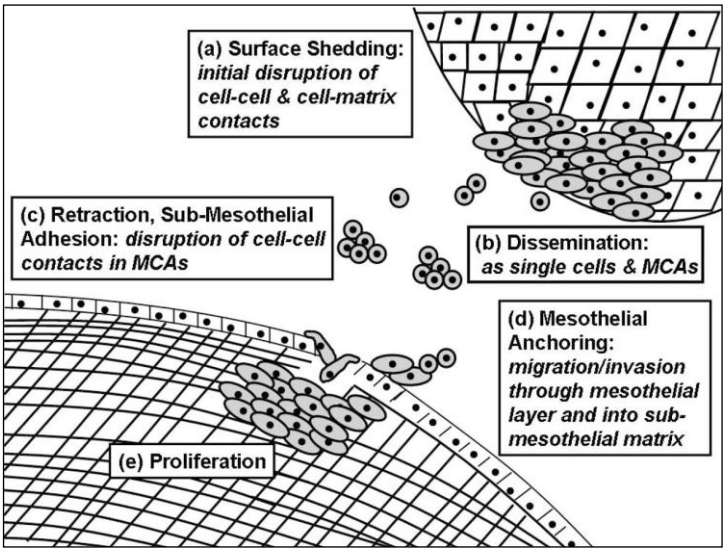

Fig. 5. The metastatization of EOC (1).

reduced in primary EOC, it could be re-expressed in metastatic lesions, where could sustain the survival of metastasis inhibiting apoptotic processes (87), suggesting that EOC cells undergo incomplete EMT. Interestingly, E-cadh engagement is necessary to the activation of PI3K/AKT-mediated proliferation (88), suggesting that E-cadh downstream signaling pathways could be

important for EOC MACs growth. During the metastatic dissemination, the attachment and invasion of EOC cells into the mesothelial cell lining the peritoneal cavity, a process call mesothelial cell clearance, requires a mesenchymal gene expression program and the de-novo expression of integrins plays an important role (89). Several groups have examined the ability of single EOC cells to pass through a mesothelial monolayer and found that the down-modulation of VCAM, α4 integrin, β1 integrin, MMP-2, or MMP-9 could decrease the extent of trans-mesothelial invasion. During the mesothelial cell clearance, mesenchymal genes appeared to be important, while epithelial genes, like E-cadh, were not associated to this process (90). All these data argue for the notion that during the re-attachment of MCAs to the mesothelium, a switch from a proliferative to a more invasive signature happens and it is driven by the down-modulation of E-cadh expression and the de-novo expression of integrins. In this contest, the activation of RTKs and the cross-talk between RTKs and adhesion molecules appears an important step in EOC progression.

Aim of the Project

The crosstalk between adhesion molecules and RTKs is considered an important driver in many types of cancers, including EOCs. Unfortunately, treatment with RTKs inhibitors resulted in a very poor clinical response in many type of tumors. For these reasons it is necessary to better investigate RTK signaling in tumor cells. A mediator of the crosstalk between adhesion molecules and RTKs is FAK. Deregulation of FAK correlates with increased survival, migration and invasion of cancer cells.

FAK has been shown to be able to regulate RTK activation, cadherin localization and expression on the membrane surface and a mediator of the integrin signaling.

Our aims are:

1. To characterize a new role of FAK phosphorylated on Serine 732 (P-FAKSer732) in tumors (**section 1**).
2. To study the crosstalk between RTKs and adhesion molecules and the contribution of FAK to these processes. In particular, the study has been focused on:
    - **i.** the crosstalk between E-cadh and EGFR (**section 2**),
    - **ii.** the crosstalk between integrins and Axl (**section 3**).

This study will contribute to identify new players that could be exploited to develop novel and more effective therapeutic approaches or as prognostic factors.

Section 1 The involvement of P-FAKSer732 in proliferation of tumor cells

Results and Discussion

1.1 FAKSer732 is accumulated in dividing tumor cells, expressed in cancer cell lines and is not localized at the FAs during migration.

First, we investigated on the localization of FAK in interphase migrating cells by immunofluorescence (IF) analysis. In particular, we analyzed whether a different FAK localization could be observed among P-FAKTyr397 (activating FAK site), P-FAKTyr576 (src-phosphorylated FAK site) and P-FAKSer732. We observed that, among all the phosphorylation of FAK, the P-FAKSer732 was not localized at FAs site but mainly present in a perinuclear region while the tyrosine phosphorylation of FAK (-Tyr397 and –Tyr576) were present at the leading edge of migrating cells at the sites where FAs assembly and disassembly (Fig. 1a). Although the role of P-FAKSer732 has been already described in nuclear movement and neuronal migration (11) and in VEGF-dependent endothelial cells migration (16), the first correlation between P-FAKSer732 and cell mitosis came from A.Y. Park in 2009, but the role of P-FAKSer732 has never been widely studied in cancer. In agreement with this previously literature knowledge, we also found that P-FAKSer732 was accumulated in mitotic cells (Fig. 1b). Seen the different localization, we then aimed to analyze if FAK phosphorylated on Ser732 was also phosphorylated at Tyr. We therefore performed an immunoprecipitaion (IP) with anti-P-FAKSer732 antibody (ab) and the presence of FAK phosphorylated on Tyr was investigated on the unbound and immunoprecipitated fractions. P-FAKSer732 in the immunoprecipitate was just poorly phosphorylated on Tyr576 while the dominant form in the unbound fraction contained P-FAKTyr576 (Fig. 1c). This result indicated that FAK could exist in two different pools on the bases of the type of phosphorylation and they might exert different roles. In several melanoma, ovarian and thyroid cancer cell lines, we tested the presence of P-

FAKSer732 together with FAK phosphorylated on Tyr 576 (P-FAKTyr576), which is the phosphorylation site responsible for the maximum activation of the tyrosine kinase (5). We observed that, in all cell lines tested, P-FAKSer732 was expressed, although at variable levels (Fig. 1d). Moreover, there was no correlation between the levels of P-FAKSer732 and the activation of the kinase activity, showed by the levels of P-FAKTyr576.

For the following analysis, the melanoma Me#28, the ovarian carcinoma OAW42 and the thyroid carcinoma NIM-1 cell lines were used as models.

1.2 P-FAKSer732 is independent from integrin engagement and FAK kinase activity.

Because P-FAKSer732 was not localized at the FA sites and is poorly phosphorylated on Tyr576, we investigated whether the phosphorylation at Ser732 residue was associated to integrin signalling cascade. To this aim, cells were grown 24 hr on plastic or fibronectin (fn). Western blot analysis on total cell lysates showed that the phosphorylation at Ser732 was not increased in cells grown on fn while P-FAKTyr397 and Tyr576 increased, as expected, in cells grown on fn (Fig. 2a). To furher investigate whether FAK auto-phosphorylation at Tyr397 was necessary for P-FAKSer732, Me#28 cells were transiently transfected with the mutant FAK construct named FRNK, which is a truncated isoform of FAK lacking the activation site (91) and the highest FRNK-expressing clone (F6) was selected by western blotting (Fig. 2b). Serum (FCS) stimulation of FRNK-transfected cells increased only P-FAKSer732 while in mock-transfected cells increased P-FAKTyr397, -Tyr576 and -Ser732 (Fig. 2c). Altogether these results indicated that the serine phosphorylation of FAK is independent from FAK kinase activity.

Hence, FAK can exert in tumor cells a dual role: one integrin-dependent linked to migration and associated to phosphorylation of Tyr397 and -576, and the

other, characterized here for the first time, integrin-independent associated to phosphorylation on Ser732.

The independence of P-FAKSer732 from integrin activation, its lack of localization at FA and its accumulation in dividing cells strongly suggest that, regardless of its involvement in migration, P-FAKSer732 play a role in the proliferation of tumor cells.

1.3 P-FAKSer732 contributes to cell proliferation exerting a role in microtubules polymerization.

To assess a role of P-FAKSer732 in proliferation, Me#28 cells were treated with a specific siRNA against FAK and growth capability was assayed. The growth rate of melanoma cells decreased 25% after 48 hr and up to 50% after 72 hr (Fig. 3a). Furthermore, phosphorylation on Ser10 of Histone H3 (herein named PHH3), a marker of mitosis (92), was 30% lower in FAK-silenced cells in comparison with cells transfected with a control siRNA (Fig. 3b), suggesting a role of FAK in the control of the mitosis. To specifically assess a role of P-FAKSer732 in cell proliferation, we transiently transfected, in control or FAK-silenced Me#28 cells, a GFP construct containing a mutated FAK on Ser732→Ala10 (11) (herein named Mut GFP-FAK) or the corresponding wild-type (wt) GFP-FAK. Control silenced cells transfected with Mut GFP-FAK displayed a reduction in the growth rate in comparison with those transfected with wt GFP-FAK that strongly decreased when Mut GFP-FAK was transfected into FAK-silenced cells (Fig. 3c). These data argue for the hypothesis that P-FAKSer732 is necessary to maintain the correct growth rate.

The above reported results were further confirmed by western blotting of cell lysates from the transfectants described above. Both wt and Mut GFP-FAK showed a decrease of PHH3 (Fig. 3d), indicating a role in the entry in mitosis. Conversely, expression of the Mut GFP-FAK increased the amount of

acetylated α-tubulin (ac-α-tubulin) which is a well-conserved post-translational modification that marks long-lived microtubules present in the cytoplasm and in the mitotic spindle during mitosis, showing that this P-FAKSer732 could exert a function in the MT dynamics.

1.4 P-FAKSer732 is localized at the mitotic spindle bound to tubulin and contributes to MTs dynamics.

It was previously reported that in migrating neural cells P-FAKSer732 was responsible for the MT assembly to generate forces for nuclear movement (11). In ECs, P-FAKSer732 was associated to the centrosome contributing to mitotic spindle formation. Deletion of FAK in primary ECs causes increases in centrosome numbers, multipolar and disorganized spindles, and unaligned chromosomes during mitosis. Re-expression of wild-type FAK, but not the mutant isoform of FAK which lacks the Ser732 site, rescued these mitotic defects (17). P-FAKSer732 was also found associated with cytoplasmic dynein, which is a MT motor protein that plays a fundamental role in mitosis (93). Confocal IF was performed to better investigate on the localization of P-FAKSer732 in dividing Me#28 cells. P-FAKSer732 co-localized with α-tubulin at the mitotic spindle during metaphase (Fig. 3a, left panel). During late anaphase, P-FAKSer732 co-localized with α-tubulin at the spindle, likely at the sites where MTs elongate and shrink (Fig. 4a, middle panel), and accumulated in the middle of the spindle, indicating an interaction with the cortical actin. Unlikely to what was reported previously by A.Y. Park, we didn't find any co-localization of P-FAKSer732 with the γ-tubulin at the centrosome (Fig. 4a right panel).

Furthermore, we also found that P-FAKSer732 was co-localized with ac-α-tubulin during all mitotic phases upon extraction of soluble tubulin (Fig. 4b) and it immunoprecipitated with both tubulin and dynein as previously reported,

assessing that dynein could be the mediator of the interaction between P-FAKSer732 and MTs. (Fig. 4c). To analyze the role of P-FAKSer732 during mitotic spindle assembly, cell lysates from Nim-1 cells transiently transfected with the Mut GFP-FAK construct were analysed by western blotting. Mut GFP-FAK showed an increased amount of polymerized MTs (2.5-fold), evaluated with anti- ac-α-tubulin ab, respect to cells that were transfected with a wt GFP-FAK (Fig. 4d). These data indicate a possible role in MTs dynamics.

To confirm this hypothesis, we performed a MT re-growth assay on Me#28 and OAW42 cells upon FAK silencing. Silenced cells were treated o.n. with nocodazole to force MT depolymerization, evaluated as the absence of ac-α-tubulin, then, nocodazole washout was performed to investigate on MT re-growth. FAK-silenced cells showed a higher amount of ac-α-tubulin indicating higher levels of polymerized MT and a better rescue of MT re-growth after nocodazole removal compared to cells transfected with control siRNA (Fig. 4e). These results clearly showed that P-FAKSer732 controls tumor cell proliferation by localizing at the mitotic spindle together with dynein and by exerting a role in MT polymerization.

1.5 The lack of P-FAKSer732 impairs mitotic spindle formation and mitosis

To specifically evaluate what could be the impact of the lack of P-FAKSer732 in mitotic spindle assembly, wt and Mut GFP-FAK were transiently transfected in Me#28 and NIM-1 cells. In interphase, wt (Fig. 5a, left panel) and Mut GFP-FAK (Fig.5b, left panel) were mainly localized at the sites of the FA, and no differences were observed between the two transfectants. In mitotic cells, wt GFP-FAK-transfected cells showed a regular spindle with wt GFP-FAK mainly localized on polar MTs (Fig. 5a, right panel). Interestingly, Mut GFP-FAK localized in randomly positioned spindle showing a diffused staining along the

entire spindle and the chromosomes appeared significantly unaligned (Fig. 5b, right panel). In agreement with these results, the number of mitosis was 6- and 3-fold lower in Mut GFP-FAK transfected Me#28 and NIM-1 cells, respectively (Fig. 5c).

1.6 The Cyclin-Dependent Kinase 5 is responsible for phosphorylation of FAK on Ser732.

Cyclin-dependent kinase 5 (CDK5) is a peculiar proline-directed serine/threonine kinase that, unlike the other members of the Cdk family, is not directly involved in cell cycle regulation but mainly present in post-mitotic neurons and its activity is tightly regulated by the interaction with the specific activators, p35 and p39 (94). In neuronal cells, CDK5 is able to phosphorylate FAKSer732 (11).

To test the hypothesis that CDK5 could be the kinase responsible for P-FAKSer732, starved Me#28, OAW42 and NIM-1 cells were treated with increasing concentrations of roscovitine, a potent CDK5 inhibitor (95). Roscovitine treatment decreased the amount of P-FAKSer732 in a dose dependent manner in all cell lines (Fig. 6a), but did not affect the level of P-FAKTyr397 and of P-ERK. Moreover, roscovitine treatment increased the amount of ac-α-tubulin in a dose-dependent manner. IF on roscovitine-treated NIM-1 cells showed impaired spindles and P-FAKSer732 staining was lower and diffused respect to that observed on untreated cells and no co-localization with acetylated α-tubulin was observed (Fig. 6b). These data demonstrated that CDK5 induces the phosphorylation of FAK at Ser732 independently from the FAK autophosphorylation thus contributing to spindle formation and mitosis of tumor cells.

1.7 The activation of the EGFR/MEK/ERK/CDK5 axis induces P-FAKSer732.

The EGFR is usually hyper-activated in many types of cancer. The MEK/ERK pathway is a downstream effector of EGFR (52) and in tumors, p35-dependent activation of CDK5 appeared to occur following ERK activation which in turn led to increased Egr1 transcriptional activity and up-regulation of p35 expression (96). To assess whether P-FAKSer732 could be downstream to the EGFR/MEK/ERK/CDK5 axis, starved Me#28, NIM-1 and OAW42 cells were stimulated with EGF. In all the three cell lines, EGF stimulation increased P-ERK together with P-FAKSer732 and P-CDK5Tyr15, the active kinase isoform (Fig. 7a). To test whether CDK5 was downstream of EGFR/MEK/ERK signaling cascade, ERK2 siRNA treated Me#28 cells were stimulated with EGF. EGF stimulation strongly increased P-FAKSer732 and P-CDK5Tyr15 of control siRNA-treated cells but not of ERK2 silenced cells showing that, upon EGFR activation, the phopshorylation of FAKSer732 induced by CDK5 needs the activation of the MEK/ERK pathway (Fig. 7b).

Conclusion and future perspectives

The results collected in this section present a deep analysis on the role of P-FAKSer732 in tumor cells. We have found that the phosphorylation of FAK at Ser732 occurs independently from integrin activation, is not localized at the sites of FAs and accumulates in mitotic cells. P-FAKSer732 plays a role in mitosis thus regulating the proliferation of tumor cells controlling the mitotic spindle assembly. We found that the phosphorylation of FAKSer732 was downstream of the EGFR/MEK/ERK pathway and we identified CDK5 as the kinase responsible for this phosphorylation.

In solid tumors, P-FAKSer732 is necessary for MT depolymerization thus maintaining normal, therefore not malignant, spindle assembly and function.

CDK5 is localized mainly in neurons and its presence, together with the presence of P-FAKSer732, should be analyzed in a large panel of solid tumors with the aim to correlate these two molecules with the malignancy and therefore with tumor growth or resistance to chemotherapy. The involvement of FAK in the mitotic spindle assembly requires further investigation to evaluate the possibility to develop specific inhibitors to this particular FAK function.

Moreover, the link between EGFR activation and P-FAKSer732, never demonstrated before, could allow a better understanding of the role of the EGFR in cancer that might be useful to design alternative therapeutic approach in tumors become resistant to anti-EGFR compounds.

Section 2 The crosstalk between RTKs and adhesion molecules and the contribution of FAK and E-cadh to these processes

Results and Discussion

During the progression of EOC, tumor cells detached from the primary tumor, persist as free-floating cells or MCAs which are able to escape from anoikis, and re-attach to a secondary site giving metastases (97). An uncontrolled integrin-independent activation of FAK responsible for the escape from anoikis in tumor cells has been already reported (41). In the previous section, we showed that the proliferation of tumor cells is strongly dependent on the presence of the EGF-induced P-FAKser732 that control mitotic spindle assembly through the binding to MTs mediated by the cytoplasmatic dynein. E-cadh expression is unusually up-regulated in EOC. It is not expressed in normal OSE cells, but is expressed in pre-malignant lesions and in well-differentiated tumors where it is membrane-associated as component of the AJs (98). E-cadh is also co-expressed with N-cadh in late-stage invasive tumors. In our lab, it was previously found that E-cadh knockdown impairs cell-cycle progression and proliferation of EOC cells and that the E-cadh-mediated AJ formation contributes to PI3K/AKT activation (88).

Here, we focused our attention on the role of FAKSer732 in EOC and in particular in MCAs biology and on the role exerted by the crosstalk between EGFR and E-cadh in this contest.

2.1 P-FAKSer732 is present in fresh EOC ascites together with E-cadh and the CDK5 activators p35 and p25.

With the aim to assess if P-FAKSer732 could be activated in EOC MCAs, we checked for its presence in several fresh EOC cells from ascites by western blotting. The characteristics of these ascites used are reported in Table I.

We also analyzed the presence of cell-cell adhesion components such as N-cadh and E-cadh together with the expression of CDK5 whose function has been reported in the previously section and in Rea K. et.,al 2013 (99).We found P-FAKSer732 expressed in 7 out of 8 EOC cells from ascites analyzed and 5 of them also co-expressed E-cadh. Seven out of 8 expressed CDK5 and its activators p35 and p25 (Fig. 8a). These findings were also confirmed by IF analysis on sample #7 where the EOC MCAs were positive for P-FAKSer732, p35 and E-cadh staining (Fig. 8b).

CDK5, a cyclin dependent kinase, is a widely expressed protein but its role in cell cycle control is not reported (100). Its activation depends on non-cyclin proteins, named p35 and p39, and the phosphorylation of CDK5 on Tyr15 increases its kinase activity. p35 and p39 resemble cyclins in their 3D structures and are almost exclusively detected in the nervous system (101). Recently, non-neuronal function of CDK5 has been also reported (102). Calpain is the mediator of the cleavage of p35 into p25. Although the levels of p25 are generally low in tissues, the interaction between CDK5 and p25 promotes CDK5 stability and enhances its kinase activity, resulting in the abnormal phosphorylation of substrates such as *tau* (94). In line with this data, we found p25 expressed in almost all the ascites analyzed, indicating an uncontrolled activation of CDK5.

In order to set up a 3D culture model resembling *in vitro* EOC MCAs, the EOC cell lines SKOV3 and OVCAR5 cells were seeded in the non-adhesive substrate alginate scaffold, the AlgiMatrix™. Alginate scaffold, to which integrins of human cells do not bind, allows the formation of spheroids and enables to study cell-cell adhesion. After 10-12 days of cultures, the MCAs were collected, fixed or lysated and analyzed by IF or by western blotting, respectively. As shown in Fig. 8c, both cell lines formed MCAs similar to those found in the EOC ascites (upper panel) and up-modulated E-cadh at the cell-cell

contacts (lower panel) respect to cells grown as monolayer (2D). Indeed, the western blotting showed that in 3D culture, E-cadh was de novo expressed in SKOV3 cells (Fig. 8d), and increased in OVCAR5 cells together with an increased level of P-FAKSer732 in both cell lines analyzed respect to cell grown on 2D.

To assess if *in vivo* the E-cadh/P-FAKSer732 axis could be present exclusively in floating MCAs, we performed a western blotting on total cell lysates obtained from two mouse xenograft models of human EOC. EOC cells from human ascites are usually injected in the peritoneum of the mice and about two months later, the mice are sacrificed and tumor cells are collected from ascites and from the solid masses grown attached to the peritoneal organs. We show here a western blotting performed on the lysates obtained from each tumor samples, the EOC MCAs from the ascites and the solid counterpart. As hypothesized, P-FAKSer732 was expressed only in the MCAs from ascites (Asc) in the 2 samples analyzed, while it was absent in the solid counterpart (st) (Fig. 8e). These observations were confirmed since P-FAKSer732 was present at higher levels in MCAs and less expressed in the solid tumors from 2 EOC patients (Fig. 8f).

Altogether the results suggest that E-cadh could be a determinant of MCAs formation and maintenance of P-FAKser732 levels.

Based on these results and those reports in the previous section, the possible existence of a crosstalk between the mechanism of cell-cell adhesion, mediated by E-cadh, and the EGFR/MEK/ERK/CDK5/P-FAKSer732 axis will be further investigated.

2.2. E-cadh induces FAKSer732 phosphorylation by modulating the CDK5 activation and CDK5 is necessary to stabilize E-cadh at the cell membrane.

It has been already showed that, upon integrins engagement, the activation of src and FAK leads to AJs disruption. Phosphorylation of β-catenin by FAK results in a loss of AJ integrity following integrin engagement (103). FAK can also regulate AJs by controlling the stability of E-cadh protein levels (22). An increased expression of E-cadh has been observed in FAK-null mouse embryonic cells, which was attributed to the regulation of the E-cadh transcriptional repressor SNAIL1 (104). FAK can also regulate the endocytosis of E-cadh and thereby its membrane localization. Depletion of FAK or β1-integrin, inhibits E-cadh endocytosis and is associated with a strengthening of cell–cell adhesions and reduced collective invasion (105).

With the aim to assess if a cooperation between the E-cadh signalling and the EGFR/MEK/ERK/CDK5/P-FAKSer732 axis exists, starved OAW42 cells were transfected with a pool of two specific E-cadh (siE-cadh) or control siRNA and a western blotting was performed on total cell lysates. As showed in Fig. 9a, E-cadh-silenced cells showed the decrease of P-FAKSer732 and P-CDK5tyr15, without affecting the other phosphorylation of FAK and the levels of P-ERK. Moreover, the E-cadh silencing also reduced the levels of the marker of mitosis PHH3 indicating that E-cadh expression has a role in cell proliferation.

To test if, as previously reported, the knockdown of FAK could have a role in modulating the expression of E-cadh influencing also the E-cadh-dependent CDK5 activation, OAW42 cells were treated with an E-cadh siRNA (siE-cadh) or with a FAK siRNA (siFAK) or with a control siRNA. Surprisingly, the western blotting performed on total cell lysates from the cells described above showed that FAK depletion affected neither the levels of E-cadh nor the levels of P-CDK5Tyr15 and the silencing of both, E-cadh plus FAK, did show a slight additive effect on the inhibition of CDK5 activation (Fig. 9b). Therefore, the

activation of CDK5/P-FAKSer732 axis depends on the presence of E-cadh. However, E-cadh protein stability is FAK independent in EOC cells.

In addition, because E-cadh silencing affects the activation of CDK5 (showed by the decreased levels of P-CDK5Tyr15) without affecting the levels of P-ERK, we speculated that direct connection between E-cadh and CDK5 could exist and it could be enhanced by the EGFR activation. In corneal epithelial cells, it has been already reported that CDK5 is localized in E-cadh containing epithelial cell-cell adhesions and co-immunoprecipitates with E-cadh (106). To test in EOC a biochemical interaction between E-cadh and CDK5, we performed an IP with anti-CDK5 ab on total cell lysates obtained from serum starved OAW42 cells stimulated or not with EGF. The western blotting confirmed that E-cadh is physically bound to CDK5 and that the amount of E-cadh/CDK5 complexes increased upon EGF stimulation (Fig. 9c). To study the meaning of the physical interaction between E-cadh and CDK5, OAW42 cells were treated with a CDK5 siRNA (siCDK5) or with a control siRNA (siCO) and IF was performed. In siCO cells, E-cadh was localized on the cell membrane at the sites of stable AJs. Upon CDK5 silencing, the stability of E-cadh at the cell membrane was impaired, as showed by the diffuse staining of E-cadh in the cytoplasm of silenced cells (Fig. 9d). In addition, CDK5 silenced cells showed longer MTs, confirming that CDK5 has a role in MTs dynamics that is mediated by P-FAKSer732 (as showed in section 1 and in Rea K. et al.,2013).

2.3 EGFR/E-cadh/CDK5 multi-protein complex regulates EGFR signaling pathway.

To assess if a multi-protein complex, constituted by EGFR/E-cadh/CDK5, could be present in MCAs complexes, we also performed an IP with anti-E-cadh in lysates obtained by *in vitro* culture of starved OAW42 cells grown in

AlgiMatrix™ and stimulated or not with EGF. The western blotting confirmed that E-cadh is also physically bound to EGFR and that the amount of E-cadh/EGFR complexes increased upon EGF stimulation (Fig. 10a) arguing for the hypothesis that a multi- protein complex composed by EGFR/E-cadh/CDK5 exists. With the aim to assess if the physical association among EGFR/E-cadh/CDK5 could influence EGFR activation, western blotting was performed on total cell lysates from starved siE-cadh or control-transfected OAW42 cells treated or not with the CDK5 inhibitor, roscovitine, upon EGF stimulation for 30 min. As showed in Fig. 10b, upon EGF stimulation control-transfected cells showed increased levels of P-EGFRTyr1068, which is the EGF-dependent autophosphorylation site, together with that of P-FAKSer732 and P-CDK5Tyr15. The phosphorylation levels of each protein were reduced in E-cadh-silenced cells and strongly impaired when E-cadh-silenced cells were treated with roscovitine (Fig. 10b). Interestingly, both E-cadh silencing and roscovitine treatment reduced the levels of EGFR arguing for the hypothesis of a regulation of EGFR stability by the E-cadh/CDK5 activation. Therefore, E-cadh regulates the EGF-dependent activation of the EGFR/CDK5/P-FAKSer732 axis.

Next, we aimed to test if E-cadh expression gives an increased sensitivity to roscovitine treatment. Two E-cadh positive (OAW42 and OVCAR5) and two E-cadh negative (SKOV3 and NL3507) cell lines were treated with roscovitine for different time point to perform a cytotoxicity assay. The results showed that the two E-cadh-positive cell lines were more sensitive to roscovitine respect to E-cadh negative cell lines (Fig. 10c, left panel and Fig. 10c right panel that shows the relative amount of E-cadh in each cell lines analyzed by western blotting).

Altogether these results confirm that E-cadh directly regulates P-FAKSer732 by the modulation of CDK5 activity in a manner that E-cadh may stabilize EGFR

expression and activation thus contributing to cell proliferation. The E-cadh/P-FAKSer732 could also be used as a signature identifying patients that will be responsive to CDK5 inhibitors.

Conclusion and future perspectives

In this section, we found that the expression of E-cadh in EOC could be an important feature during EOC progression contributing to cell proliferation and survival by the crosstalk with EGFR and the CDK5-mediated P-FAKSer732. As showed in section 1, P-FAKSer732 exerts an important role in MT polymerization and mitotic spindle formation thus modulating mitosis. Although, we found that P-FAKSer732 is independent from cell-ECM adhesion, in the current section we showed that it is dependent on E-cadh mediated cell-cell adhesion. EOC is the fifth leading cause of cancer-related deaths among women, and the leading cause of death from gynecological cancer. During EOC progression, small clusters of cancer cells shed from the primary tumor survive and proliferate as free floating cells. Subsequently these MCAs attach on the abdominal peritoneum giving a secondary lesion (97). This particular behaviour argues for the hypothesis that cell-cell and cell-ECM adhesion can contribute to mechanisms of proliferation/survival and of migration/invasion. We found that EOC cells, purified from ascites, express E-cadh at cell-cell contact. These EOC cells also expressed P-FAKSer732 and p35, the CDK5 activator. Because we found E-cadh is involved in modulating the EGFR/CDK5/P-FAKSer732 and, previously, our group demonstrated that E-cadh contributes EOC cell growth by recruitment of the PI3K-p85 subunit to the cell membrane (88) while P-FAKSer732 contributes to cell proliferation by regulating mitotic spindle formation (99), we can speculate that both signallings cooperate leading to growth and maintenance of MCAs present in the malignant ascites.

We introduced here some important steps in this complex scenario that clarified some mechanisms of MCAs biology.

Section 3 The crosstalk between RTKs and adhesion molecules and the contribution of FAK to these processes: the role of Axl.

Results and Discussion

As reported in the section "State of Art", a critical step in ovarian cancer metastasis is the transition of EOC cells from a proliferative to a more invasive phenotype necessary to establishing secondary lesion within the peritoneal cavity (107).

The MCAs present in the ascites form a reservoir of cancer cells that continuously re-populate the abdominal cavity leading to metastasis. The re-attachement to the peritoneal cavity requires that the MCAs loss cell-cell adhesion contacts and express de-novo integrins such as αvβ3 integrin, secretion of ECM component such as fn (107) and metalloproteases such as MMP-2 (108). All these events are induced by multiple biochemical changes that enable cells to assume a mesenchymal phenotype, which includes enhanced migratory capacity and invasiveness. These molecular changes are the basis of the EMT (109). MCAs can attach and spread on multiple ECM proteins associated with the mesothelium and then they need to pass through (or "clear") the mesothelial cells and take contact with the underlying basement membrane. This process is known as mesothelial clearance (89). In a recent study, EOC cell lines were divided in mesothelial clearance competent or incompetent cells on the basis of a mesenchymal gene expression profile which was positively correlated with clearance competency. Axl was one of the genes correlated with the clearance competency (90). Axl is a member of the TAM family of RTKs which is composed of three members: Axl, Mer, and Tyro-3. Axl has not a prominent role as oncogenic driver but it has been found overexpressed in many type of cancers and related to cancer progression (58).

The exact mechanisms that allow cells to undergo to EMT and to secondary lesions are largely unknown.

In this scenario, the roles of the TAM receptor and the ligand Gas6 have been investigated.

3.1 The expression of Gas6 and TAM receptor in EOC stable cell lines.

As first, we checked the expression of Gas6 and the three TAM receptors in a panel of human EOC cell lines by RT-PCR and western blotting. OVCAR4, and SKOV3 cells expressed the highest levels of Gas6 (Fig. 11a), while OVCAR5 and NL3507 barely showed detectable Gas6 transcript. The expression of the three TAM receptors was heterogeneous with Axl expressed at high levels in OVCAR5, NL3507 and SKOV3 cells as resulted by both real time RT-PCR and western blotting (Fig. 11a and b).

3.2 Axl is the TAM receptor specifically activated by the Gas6.

To assess which TAM receptors was activated by Gas6 stimulation, an IP with an anti-phosphotyrosine ab (p-Tyr) was performed on starved SKOV3 cells, expressing the TAM receptors Axl and Tyro-3, and on starved NL3507 cells, expressing Axl and Mer, stimulated or not with Gas6. In both starved cell lines, Axl was already slightly tyrosine phosphorylated compatible with stimulation by endogenously produced Gas6, and de novo Gas6 stimulation induced higher levels of Axl phosphorylation (Fig. 12a). In SKOV3 cell, a slight amount of phosphorylated Tyro-3 was observed, while in NL3507 neither Mer nor Tyro-3 resulted tyrosine phosphorylated upon Gas6 stimulation.

In line with these results, in both Gas6-stimulated cell lines the phosphorylation of Axl was inhibited by the presence of a recombinant Axl-Fc protein (Fig. 12b).

3.3 Gas6 and sAxl expression in EOC ascites

Next, we aimed to investigate on both the presence of Gas6 and Axl in EOC ascites. We therefore analyzed 22 EOC ascites by ELISA and found that the levels of Gas6 ranged from 43 to 103ng/ml with a mean value of 74.1ng/ml and were statistically higher compared to levels in 22 ascites from non-malignant pathologies (Fig 13a and Table II for the main characteristics of the ascites used). To evaluate if the soluble Axl ectodomain (sAxl) is able to sequester Gas6, its levels were also measured. As shown in Fig. 13b, Axl molecules were not sufficient to completely sequester Gas6 molecules in 20 out of 22 ascites indicating that Gas6 present in the EOC ascites was available for the stimulation of TAM receptors eventually expressed by EOC cells. In oral squamous cell carcinoma (OSCC) Gas6 released from the tumor-associated macrophages (TAMs) has been shown to promote tumor metastasis through the activation of Axl (110). As observed in OSCC, the presence of Gas6 in EOC ascites suggests that it acts like a fuel, maybe released by EOC cells or by the cells of the the immune system present in the microenvironment, favoring tumor invasion and the establishment of secondary lesions.

3.4 The Gas6/Axl activation doesn't affect cell proliferation but is involved in cell migration and actin cytoskeleton remodeling and invasion.

Once assessed that Axl and its ligand Gas6 were expressed in EOC cells and that Gas6 specifically actives Axl, we next aimed to get information about their functions.

A role for Gas6/Axl in proliferation of normal lens epithelial cells (111) and in proliferation of prostate human carcinoma (112) and colon cancer (113) has been already reported. We performed a proliferation assay on Gas6-stimulated SKOV3 transfected with a control siRNA (siCO) or with an Axl siRNA (siAxl)

showing that Gas6-dependent Axl activation didn't affect cell proliferation in EOC (Fig. 14a).

Following, we tested whether Gas6 was able to induce cancer cell migration by wound healing assay performed on starved SKOV3 and NL3507 cells upon Gas6 stimulation. Wounds were created in cell monolayers, and the wound repair was recorded at different time point post-wounding. Gas6-stimulated SKOV3 cells repaired the wound after 30 hr, while, at the same time, starved SKOV3 cells only showed 39% of wound repair. NL3507 cells repaired 21% of the wound after 30 hr in presence of Gas6 and only 10% in serum-free condition (Fig. 14b).

Next, we investigated whether the Gas6-dependent Axl activation leads to cytoskeleton remodeling by IF performed on starved SKOV3 and NL3507 cells in presence or not of Gas6. In both cell lines Gas6 stimulation led to membrane protrusion formation in a sheet-like conformation, such as lamellipodia, induced by actin polymerization at the leading edge (Fig. 14c lower panel) that were not visible in serum starved cells (Fig. 14c upper panel). Filopodia-like structures were also observed at the migrating front of cells together with large focal adhesions (Fig. 14c lower panel). These results demonstrated that Gas6/Axl pathway induces EOC cell migration through the remodeling of the actin cytoskeleton.

3.5 The Gas6/Axl pathway enhances cancer cell invasion.

To assess whether The Gas6/Axl signaling could be involved also in cancer cell invasion, we performed reduced growth factor matrigel-embedded 3D cultures of SKOV3 and NL3507 cells, to drive the formation of spheroids, with the aim to resemble the invasion process occurring *in vivo*. After 5 days, single cells from both EOC cell lines were able to form spheres in matrigel (Fig. 15a, left panels). These spheroids were serum-starved and stimulated or not with Gas6 to

evaluate its effect on cell behavior. Gas6 stimulation of the spheres induced the formation of a stellate invasive phenotype characterized by invadopodia and chains of cells that invade through the surrounding matrigel (Fig. 15a, right panel). To test if the interaction with component of the ECM was essential in the Gas6-induced invasion, we used the AlgiMatrix™, to which human integrins do not interact. SKOV3 spheroids, grown in AlgiMatrix™ for 12 days, were serum starved and stimulated or not with Gas6. Opposite to what we observed in matrigel, Gas6 did not induce any morphological change (Fig. 15b, left panel). These spheres were then taken from AlgiMatrix™, embedded in matrigel and stimulated or not with Gas6, as above. An invasive morphology was observed only in the presence of Gas6 (Fig. 15b, right panel).

These results indicate that Gas6 stimulation alone is not sufficient to induce cell invasion but it needs the interaction with the ECM.

Moreover, we found that, in starved SKOV3 and NL3507 cells allowed to adhere for a short time (30 min) on fn coated dishes, the levels of Axl activation upon Gas6 stimulation, reported as the level of Axl phosphorylated on Tyr702 (P-AxlTyr702) analyzed by western blotting, were higher in cells adherent on fn respect to cells simply adherent on plastic as explained by the quantitative analysis of three independent experiments reported in the graph (Fig. 15c upper and lower panels). These results showed that the interaction with ECM and the integrin engagement could enhance Gas6-mediated Axl activation.

Among the different β chain of the integrin molecules, SKOV3 and NL3507 cells express the integrin β3, as assessed by FACS analysis (Fig. 15d, upper panel). To assess in NL3507 whether indeed this integrin was involved in Gas-stimulated Axl activation, the previous experiment was performed in the presence of an ab able to inhibit integrin β3/fn interaction. As expected, the inhibition of the integrin β3 to bind the ECM protein completely abolished Gas6-induced Axl tyrosine phosphorylation (Fig. 15d, lower panel).

These data showed that, in EOC, the activation of Gas-stimulated Axl signaling pathway is dependent on the interaction with the ECM.

3.6 The Gas6-dependent activation of Axl requires the cross-signal with integrins mediated by the scaffold protein p130cas.

The synergism between RTKs and integrins is mediated by intracellular scaffold proteins, such as FAK and p130Cas, which integrate both signaling leading to the intracellular response (9). To study if these scaffold proteins could be the mediator(s) between Gas6/Axl and integrin/ECM signallings, the possible interaction between Axl and p130Cas or FAK was analyzed by IP performed on starved SKOV3 stimulated or not with Gas6. Total cell lysates were immunoprecipitated with anti-p130Cas (Fig. 16a) or-FAK Abs (Fig. 16b) and the obtained protein complexes were analyzed by western blotting with anti-Axl ab. We found that Axl co-immunoprecipitated with the p130Cas scaffold protein in absence and in presence of Gas6 (Fig 16a), while it only slightly interacted with FAK (Fig. 16b).

p130Cas is a scaffold protein involved in the process of cell adhesion and migration upon integrin engagements with the ECM (114). In EOC, high p130Cas expression has been reported to be associated with advanced tumor stage and inversely associated with overall survival and progression-free survival (115).

To test if p130Cas could be essential for Gas6-dependent activation of Axl, SKOV3 were transiently silenced for p130Cas (sip130Cas) or with a control siRNA, plated on fn coating or on plastic, serum starved and then stimulated or not with Gas6. Upon Gas6 stimulation, control silenced cells showed, as expected, an increased level of phosphorylated Axl respect to cells in serum-free medium (Fig. 16c). Interestingly, both starved and Gas6-stimulated fn adherent cells showed higher levels of Axl phosphorylation respect to cells

adherent on plastic. These results showed that Gas6 requires the synergism between Axl and integrins which is mediated by the intracellular scaffold proteins p130Cas.

3.7 Altering p130Cas/Axl interactions reduces Gas6-dependent adhesion and invasion.

To further clarify the role of p130Cas in the Gas6-dependent Axl activation and its contribution to EOC cell interaction with the ECM, the mechanism of cell adhesion was analyzed. To this aim, SKOV3 cells were transiently silenced for p130Cas (sip130Cas) or with a control siRNA (siCO), plated on fn and the cell adhesion was monitored up to 1 h by live imaging in presence or not of Gas6. Upon Gas6 stimulation, siCO cells started to adhere on fn after 10 min and after 20 min were completely spread on the substrate while Gas6-stimulated sip130Cas cells were not yet adherent on fn at the same time point (Fig.17a left panel) but same number of cells resulted adherent to fn in starved siCO cells and in sip130Cas cells stimulated with Gas6 (Fig. 17a right panel) meaning that the p130Cas-silenced cells were not activated by Gas6.

To further investigate on the cellular effect of p130Cas in the Gas6-dependent Axl activation, starved sip130Cas or control transfected SKOV3 cells were plated on fn and IF analysis of actin cytoskeleton was performed in presence or not of Gas6. Upon Gas6 stimulation, siCO cells plated on fn showed the formation of filopodia-like structure, while p130Cas-silenced cells appeared rounded and not attached to the substrate (Fig 17b).

To assess if the presence of p130Cas is necessary also in Gas6/Axl mediated cell invasion, stable control or p130Cas-silenced SKOV3 cells (Mock- and shp130Cas-SKOV3, respectively) were then embedded in reduced-growth factor matrigel and the obtained spheroids were then stimulated or not with Gas6. Upon Gas6 stimulation, shp130Cas-SKOV3 cells maintained a spherical

shape, while Mock-SKOV3 spheroids formed structures that invade into the surrounding thick matrigel (Fig. 17c).

These data strongly indicated that in the Gas6-dependent integrin-dependent adhesion, p130Cas is essential for invasion into ECM of EOC cells.

3.8 Gas6/Axl signaling triggered PI3K/AKT/rac activation.

In order to better clarify the downstream signaling pathway which is responsible for Gas6/Axl-dependent migration and invasion, SKOV3 were Gas6 stimulated while adhering to fn and the actin assembly was evaluated by IF with labeled phalloidin. Gas6 induced protrusive structures at the leading edge associated to the presence of stress fibers (Fig. 18a). In the presence of the compounds R428, an inhibitor of Axl phosphorylation, actin nucleation was inhibited as well as the formation of stress fibers. Interestingly, treatment of fn-adherent SKOV3 cells with the rac inhibitor EHT1864 recapitulated the effect of the Axl inhibitor on actin assembly and formation of stress fibers. Western blotting on total lysates from the same treated cells showed that R428 inhibited Axl and AKT phosphorylations (Fig. 18b). The phosphorylation of the src kinase, known to be activated by the adhesion to ECM proteins, resulted increased upon adhesion on fn and did not increase upon Gas6 stimulation, but it slightly increased in R428 treated cells only, arguing for the hypothesis that Axl activation could partially inhibit ECM-dependent src activation. On the other hand, rac inhibitor could decrease src phosphorylation but not Gas6-dependent AKT phosphorylation.

These results were further supported by inhibition of the invasion of Gas6-stimulated SKOV3 spheroids in matrigel by both the Axl and rac inhibitors (Fig. 18c).

Altogether these data suggest that Gas6/Axl signaling led to PI3K/AKT/rac activation in ECM-adherent EOC cells in a src-independent way.

3.9 Validation of the Gas6/Axl signaling in "*in vivo*" EOC samples.

The results obtained highlighted that the Gas6/Axl axis could be very important in metastasis formation. To test Gas6/Axl signaling also in *in vivo* samples, EOC MCAs were allowed to adhere on matrigel in presence or not of Gas6 and cancer cells invasion into matrigel was monitored by phase contrast microscopy. Accordingly to that observed for EOC cell lines, Gas6 induced in EOC MCAs morphological transformation such as the acquisition of a stellate invasive phenotype (Fig. 19a). An IP performed with an anti-p130Cas ab on a MCA lysates confirmed that, Axl is physically bound to p130Cas also *in vivo* (fig. 19b).

Accordingly, immunohistochemistry (IHC) on an archival case material showed that, among 72 EOC primary tumors, the majority expresses Axl at the cell membrane (80%) (Table III). Eighty % of these EOC samples also co-expressed p130Cas in the cytoplasm (representative samples in Fig.19c).

In particular, Axl and p130Cas co-expression could distinguish type I from type II EOCs as evaluated by Fisher's Exact Test (p=0,0009, Fig. 19d). These data, together with the biochemical and cellular data obtained *in vitro*, argue for the notion that EOCs susceptible to Gas6 activation are only those co-expressing Axl and p130Cas and that the Gas6/Axl signaling cascade is activated preferentially in p130Cas-expressing type II EOCs.

Conclusion and future perspectives

This section uncovers a new role of Gas6/Axl pathway during the progression of EOCs. The main novelties are: 1) the founding that Gas6, present at high levels in EOC ascites, is involved in EOC cell migration and invasion 2) the assessment that Gas6/Axl signaling requires an integrin-dependent pathway mediated by the scaffold protein p130Cas for activation.

In oral squamous cell carcinoma (OSCC) Gas6 released from the tumor-associated macrophages (TAMs) has been shown to promote tumor metastasis through the activation of Axl (110). Accordingly with these previous observations, we showed that Gas6/Axl pathway was able to promote cell invasion in integrin-dependent fashion. We also outlined that the crosstalk between integrins and Axl was mediated by a direct interaction with p130Cas but not with FAK. In fact, the p130Cas knocking-down reduced the capability of EOC cells to invade into matrigel and inhibited the cytoskeleton remodeling observed upon Gas6 stimulation. In line with our results, high p130cas expression was previously found in EOC and it was associated with advanced tumor stage and inversely associated with overall survival and progression-free survival (115). It is widely reported the role of p130Cas in regulating cell invasion through the release of matrix metalloproteinases such as MMP-9 (116). In EOC, Axl activation has been linked with cell invasion through the induction of MMP-1 and MMP-9 (68). Our results indicate that high levels of Gas6 in the EOC microenvironment activates actin re-organization and in turn adhesion and invasion. These functions are mediated by the interaction between Axl and p130Cas. We also demonstrated that all these processes downstream of Gas6/Axl/p130Cas axis are driven by the PI3K/Akt/rac activation.

All together, our experimental data suggest that Gas6/Axl/p130Cas axis is involved in EOC dissemination and metastasis formation.

A larger analysis of the expression of Gas6, Axl and p130Cas is ongoing in EOC and preliminary data indicate that the presence of an activated GAS6/Axl/p130Cas signaling pathway could be exploited as an indicator of an invasive EOC phenotype. The possibility to discriminate among different EOC phenotypes through the identification of new molecules that play a key role in the different step of EOC progression, as the Gas6/Axl/p130Cas axis, could lead to new and more specific therapeutic approaches.

The exploitation of therapeutic strategies targeting each of these molecules might be successful in the inhibition of EOC dissemination, especially for those patients, resistant to the conventional chemotherapies, who unfortunately recur with uncontrolled dissemination.

FIGURES AND TABLES

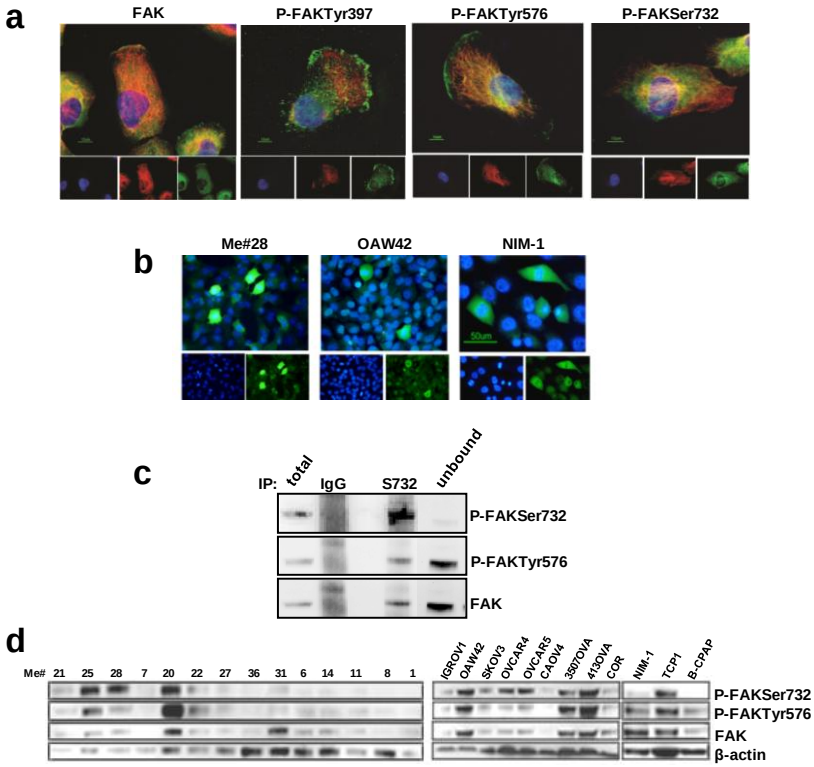

Fig. 1. FAKSer732 is accumulated in dividing tumor cells, expressed in cancer cell lines and is not localized at the FAs during migration.

a. IF performed on starved Me#28 cells induced to migrate through a wound. Cells were stained for P-FAKSer732, -Tyr 397, -Tyr 576, FAK (green) and α-tubulin (red). Nuclei were stained with DAPI (blue). Merged images are reported on the upper panels. **b.** IF performed on fixed cells upon FCS stimulation with anti-P-FAKSer732 ab (green). Nuclei were stained with DAPI (blue). **c.** IP performed with anti-PFAKSer732 ab on total cell lysates obtained from Me#28 cells. Normal rabbit (IgG) sera was used as negative control. Immunoprecipitated and unbound samples were analyzed by western blotting. **d.** Western blotting performed on total cell lysates from melanoma (n=14), ovarian (n=9) and thyroid (n=3) cancer cell lines. β-actin was used as control of gel loading.

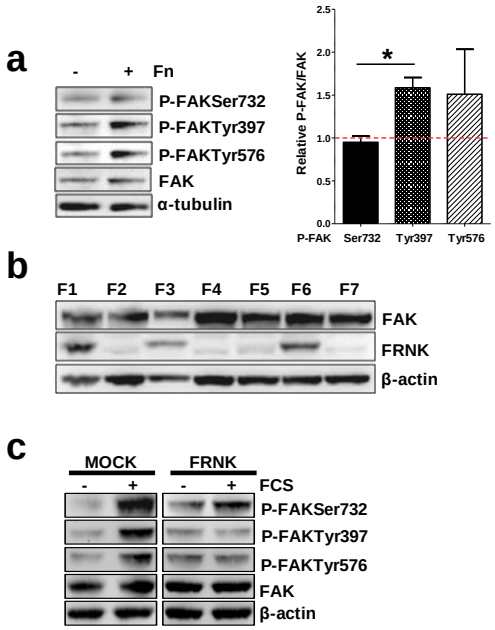

Fig. 2. P-FAKSer732 is independent from integrin engagement and FAK kinase activity.
a. Left panel: western blotting performed on total cell lysates from starved Me#28 cells grown on plastic (-) or fibronectin (fn). α-tubulin was used as control of gel loading. Right panel: densitometric analysis reporting the levels of FAK phosphorylated isoforms respect to total FAK expression of cells grown on fn. The medium values of three experiments are reported. Asterisk, $p \leq 0.05$. **b.** Western blotting performed on total cell lysates of the clones obtained from FRNK-transfected (Me)#28. The clone F6, expressing the highest levels of FRNK protein, was selected for the experiment reported on Fig. 2c. **c.** Western blotting performed on total cell lysates from Mock- or FRNK-transfected (clone F6) Me#28 cells. β-actin was used as control of gel loading.

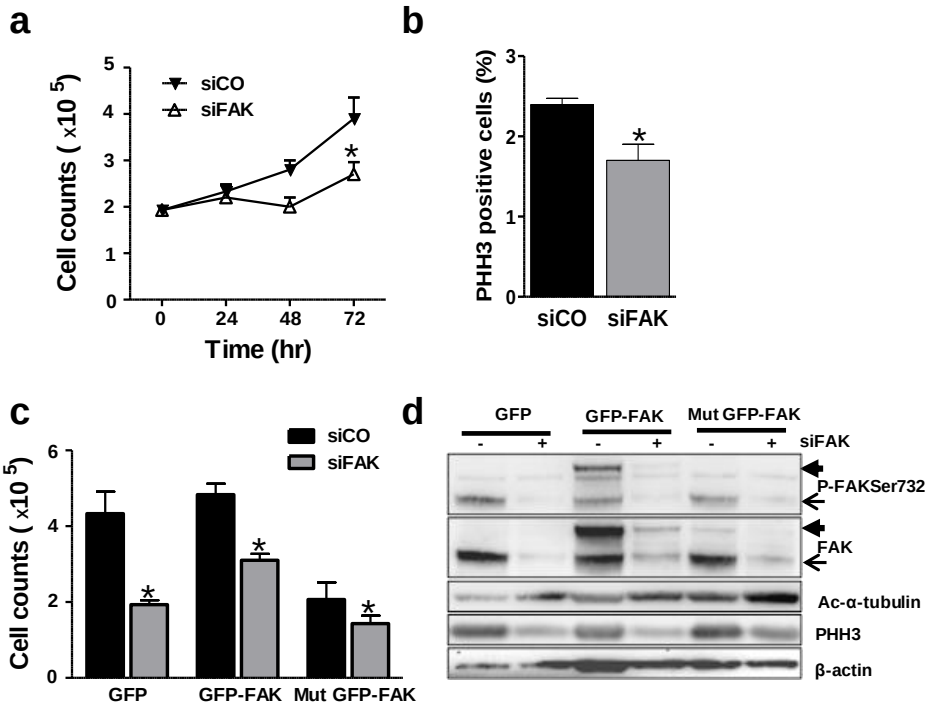

Fig. 3. P-FAKSer732 contributes to cell proliferation exerting a role in microtubules polymerization.

a. Proliferation assay performed on cells transiently transfected with control- (siCO) or FAK- (siFAK) siRNA. Representative growth curves of one of three independent experiments are shown; each point represents the mean of four replicates. Error bars, SD. **b.** Mitotic index performed on control- (siCO) or FAK- (siFAK) silenced (Me)#28 cells. The level of mitosis is reported as the percentage of PHH3 positive cells measured by FACS. Asterisk, $p \leq 0.05$. **c.** Proliferation rate of control- (siCO)- or FAK- (siFAK)-silenced Me#28 cells transfected with wt or Mut GFP-FAK vectors. The experiment was done three times in quintuplicate. The percentage of proliferation rate was calculated normalizing the values of each sample with those obtained in cells transfected with the GFP-containing vector only. Asterisks indicate statistical significant values ($p<0.001$). Error bars, SD. **d.** Western blotting performed on total cell lysates of the transfectants described above. β-actin was used as control of gel loading. Endogenous FAK, thin arrow, ectopic FAK, thick arrow.

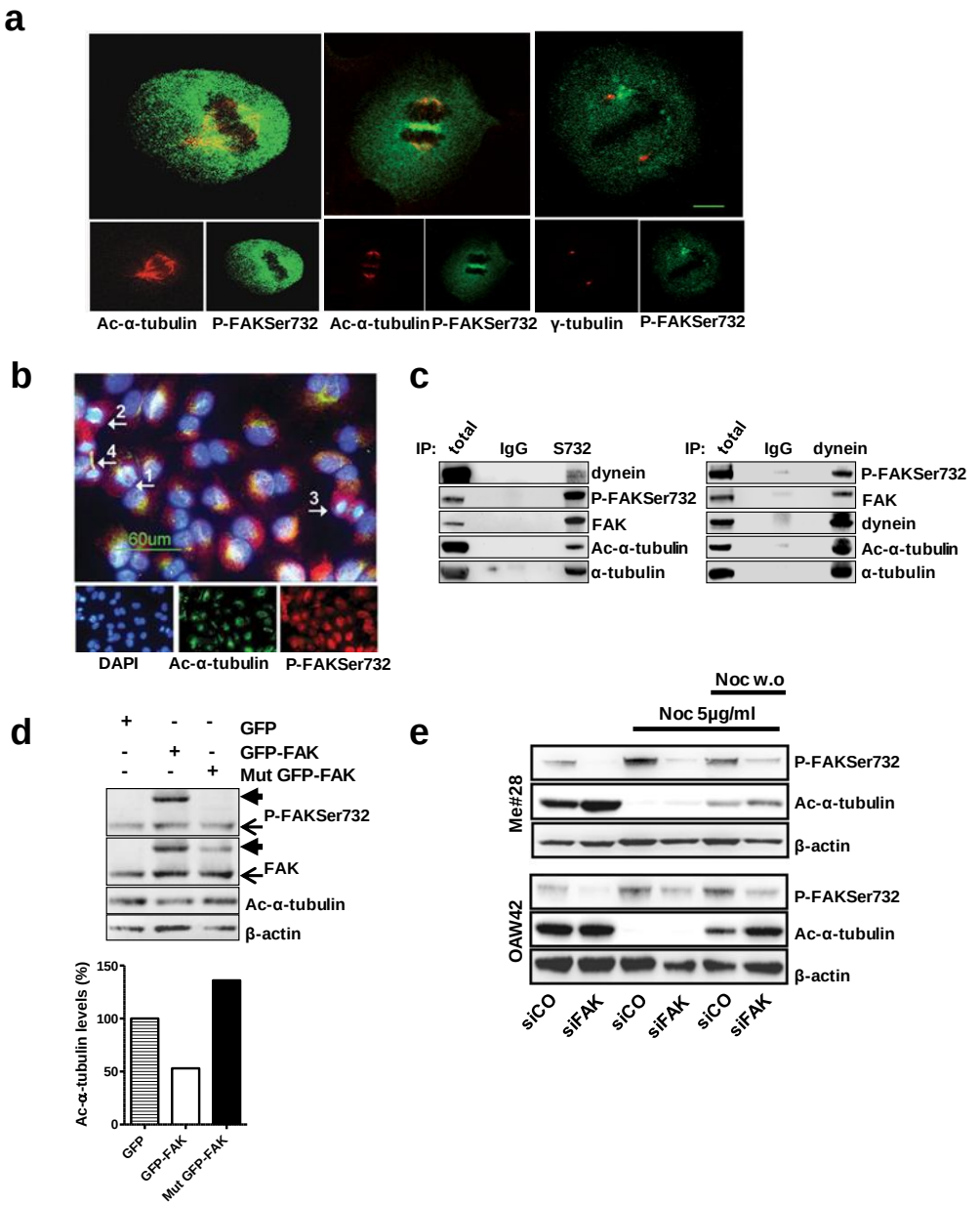

Fig. 4. P-FAKSer732 is localized at the mitotic spindle bound to tubulin and contributes to MTs dynamics.

a. Confocal IF performed on fixed Me#28 cells with anti-P-FAKSer732 and ac-α- (left and middle panels) or γ-tubulin abs (right panel). Images of metaphases (left and right panels, section 14 and 12, respectively) and late anaphase (section 11, middle panel) are shown. Bars,

10µm. **b.** IF performed on (Me)#28 cells upon extraction of free tubulin. The white arrows indicate the mitotic phases: 1, prophase; 2 anaphase; 3, telophase; 4, cytokinesis. The immunostaining was performed with anti-P-FAKSer732 (red) and ac-α-tubulin (green) abs. Nuclei were stained with DAPI (blue). Bars, 60µm. **c.** IP performed with anti-P-FAKSer732 (S732) and -dynein intermediate chain abs on lysates from Me#28 cells. Normal rabbit or mouse (IgG) sera were used as negative control. Immunoprecipitated samples were analyzed by western blotting. **d.** Upper panel: western blotting performed on total cell lysates from NIM-1 cells transfected with GFP alone, wt or Mut GFP-FAK vectors. Endogenous FAK, thin arrow, ectopic FAK, thick arrow. Lower panel: densitometric analysis performed on the western blotting shown in the upper panel. The results of an experiment of three performed are shown. **e.** MT re-growth assay was performed on Me#28 and OAW42 cells transiently transfected with control (siCO) or FAK (siFAK) siRNA. MTs were depolymerized treating the cells with 5 µg/ml nocodazole in complete medium at 37 °C o.n. Cells were washed with complete medium once and incubated at 37 °C. For Me#28 and OAW42 cells, the MT re-growth was allowed for 30 min and 3 h, respectively. Total cell lysates were analyzed by western blotting. β-actin was used as control of gel loading.

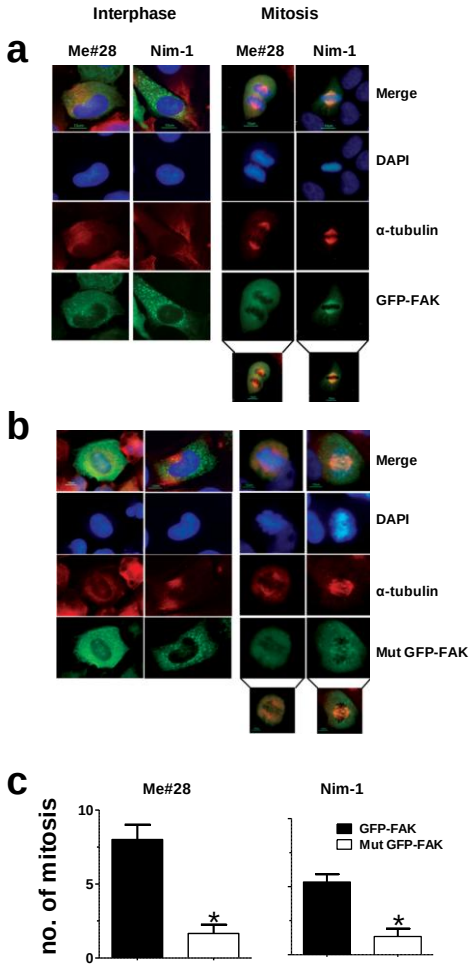

Fig. 5. The lack of P-FAKSer732 impaires mitotic spindle formation and mitosis.

Me#28 and NIM-1 cells transiently transfected with wt **(a)** or Mut GFP-FAK **(b)** vectors. IF was performed with anti-α-tubulin (red) ab on fixed cells. Nuclei were stained with DAPI (blue). Inserts on the bottom report green/red merge showing the localization in the spindle of the exogenous wt or Mut GFP-FAK. Bars, 10μm. **c.** Number of mitosis in transfected cells. Error bars, SD. Asterics indicate $p \leq 0.05$.

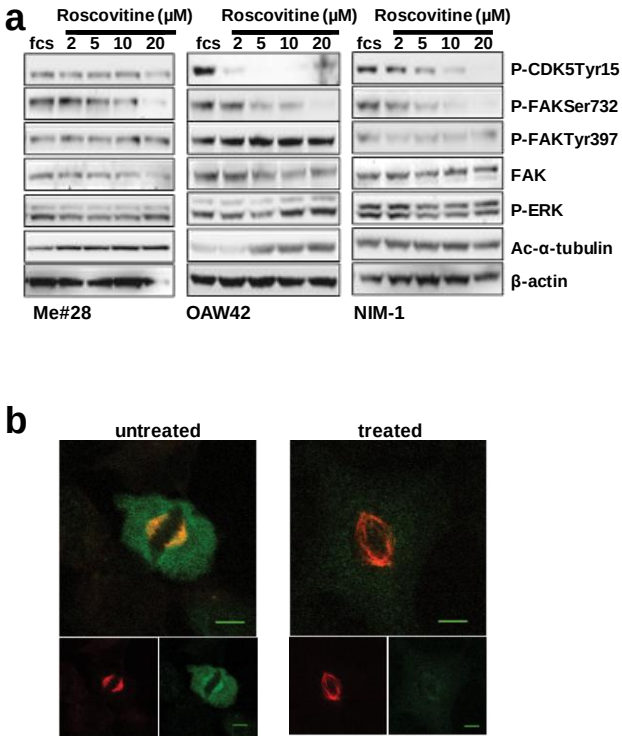

Fig. 6 The Cyclin-Dependent Kinase 5 is responsible for phosphorylation of FAK on Ser732.

a. Western blotting performed on total cell lysates from starved Me#28, OAW42 and NIM 1 cells untreated or treated with roscovitine (2-20 μM) and stimulated with FCS. β-actin was used as control of gel loading. **b.** Confocal IF performed on fixed NIM-1 cells untreated or treated with roscovitive (10μM) and stained with anti-P-FAKSer732 (green) and α-tubulin (red) abs. Bars, 20μm.

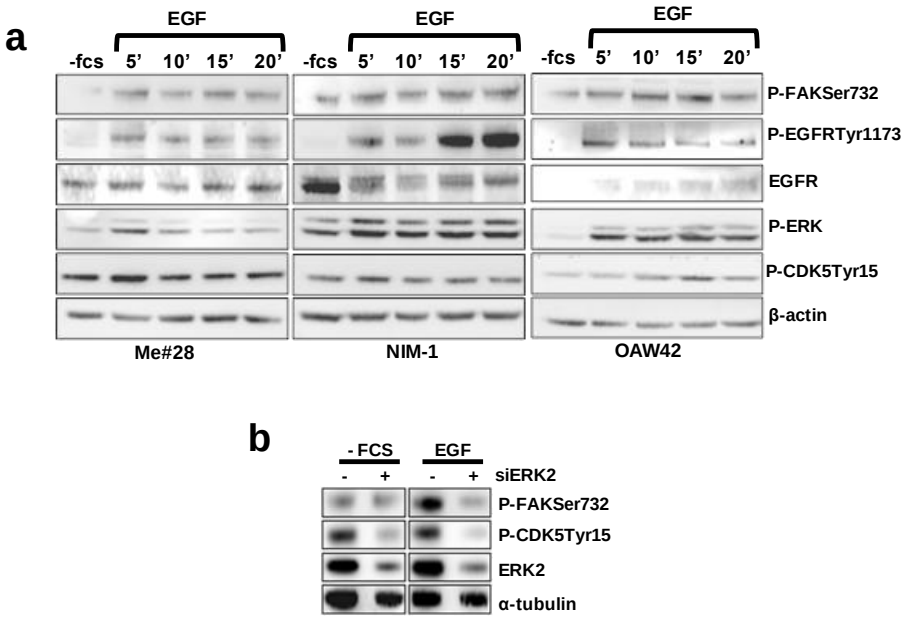

Fig. 7. The activation of the EGFR/MEK/ERK/CDK5 axis induces P-FAKSer732.

a. Western blotting performed on total cell lysates from starved Me#28, NIM-1 and OAW42 cells stimulated with EGF (20 ng/ml) for up to 20 min. β-actin was used as control of gel loading. **b.** Western blotting performed on total cell lysates from Me#28 cells silenced with control (-) or ERK2 (+) siRNA, starved and then stimulated with EGF (20 ng/ml) for 15 min. α-tubulin was used as control of gel loading.

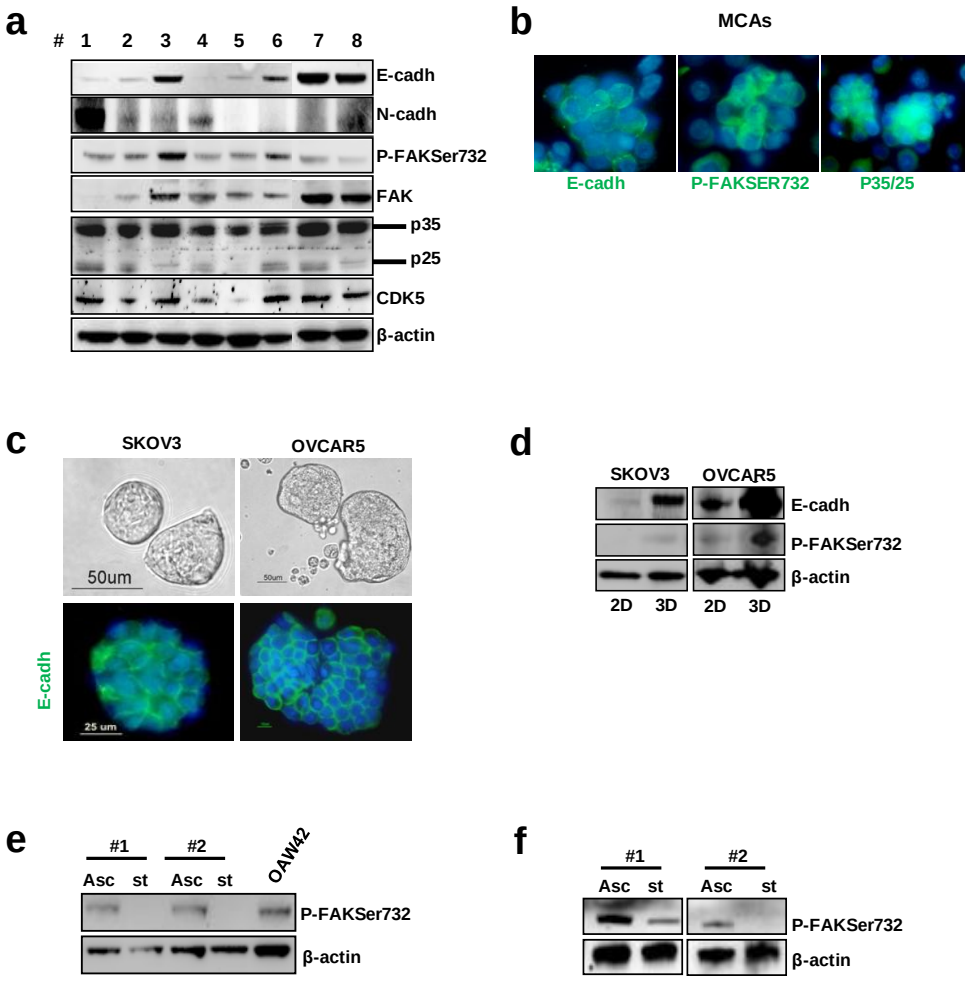

Fig. 8. P-FAKSer732 is present in fresh ascites together with E-cadh and the CDK5 activators p35 and p25.

a. Western blotting performed on total cell lysates from cells of EOC ascites. β-actin was used as control of gel loading. **b.** IF performed on cells of EOC ascites sample #7. The immunostaining was performed with anti-E-cadh, anti-P-FAKSer732 and anti-p35/p25 (green) abs. Nuclei were stained with DAPI (blue). **c.** Upper panel: phase contrast microscopy performed on SKOV3 and OVCAR5 cells grown on AlgiMatrix™. Lower panel: IF performed on fixed cells upon scaffold dissolution. The immunostaining was performed with anti-E-cadh (green) ab. Nuclei were stained with DAPI (blue). **d.** Western blotting performed on total cell

lysates from SKOV3 and OVCAR5 cells grown on plastic (2D) or AlgiMatrix™ (3D). β-actin was used as control of gel loading. **e.** Western blotting performed on total cell lysates from cells of two human EOC ascites and the corresponding solid tumors obtained by two mouse xenograft tumors. OAW42 lysates were used as positive control. β-actin was used as control of gel loading. **e.** Western blotting performed on total cell lysates from cells of two EOC matched samples: ascites and the tumor cells from the corresponding solid tumors. β-actin was used as control of gel loading.

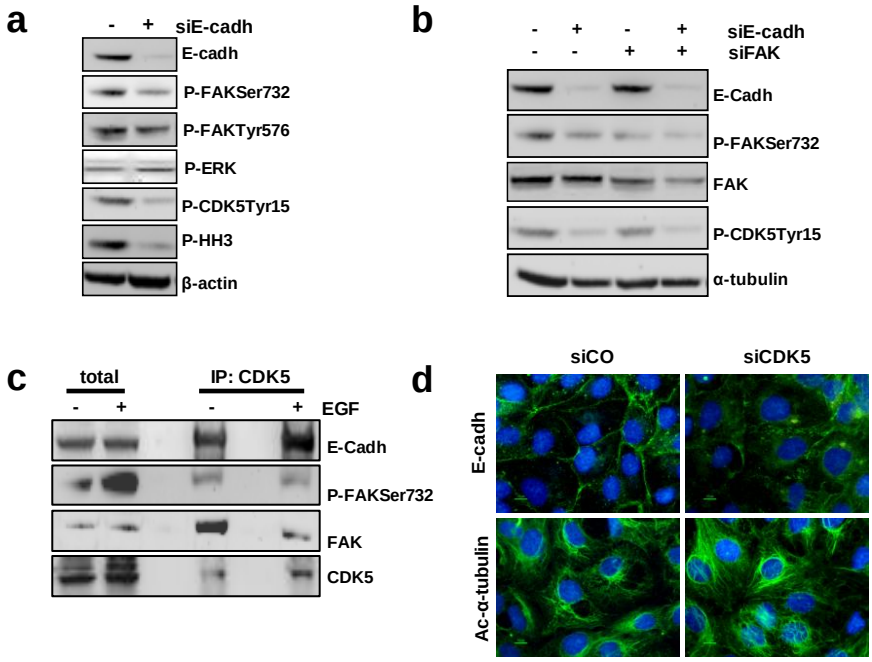

Fig. 9. E-cadh induces FAKSer732 phosphorylation by modulating the CDK5 activation and CDK5 is necessary to stabilize E-cadh at the cell membrane.

a. Western blotting performed on total cell lysates from OAW42 cells transiently transfected with control (-) or E-cadh (siE-cadh) siRNA. β-actin was used as control of gel loading. **b**. Western blotting performed on total cell lysates from OAW42 cells silenced with control (-) or E-cadh (siE-cadh) or FAK (siFAK) siRNA. α-tubulin was used as control of gel loading. **c.** IP performed with anti-CDK5 ab on lysates from starved or EGF-stimulated OAW42 cells. Immunoprecipitated samples were analyzed by western blotting**. d.** IF performed on fixed OAW42 cells transiently transfected with control- (siCO) or CDK5- (siCDK5) siRNA. Cells were starved and then stimulated with EGF (20 ng/ml) for 30 min. The immunostaining was performed with anti-E-cadh and ac-α-tubulin (green) abs. Nuclei were stained with DAPI (blue).

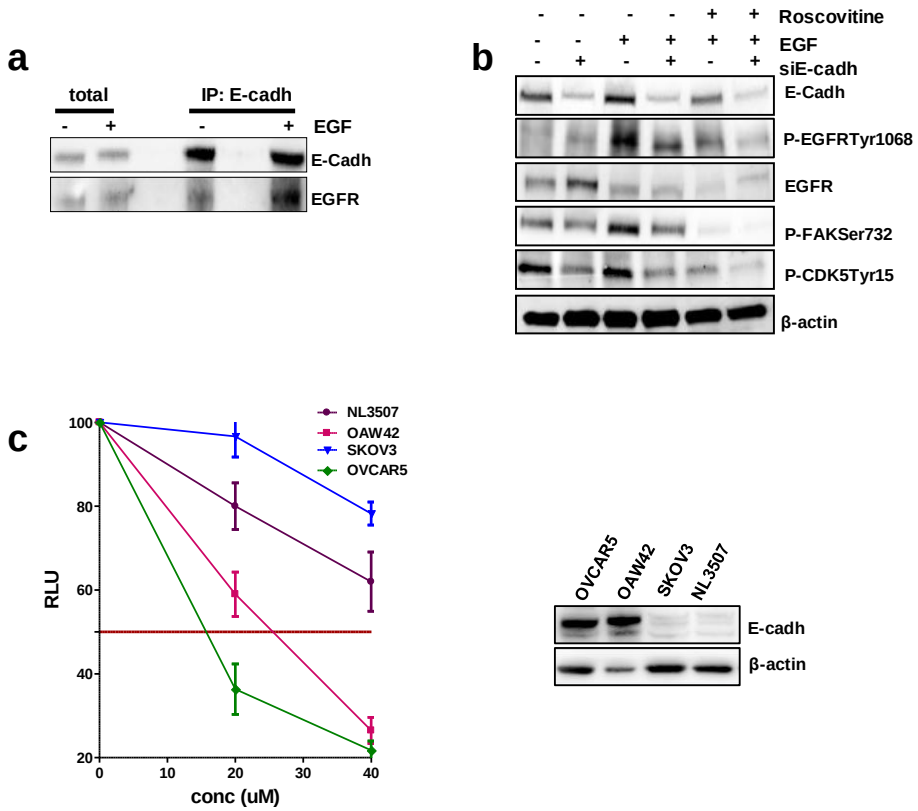

Fig. 10. EGFR/E-cadh/CDK5 multi-protein complex regulates EGFR signaling pathway.

a. IP performed with anti-E-cadh ab on lysates from starved or EGF-stimulated OAW42 cells grown on AlgiMatrix™. Immunoprecipitated samples were analyzed by western blotting. **b.** Western blotting performed on total cell lysates from OAW42 transiently transfected with a control (-) or E-cadh (siE-cadh) siRNA, starved, treated with roscovitine and then stimulated with EGF (20 ng/ml) for 30 min. β-actin was used as control of gel loading. **c.** Left panel: NL3507, OAW42, SKOV3 and OVCAR5 cells were treated with roscovitine up to 96 hr and cell viability was measured by CellTiter-Glo® Luminescent Cell Viability Assay. Representative growth curves of one of three independent experiments are shown; each point represents the mean of three replicates. Error bars, SD. Right panel: Western blotting performed on total cell lysates from NL3507; OAW42; SKOV3 and OVCAR5 cells. β-actin was used as control of gel loading.

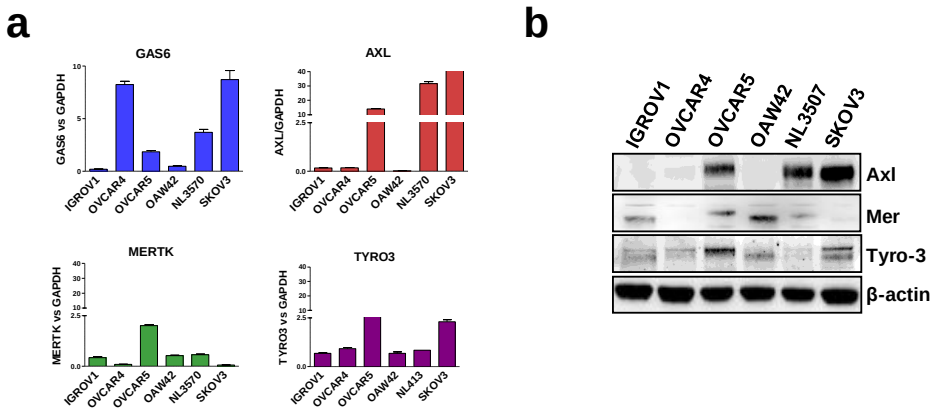

Fig. 11. The expression of Gas6 and TAM receptor in EOC stable cell lines.

a. Real-time PCR for Gas6, AXL, MERTK, and TYRO-3 genes of total RNA from six EOC cell lines. Results are presented as relative expression normalized to GAPDH mRNA levels. **b.** Western blotting performed on total cell lysates from the same six EOC cell lines. β-actin was used as control of gel loading.

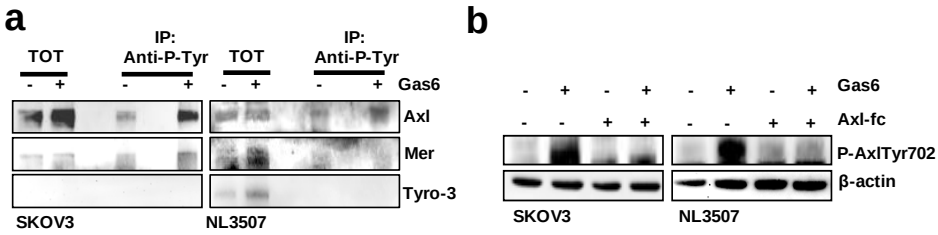

Fig. 12. Axl is the TAM receptor specifically activated by the Gas6.

a. IP performed with Anti-P-Tyrosine (P-Tyr) ab on lysates from starved or Gas6-stimulated SKOV3 and NL3507 cells. Immunoprecipitated samples were analyzed by western blotting. **b.** Western blotting performed on total cell lysates from starved SKOV3 and NL3507 cells pre-treated with Axl-Fc (2.5 μg/ml) and stimulated or not with Gas6. β-actin was used as control of gel loading.

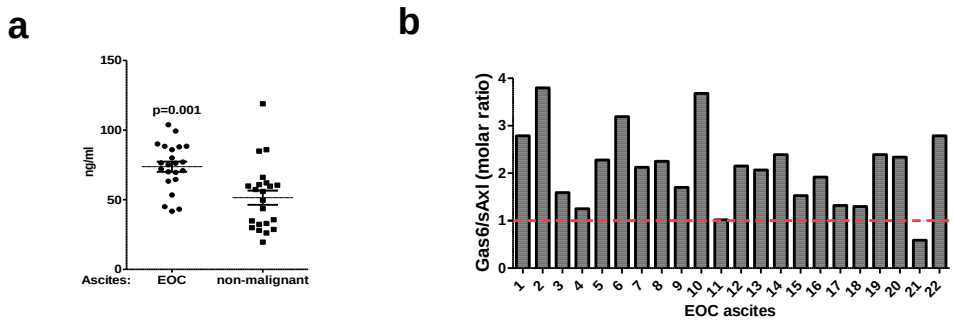

Fig. 13. Gas6 and sAxl expression in EOC ascites.

a. Gas6 levels measured by ELISA on 22 EOC ascites and 22 non malignant ascites. **b.** Evaluation in the EOC ascites of the sequestration by Axl ectodomain of Gas6. The graph reports the molar ratio between Gas6 and Axl ectodomain (sAxl). The red line represents the equimolar ratio.

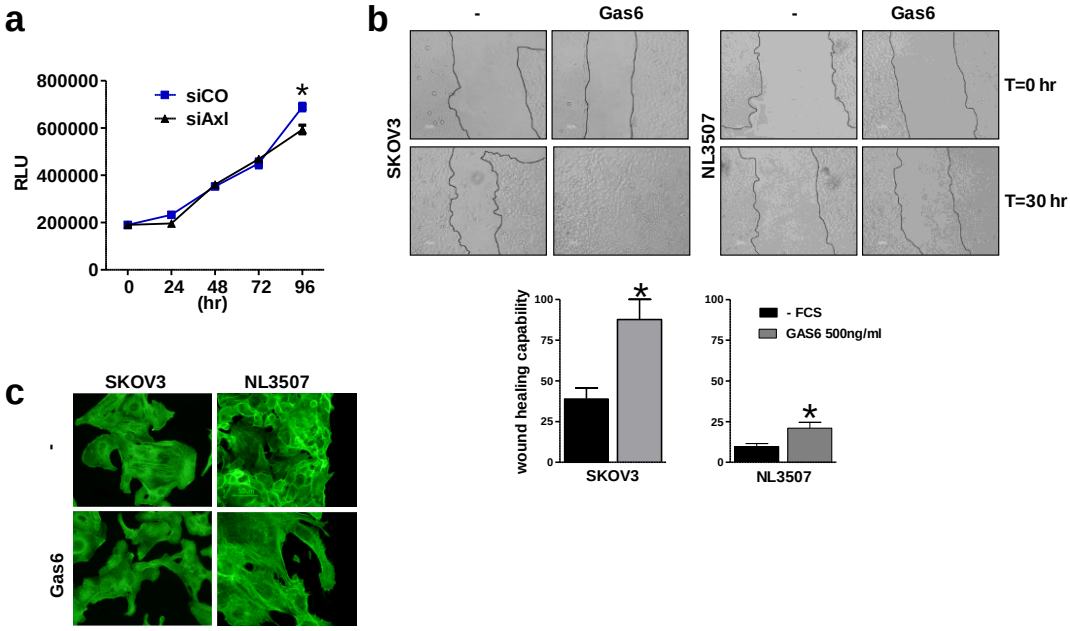

Fig. 14. The Gas6/Axl activation doesn't affect cell proliferation but is involved in cell migration and actin cytoskeleton remodeling and invasion.

a. Proliferation assay performed on SKOV3 cells transiently transfected with control (siCO) or Axl- (siAxl) siRNA. Representative growth curves of one of three independent experiments are shown; each point represents the mean of four replicates. Error bars, SD. **b.** Wound-healing assay performed on starved SKOV3 and NL3507 upon GAS6 stimulation. Upper panel: representative images reporting the wounds at the starting point (T=0 hr) and at the end of the experiment (T=30 hr). Lower panel: wound-healing repair capability at 30 h from the scratch. Asterisks p=0.01. Error bars, S.D. **c.** IF performed on starved SKOV3 and NL3507 induced to migrate through a wound in presence or not (-) of Gas6. F-actin was stained with phalloidin.

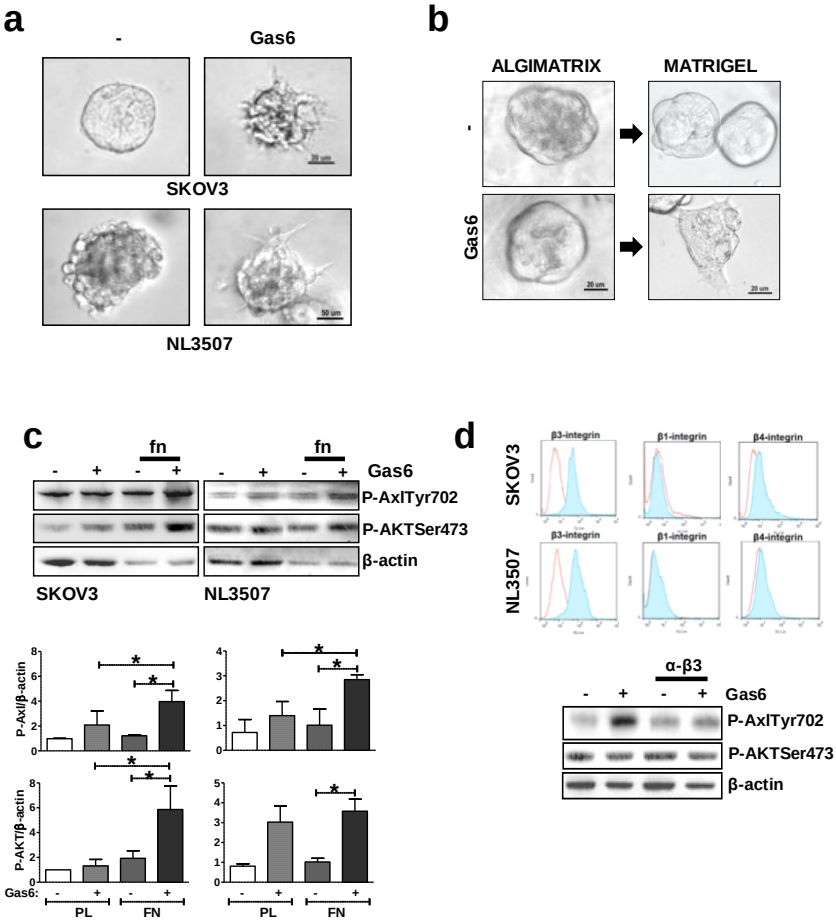

Fig. 15. The Gas6/Axl pathway enhances cancer cell invasion.

a. Invasion assay of starved (-) or Gas6-stimulated SKOV3 and NL3507 cells grown in Matrigel®. **b.** Left panel: phase contrast microscopy performed on starved (-) or Gas6-stimulated SKOV3 cells grown on AlgiMatrix™. Right panel**:** the spheres were dissolved from the AlgiMatrix™ and passed in Matrigel® in presence or not (-) of Gas6. **c.** Upper panel: western blotting performed on total cell lysates from starved or Gas6-stimulated SKOV3 and NL3507 cells seeded on fn for 30 min. A representative experiment of three performed is shown. β-actin was used as control of gel loading. Lower panel: quantitative evaluation of phosphorylated Axl in Gas6-stimulated cells upon adhesion on fn. The graph reports the mean±SD from three independent experiments. **D.** Upper panel: membrane staining of the integrin β3, β1 and β4 receptor was determined by flow cytometry on NL3507 cell line. The red

and light blue peaks, respectively, represent the fluorescence of the cells incubated with the secondary antibody alone as control (α-mouse) and the anti-integrins ab. Lower panel: western blotting performed on total cell lysates from starved or Gas6-stimulated NL3507 cells, in the absence or in the presence of the anti-integrin β3 ab. A representative experiment is shown. β-actin was used as control of gel loading.

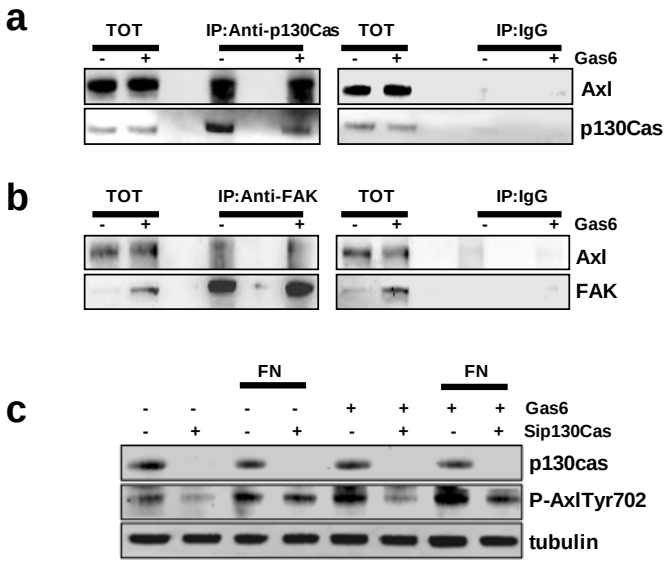

Fig.16. The Gas6-dependent activation of Axl requires the cross-signal with integrins mediated by the scaffold protein p130cas.

IP performed with anti-p130Cas **(a)** or with anti-FAK **(b)** abs on lysates of starved or Gas6-stimulated SKOV3 cells. Normal mouse or rabbit (IgG) sera were used as negative control, respectively. Immunoprecipitated samples were analyzed by western blotting. **c.** Western blotting performed on total cell lysates from SKOV3 cells transiently transfected with control or p130Cas (sip130Cas) siRNA. Cells were starved and seeded on fn for 30 min in presence or not of Gas6. α-tubulin was used as control of gel loading.

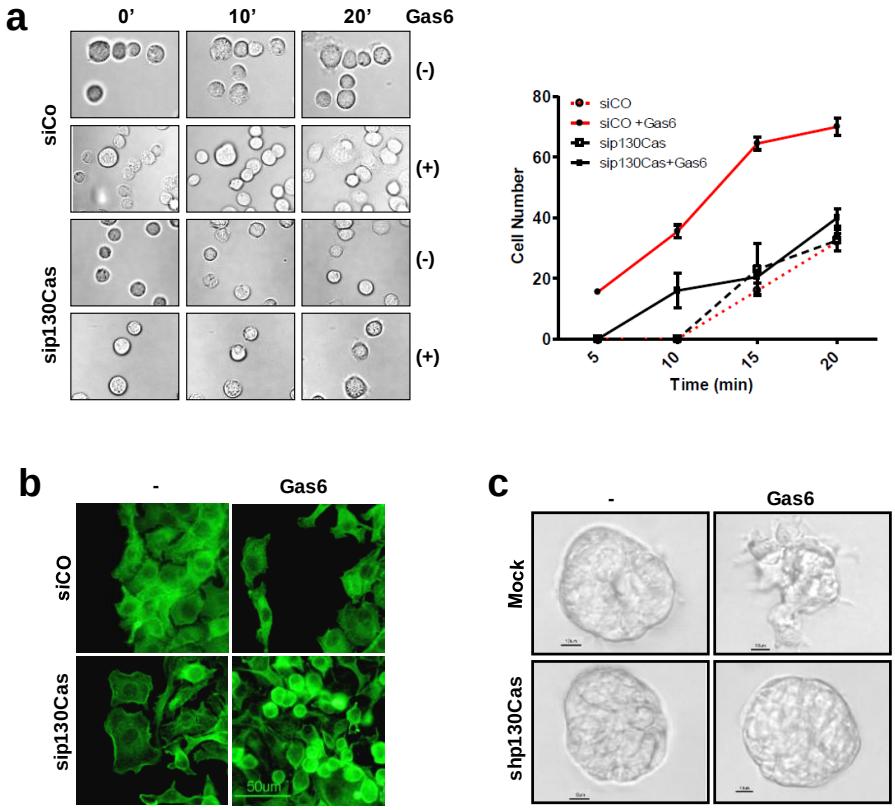

Fig.17. Altering p130Cas/Axl interactions reduces Gas6-dependent adhesion and invasion. **a.** Left panel: live cell imaging performed on starved (-) or Gas6-stimulated (+) control- (siCO) and p130Cas- (sip130Cas) silenced SKOV3 cells during adhesion on fn. Representative frames at 0, 10' and 20' hr are reported; frames were taken up to 1 hr. Right panel: graph reporting the number of siCo- or sip130Cas-silenced SKOV3 cells adherent on fn at different time point in presence or not of Gas6. **b.** IF performed on starved (-) or Gas6-stimulated siCo- or sip130Cas-silenced NL3507 cells upon 20 min of adhesion on fn. The F-actin was stained with phalloidin. **c.** Invasion assay performed on starved (-) or Gas6-stimulated SKOV3 cells stably p130Cas-silenced (shp130Cas) or transfected with a control shRNA (Mock) and then grown in Matrigel®.

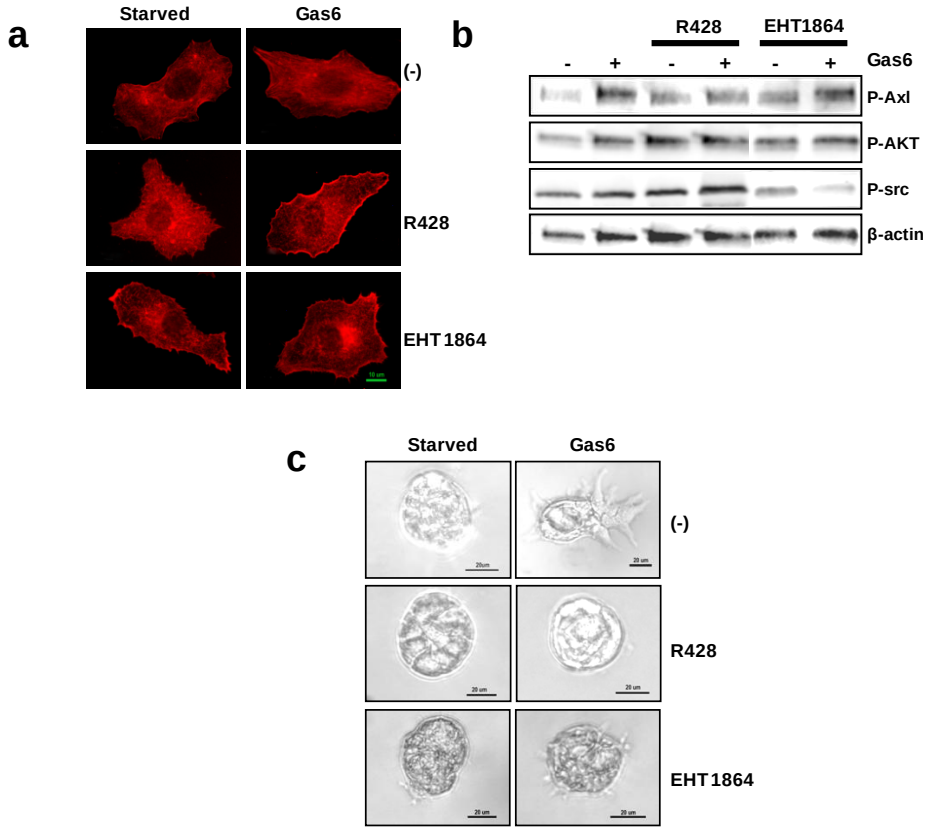

Fig.18. Gas6/Axl signaling triggered PI3K/AKT/rac activation.

a. IF performed on SKOV3 cells grown on fn, starved and then induced to migrate through a wound in presence or not of Gas6. Cells were treated with the reported inhibitors and F-actin was stained with phalloidin (red). **b.** Western blotting performed on total cell lysates from starved or Gas6-stimulated SKOV3 cells seeded on fn and treated with the reported inhibitors. A representative experiment of three performed is shown. β-actin was used as control of gel loading. **c.** Invasion assay performed on starved or Gas6-stimulated SKOV3 and NL3507 cells grown in Matrigel®. Cells were treated with the reported inhibitors.

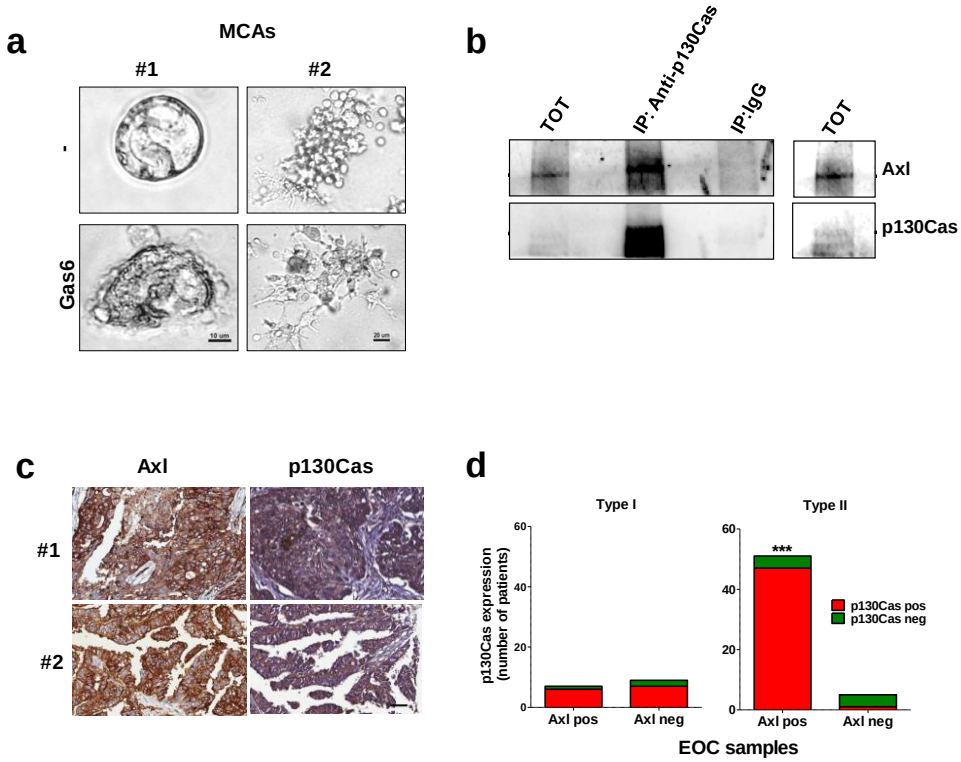

Fig.19. Validation of the Gas6/Axl signaling in *"in vivo"* EOC samples.

a. Invasion assay performed on starved (-) or Gas6-stimulated EOC MCAs from two representative Axl-positive ascites grown in matrigel. **b.** IP performed with anti-p130Cas ab on total cell lysates obtained from the EOC of patient #1. A normal mouse (IgG) serum was used as negative control. Immunoprecipitated samples were analyzed by western blotting. **c.** Representative images of anti-Axl and anti-p130Cas abs staining on FFPE EOC sections. Scale bar, 50 μm. **d.** Graph reporting the correlation between p130Cas and Axl expressions in Type I and Type II EOC. Contingency analysis was performed by Fisher's exact test, p=0,0009.

Table 1. Characteristics of the EOC samples evaluated in the present study.

Sample ID	**Histotype**	**Grading**	**FIGO[a] Stage**	**Presence of tumor cells[b]**
1	Serous	G2	III	Abundant
2	Serous	G3	III	Present
3	Mixed	G3	III	Abundant
4	Serous	G3	III	Abundant
5	Undifferentiated	Undifferentiated	III	Abundant
6	[c]	NA	III	Present
7	Serous	G2	III	Present
8	Serous	G3	III	Abundant

[a] Federation of Gynecologists and Obstetricians.

[b] The amount of cells present in ascites of EOC patients as defined

[c] Endometrial cancer with metastasis to the ovary as subsequently evaluated by the pathologist.

NA, not applicable.

Table 2. Characteristics of the EOC patients evaluated in the present study.

Sample ID	Histotype	Grading	FIGO[a] Stage	Presence of:	
				Tumor cells[b]	Mesothelial cells[b]
1	Serous	G3	IV	Abundant	Present
2	Serous	G3	IIIC	Abundant	Present
3	Serous	G3	IIIC	Abundant	Present
4	Serous	G3	III	Rare	Present
5	Serous	G3	IIIC	Abundant	Abundant
6	Serous	G3	IIIC	Present	Present
7	Serous	G3	IIIC	Rare	Abundant
8	Serous and endometroid	G3	IV	Abundant	Present
9	Serous	G3	IIIC	Abundant	Rare
10	Mullerian mixed	NA	IIIC	Present	Abundant
11	Serous	G3	IIIC	Rare	Present
12	Serous	G2	IIIC	Abundant	Present
13	Serous	G2	IIIC	Abundant	NA
14	Serous	G3	IIIC	Rare	Abundant
15	Endometroid	G3	IV	Rare	Abundant
16	Serous	G3	IIIC/IV	Present	Abundant
17	Serous	G3	IV	Abundant	Rare
18	Endometroid	NA	IIIC	Present	Abundant
19	Serous	NA	IIIC	Abundant	Rare
20	Serous	G3	IIIC	Present	Present
21	Serous	G2/G3	IIIC	Abundant	Rare
22	Serous	G3	IIIC	Abundant	Present

[a] Federation of Gynecologists and Obstetricians.

[b]The amount of cells present in ascites of EOC patients as defined by the cytopathologist at diagnosis.

Table 3. Clinicopathological characteristics of EOC biopsies evaluated by IHC with the Abs anti-Axl and –p130Cas.

Clinicopathological characteristics	Total	(%)	AXL positive cases	(%)	AXL negative cases		p130 cas positive cases	(%)	p130 cas negative cases	(%)
Tumor stage										
I	19	26.39	12	63.16	7	36.84	13	68.42	6	31.58
II	6	8.33	5	83.33	1	16.67	4	66.67	2	33.33
III	47	65.28	41	87.23	6	12.77	42	89.36	5	10.64
Tumor grade										
1	10	13.89	5	50	5	50	5	50	5	50
2	23	31.94	16	69.57	7	30.43	20	86.96	3	13.04
3	37	51.39	35	94.59	2	5.41	32	86.49	5	13.51
Undifferentiated	2	2.78	2	100	0	0	2	100	0	0
Histologic subtype										
LGEC	4	5.56	3	75	1	25	3	75	1	25
MOC	10	13.89	2	20	8	80	3	30	7	70
COC	2	2.78	2	100	0	0	2	100	0	0
HGSC	51	70.83	46	90.2	5	9.8	46	90.2	5	9.8
HGEC	3	4.17	3	100	0	0	3	100	0	0
Undifferentiated	2	2.78	2	100	0	0	2	100	0	0
Tumor Type										
Type I	16	22.22	7	43.75	9	56.25	8	50	8	50
Type II	56	77.78	51	91.07	5	8.93	51	91.07	5	8.93

References

(1) Hudson LG, Zeineldin R, Stack MS. Phenotypic plasticity of neoplastic ovarian epithelium: unique cadherin profiles in tumor progression. Clin Exp Metastasis 2008;25(6):643-55.

(2) Burridge K, Chrzanowska-Wodnicka M. Focal adhesions, contractility, and signaling. Annu Rev Cell Biol 1996;12:463-518.

(3) Guan J-L, Shalloway D. Regulation of focal adhesion-associated protein tyrosine kinase by both cellular adhesion and oncogenic transformation. Nature 1992;358:690-2.

(4) Schaller MD, Borgman CA, Cobb BS, Vines RR, Reynolds AB, Parsons JT. pp125FAK a structurally distinctive protein-tyrosine kinase associated with focal adhesions. Proc Natl Acad Sci U S A 1992;89(11):5192-6.

(5) Mitra SK, Hanson DA, Schlaepfer DD. Focal adhesion kinase: in command and control of cell motility. Nat Rev Mol Cell Biol 2005;6(1):56-68.

(6) Chen HC, Guan JL. Association of focal adhesion kinase with its potential substrate phosphatidylinositol 3-kinase. Proc Natl Acad Sci U S A 1994;91(21):10148-52.

(7) Zhang X, Chattopadhyay A, Ji QS, Owen JD, Ruest PJ, Carpenter G, et al. Focal adhesion kinase promotes phospholipase C-gamma1 activity. Proc Natl Acad Sci U S A 1999;96(16):9021-6.

(8) Schlaepfer DD, Hanks SK, Hunter T, van der GP. Integrin-mediated signal transduction linked to Ras pathway by GRB2 binding to focal adhesion kinase. Nature 1994;372(6508):786-91.

(9) Polte TR, Hanks SK. Interaction between focal adhesion kinase and Crk-associated tyrosine kinase substrate p130Cas. Proc Natl Acad Sci U S A 1995;92(23):10678-82.

(10) Ma A, Richardson A, Schaefer EM, Parsons JT. Serine phosphorylation of focal adhesion kinase in interphase and mitosis: a possible role in modulating binding to p130(Cas). Mol Biol Cell 2001;12(1):1-12.

(11) Xie Z, Sanada K, Samuels BA, Shih H, Tsai LH. Serine 732 phosphorylation of FAK by Cdk5 is important for microtubule organization, nuclear movement, and neuronal migration. Cell 2003;114(4):469-82.

(12) Yamakita Y, Totsukawa G, Yamashiro S, Fry D, Zhang X, Hanks SK, et al. Dissociation of FAK/p130(CAS)/c-Src complex during mitosis: role of mitosis-specific serine phosphorylation of FAK. J Cell Biol 1999;144(2):315-24.

(13) Bianchi M, De LS, Marin O, Turner DL, Hanks SK, Villa-Moruzzi E. Regulation of FAK Ser-722 phosphorylation and kinase activity by GSK3 and PP1 during cell spreading and migration. Biochem J 2005;391(Pt 2):359-70.

(14) Hunger-Glaser I, Fan RS, Perez-Salazar E, Rozengurt E. PDGF and FGF induce focal adhesion kinase (FAK) phosphorylation at Ser-910: dissociation from Tyr-397 phosphorylation and requirement for ERK activation. J Cell Physiol 2004;200(2):213-22.

(15) Xie Z, Tsai LH. Cdk5 phosphorylation of FAK regulates centrosome-associated miocrotubules and neuronal migration. Cell Cycle 2004;3(2):108-10.

(16) Le Boeuf F, Houle F, Sussman M, Huot J. Phosphorylation of focal adhesion kinase (FAK) on Ser732 is induced by rho-dependent kinase and is essential for proline-rich tyrosine kinase-2-mediated phosphorylation of FAK on Tyr407 in response to vascular endothelial growth factor. Mol Biol Cell 2006;17(8):3508-20.

(17) Park AY, Shen TL, Chien S, Guan JL. Role of focal adhesion kinase Ser-732 phosphorylation in centrosome function during mitosis. J Biol Chem 2009;284(14):9418-25.

(18) Daval M, Gurlo T, Costes S, Huang CJ, Butler PC. Cyclin-dependent kinase 5 promotes pancreatic beta-cell survival via Fak-Akt signaling pathways. Diabetes 2011;60(4):1186-97.

(19) Zhao J, Pestell R, Guan JL. Transcriptional activation of cyclin D1 promoter by FAK contributes to cell cycle progression. Mol Biol Cell 2001;12(12):4066-77.

(20) Kadare G, Toutant M, Formstecher E, Corvol JC, Carnaud M, Boutterin MC, et al. PIAS1-mediated sumoylation of focal adhesion kinase activates its autophosphorylation. J Biol Chem 2003;278(48):47434-40.

(21) Golubovskaya VM, Finch R, Cance WG. Direct interaction of the N-terminal domain of focal adhesion kinase with the N-terminal transactivation domain of p53. J Biol Chem 2005;280(26):25008-21.

(22) Cicchini C, Laudadio I, Citarella F, Corazzari M, Steindler C, Conigliaro A, et al. TGFbeta-induced EMT requires focal adhesion kinase (FAK) signaling. Exp Cell Res 2008;314(1):143-52.

(23) Braren R, Hu H, Kim YH, Beggs HE, Reichardt LF, Wang R. Endothelial FAK is essential for vascular network stability, cell survival, and lamellipodial formation. J Cell Biol 2006;172(1):151-62.

(24) Xia H, Nho RS, Kahm J, Kleidon J, Henke CA. Focal adhesion kinase is upstream of phosphatidylinositol 3-kinase/Akt in regulating fibroblast survival in response to contraction of type I collagen matrices via a beta 1 integrin viability signaling pathway. J Biol Chem 2004;279(31):33024-34.

(25) Deramaudt TB, Dujardin D, Noulet F, Martin S, Vauchelles R, Takeda K, et al. Altering FAK-paxillin interactions reduces adhesion, migration and invasion processes. PLoS One 2014;9(3):e92059.

(26) Tomar A, Schlaepfer DD. Focal adhesion kinase: switching between GAPs and GEFs in the regulation of cell motility. Curr Opin Cell Biol 2009;21(5):676-83.

(27) Ren XD, Kiosses WB, Sieg DJ, Otey CA, Schlaepfer DD, Schwartz MA. Focal adhesion kinase suppresses Rho activity to promote focal adhesion turnover. J Cell Sci 2000;113 (Pt 20):3673-8.

(28) Wu X, Suetsugu S, Cooper LA, Takenawa T, Guan JL. Focal adhesion kinase regulation of N-WASP subcellular localization and function. J Biol Chem 2004;279(10):9565-76.

(29) Parsons JT, Horwitz AR, Schwartz MA. Cell adhesion: integrating cytoskeletal dynamics and cellular tension. Nat Rev Mol Cell Biol 2010;11(9):633-43.

(30) Kaverina I, Rottner K, Small JV. Targeting, capture, and stabilization of microtubules at early focal adhesions. J Cell Biol 1998;142(1):181-90.

(31) Efimov A, Schiefermeier N, Grigoriev I, Ohi R, Brown MC, Turner CE, et al. Paxillin-dependent stimulation of microtubule catastrophes at focal adhesion sites. J Cell Sci 2008;121(Pt 2):196-204.

(32) Palazzo AF, Eng CH, Schlaepfer DD, Marcantonio EE, Gundersen GG. Localized stabilization of microtubules by integrin- and FAK-facilitated Rho signaling. Science 2004;303(5659):836-9.

(33) Ezratty EJ, Partridge MA, Gundersen GG. Microtubule-induced focal adhesion disassembly is mediated by dynamin and focal adhesion kinase. Nat Cell Biol 2005;7(6):581-90.

(34) Heng YW, Koh CG. Actin cytoskeleton dynamics and the cell division cycle. Int J Biochem Cell Biol 2010;42(10):1622-33.

(35) Tancioni I, Miller NL, Uryu S, Lawson C, Jean C, Chen XL, et al. FAK activity protects nucleostemin in facilitating breast cancer spheroid and tumor growth. Breast Cancer Res 2015;17(1):47.

(36) Li J, He X, Dong R, Wang Y, Yu J, Qiu H. Frequent loss of NISCH promotes tumor proliferation and invasion in ovarian cancer via inhibiting the FAK signal pathway. Mol Cancer Ther 2015.

(37) Ucar DA, Kurenova E, Garrett TJ, Cance WG, Nyberg C, Cox A, et al. Disruption of the protein interaction between FAK and IGF-1R inhibits melanoma tumor growth. Cell Cycle 2012;11(17):3250-9.

(38) Lahlou H, Sanguin-Gendreau V, Frame MC, Muller WJ. Focal adhesion kinase contributes to proliferative potential of ErbB2 mammary tumour cells but is dispensable for ErbB2 mammary tumour induction in vivo. Breast Cancer Res 2012;14(1):R36.

(39) Shibue T, Weinberg RA. Integrin beta1-focal adhesion kinase signaling directs the proliferation of metastatic cancer cells disseminated in the lungs. Proc Natl Acad Sci U S A 2009;106(25):10290-5.

(40) Ding Q, Grammer JR, Nelson MA, Guan JL, Stewart JE, Jr., Gladson CL. p27Kip1 and cyclin D1 are necessary for focal adhesion kinase regulation of cell cycle progression in glioblastoma cells propagated in vitro and in vivo in the scid mouse brain. J Biol Chem 2005;280(8):6802-15.

(41) Duxbury MS, Ito H, Zinner MJ, Ashley SW, Whang EE. Focal adhesion kinase gene silencing promotes anoikis and suppresses metastasis of human pancreatic adenocarcinoma cells. Surgery 2004;135(5):555-62.

(42) Sood AK, rmaiz-Pena GN, Halder J, Nick AM, Stone RL, Hu W, et al. Adrenergic modulation of focal adhesion kinase protects human ovarian cancer cells from anoikis. J Clin Invest 2010;120(5):1515-23.

(43) Wu X, Gan B, Yoo Y, Guan JL. FAK-mediated src phosphorylation of endophilin A2 inhibits endocytosis of MT1-MMP and promotes ECM degradation. Dev Cell 2005;9(2):185-96.

(44) Wang Y, McNiven MA. Invasive matrix degradation at focal adhesions occurs via protease recruitment by a FAK-p130Cas complex. J Cell Biol 2012;196(3):375-85.

(45) Chen JS, Huang XH, Wang Q, Huang JQ, Zhang LJ, Chen XL, et al. Sonic hedgehog signaling pathway induces cell migration and invasion through focal adhesion kinase/AKT signaling-mediated activation of matrix metalloproteinase (MMP)-2 and MMP-9 in liver cancer. Carcinogenesis 2013;34(1):10-9.

(46) Sulzmaier FJ, Jean C, Schlaepfer DD. FAK in cancer: mechanistic findings and clinical applications. Nat Rev Cancer 2014;14(9):598-610.

(47) Lemmon MA, Schlessinger J. Cell signaling by receptor tyrosine kinases. Cell 2010;141(7):1117-34.

(48) Citri A, Yarden Y. EGF-ERBB signalling: towards the systems level. Nat Rev Mol Cell Biol 2006;7(7):505-16.

(49) Seshacharyulu P, Ponnusamy MP, Haridas D, Jain M, Ganti AK, Batra SK. Targeting the EGFR signaling pathway in cancer therapy. Expert Opin Ther Targets 2012;16(1):15-31.

(50) Siwak DR, Carey M, Hennessy BT, Nguyen CT, McGahren Murray MJ, Nolden L, et al. Targeting the epidermal growth factor receptor in epithelial ovarian cancer: current knowledge and future challenges. J Oncol 2010;2010:568938.

(51) Lemmon MA, Schlessinger J. Cell signaling by receptor tyrosine kinases. Cell 2010;141(7):1117-34.

(52) Normanno N, De LA, Bianco C, Strizzi L, Mancino M, Maiello MR, et al. Epidermal growth factor receptor (EGFR) signaling in cancer. Gene 2006;366(1):2-16.

(53) Stewart EL, Tan SZ, Liu G, Tsao MS. Known and putative mechanisms of resistance to EGFR targeted therapies in NSCLC patients with EGFR mutations-a review. Transl Lung Cancer Res 2015;4(1):67-81.

(54) Lafky JM, Wilken JA, Baron AT, Maihle NJ. Clinical implications of the ErbB/epidermal growth factor (EGF) receptor family and its ligands in ovarian cancer. Biochim Biophys Acta 2008;1785(2):232-65.

(55) Vermeij J, Teugels E, Bourgain C, Xiangming J, in ', V, Ghislain V, et al. Genomic activation of the EGFR and HER2-neu genes in a significant proportion of invasive epithelial ovarian cancers. BMC Cancer 2008;8:3.

(56) Lassus H, Sihto H, Leminen A, Joensuu H, Isola J, Nupponen NN, et al. Gene amplification, mutation, and protein expression of EGFR and mutations of ERBB2 in serous ovarian carcinoma. J Mol Med (Berl) 2006;84(8):671-81.

(57) Stitt TN, Conn G, Gore M, Lai C, Bruno J, Radziejewski C, et al. The anticoagulation factor protein S and its relative, Gas6, are ligands for the Tyro 3/Axl family of receptor tyrosine kinases. Cell 1995;80(4):661-70.

(58) Verma A, Warner SL, Vankayalapati H, Bearss DJ, Sharma S. Targeting Axl and Mer kinases in cancer. Mol Cancer Ther 2011;10(10):1763-73.

(59) Korshunov VA. Axl-dependent signalling: a clinical update. Clin Sci (Lond) 2012;122(8):361-8.

(60) Hasanbasic I, Cuerquis J, Varnum B, Blostein MD. Intracellular signaling pathways involved in Gas6-Axl-mediated survival of endothelial cells. Am J Physiol Heart Circ Physiol 2004;287(3):H1207-H1213.

(61) McCarty JH. The Nck SH2/SH3 adaptor protein: a regulator of multiple intracellular signal transduction events. Bioessays 1998;20(11):913-21.

(62) Gallicchio M, Mitola S, Valdembri D, Fantozzi R, Varnum B, Avanzi GC, et al. Inhibition of vascular endothelial growth factor receptor 2-mediated endothelial cell activation by Axl tyrosine kinase receptor. Blood 2005;105(5):1970-6.

(63) Rothlin CV, Ghosh S, Zuniga EI, Oldstone MB, Lemke G. TAM receptors are pleiotropic inhibitors of the innate immune response. Cell 2007;131(6):1124-36.

(64) Asiedu MK, Beauchamp-Perez FD, Ingle JN, Behrens MD, Radisky DC, Knutson KL. AXL induces epithelial-to-mesenchymal transition and regulates the function of breast cancer stem cells. Oncogene 2014;33(10):1316-24.

(65) Paccez JD, Vogelsang M, Parker MI, Zerbini LF. The receptor tyrosine kinase Axl in cancer: biological functions and therapeutic implications. Int J Cancer 2014;134(5):1024-33.

(66) Sensi M, Catani M, Castellano G, Nicolini G, Alciato F, Tragni G, et al. Human cutaneous melanomas lacking MITF and melanocyte differentiation antigens express a functional Axl receptor kinase. J Invest Dermatol 2011;131(12):2448-57.

(67) Sun W, Fujimoto J, Tamaya T. Coexpression of Gas6/Axl in human ovarian cancers. Oncology 2004;66(6):450-7.

(68) Rankin EB, Fuh KC, Taylor TE, Krieg AJ, Musser M, Yuan J, et al. AXL is an essential factor and therapeutic target for metastatic ovarian cancer. Cancer Res 2010;70(19):7570-9.

(69) Macleod K, Mullen P, Sewell J, Rabiasz G, Lawrie S, Miller E, et al. Altered ErbB receptor signaling and gene expression in cisplatin-resistant ovarian cancer. Cancer Res 2005;65(15):6789-800.

(70) Phillips-Mason PJ, Craig SE, Brady-Kalnay SM. Should I stay or should I go? Shedding of RPTPs in cancer cells switches signals from stabilizing cell-cell adhesion to driving cell migration. Cell Adh Migr 2011;5(4):298-305.

(71) Baum B, Georgiou M. Dynamics of adherens junctions in epithelial establishment, maintenance, and remodeling. J Cell Biol 2011;192(6):907-17.

(72) Andl CD, Rustgi AK. No one-way street: cross-talk between e-cadherin and receptor tyrosine kinase (RTK) signaling: a mechanism to regulate RTK activity. Cancer Biol Ther 2005;4(1):28-31.

(73) Berx G, Van Roy F. Involvement of members of the cadherin superfamily in cancer. Cold Spring Harb Perspect Biol 2009;1(6):a003129.

(74) Qian X, Karpova T, Sheppard AM, McNally J, Lowy DR. E-cadherin-mediated adhesion inhibits ligand-dependent activation of diverse receptor tyrosine kinases. EMBO J 2004;23(8):1739-48.

(75) Xin HW, Yang JH, Nguyen DM. Sensitivity to epidermal growth factor receptor tyrosine kinase inhibitor requires E-cadherin in esophageal cancer and malignant pleural mesothelioma. Anticancer Res 2013;33(6):2401-8.

(76) Desgrosellier JS, Cheresh DA. Integrins in cancer: biological implications and therapeutic opportunities. Nat Rev Cancer 2010;10(1):9-22.

(77) Guo W, Pylayeva Y, Pepe A, Yoshioka T, Muller WJ, Inghirami G, et al. Beta 4 integrin amplifies ErbB2 signaling to promote mammary tumorigenesis. Cell 2006;126(3):489-502.

(78) Ricono JM, Huang M, Barnes LA, Lau SK, Weis SM, Schlaepfer DD, et al. Specific cross-talk between epidermal growth factor receptor and integrin alphavbeta5 promotes carcinoma cell invasion and metastasis. Cancer Res 2009;69(4):1383-91.

(79) Bertotti A, Comoglio PM, Trusolino L. Beta4 integrin activates a Shp2-Src signaling pathway that sustains HGF-induced anchorage-independent growth. J Cell Biol 2006;175(6):993-1003.

(80) Bast RC, Jr., Hennessy B, Mills GB. The biology of ovarian cancer: new opportunities for translation. Nat Rev Cancer 2009;9(6):415-28.

(81) Morice P, Uzan C, Fauvet R, Gouy S, Duvillard P, Darai E. Borderline ovarian tumour: pathological diagnostic dilemma and risk factors for invasive or lethal recurrence. Lancet Oncol 2012;13(3):e103-e115.

(82) Kurman RJ, Shih I. Molecular pathogenesis and extraovarian origin of epithelial ovarian cancer--shifting the paradigm. Hum Pathol 2011;42(7):918-31.

(83) Kenny HA, Krausz T, Yamada SD, Lengyel E. Use of a novel 3D culture model to elucidate the role of mesothelial cells, fibroblasts and extra-cellular matrices on adhesion and invasion of ovarian cancer cells to the omentum. Int J Cancer 2007;121(7):1463-72.

(84) Ahmed N, Thompson EW, Quinn MA. Epithelial-mesenchymal interconversions in normal ovarian surface epithelium and ovarian carcinomas: an exception to the norm. J Cell Physiol 2007;213(3):581-8.

(85) Tomassetti A, De Santis G, Castellano G, Miotti S, Mazzi M, Tomasoni D, et al. Variant HNF1 Modulates Epithelial Plasticity of Normal and Transformed Ovary Cells. Neoplasia 2008;10(12):1481-92.

(86) Strauss R, Li ZY, Liu Y, Beyer I, Persson J, Sova P, et al. Analysis of epithelial and mesenchymal markers in ovarian cancer reveals phenotypic heterogeneity and plasticity. PLoS One 2011;6(1):e16186.

(87) Davidson B, Gotlieb WH, Ben-Baruch G, Nesland JM, Bryne M, Goldberg I, et al. E-Cadherin complex protein expression and survival in ovarian carcinoma. Gynecol Oncol 2000;79(3):362-71.

(88) De Santis G, Miotti S, Mazzi M, Canevari S, Tomassetti A. E-cadherin directly contributes to PI3K/AKT activation by engaging the

PI3K-p85 regulatory subunit to adherens junctions of ovarian carcinoma cells. Oncogene 2009;28(9):1206-17.

(89) Davidowitz RA, Iwanicki MP, Brugge JS. In vitro mesothelial clearance assay that models the early steps of ovarian cancer metastasis. J Vis Exp 2012;(60).

(90) Davidowitz RA, Selfors LM, Iwanicki MP, Elias KM, Karst A, Piao H, et al. Mesenchymal gene program-expressing ovarian cancer spheroids exhibit enhanced mesothelial clearance. J Clin Invest 2014.

(91) Schaller MD, Borgman CA, Parsons JT. Autonomous expression of a noncatalytic domain of the focal adhesion-associated protein tyrosine kinase pp125^{FAK}. Mol Cell Biol 1993;13:785-91.

(92) Juan G, Traganos F, James WM, Ray JM, Roberge M, Sauve DM, et al. Histone H3 phosphorylation and expression of cyclins A and B1 measured in individual cells during their progression through G2 and mitosis. Cytometry 1998;32(2):71-7.

(93) Laan L, Pavin N, Husson J, Romet-Lemonne G, van DM, Lopez MP, et al. Cortical dynein controls microtubule dynamics to generate pulling forces that position microtubule asters. Cell 2012;148(3):502-14.

(94) Lopes JP, Agostinho P. Cdk5: multitasking between physiological and pathological conditions. Prog Neurobiol 2011;94(1):49-63.

(95) Meijer L, Borgne A, Mulner O, Chong JP, Blow JJ, Inagaki N, et al. Biochemical and cellular effects of roscovitine, a potent and selective inhibitor of the cyclin-dependent kinases cdc2, cdk2 and cdk5. Eur J Biochem 1997;243(1-2):527-36.

(96) Harada T, Morooka T, Ogawa S, Nishida E. ERK induces p35, a neuron-specific activator of Cdk5, through induction of Egr1. Nat Cell Biol 2001;3(5):453-9.

(97) Barbolina MV, Moss NM, Westfall SD, Liu Y, Burkhalter RJ, Marga F, et al. Microenvironmental regulation of ovarian cancer metastasis. Cancer Treat Res 2009;149:319-34.

(98) Wu C, Cipollone J, Maines-Bandiera S, Tan C, Karsan A, Auersperg N, et al. The morphogenic function of E-cadherin-mediated adherens junctions in epithelial ovarian carcinoma formation and progression. Differentiation 2008;76(2):193-205.

(99) Rea K, Sensi M, Anichini A, Canevari S, Tomassetti A. EGFR/MEK/ERK/CDK5-dependent integrin-independent FAK phosphorylated on serine 732 contributes to microtubule depolymerization and mitosis in tumor cells. Cell Death Dis 2013;4:e815.

(100) Dhavan R, Tsai LH. A decade of CDK5. Nat Rev Mol Cell Biol 2001;2(10):749-59.

(101) Smith DS, Greer PL, Tsai LH. Cdk5 on the brain. Cell Growth Differ 2001;12(6):277-83.

(102) Arif A. Extraneuronal activities and regulatory mechanisms of the atypical cyclin-dependent kinase Cdk5. Biochem Pharmacol 2012;84(8):985-93.

(103) Koenig A, Mueller C, Hasel C, Adler G, Menke A. Collagen type I induces disruption of E-cadherin-mediated cell-cell contacts and promotes proliferation of pancreatic carcinoma cells. Cancer Res 2006;66(9):4662-71.

(104) Li XY, Zhou X, Rowe RG, Hu Y, Schlaepfer DD, Ilic D, et al. Snail1 controls epithelial-mesenchymal lineage commitment in focal adhesion kinase-null embryonic cells. J Cell Biol 2011;195(5):729-38.

(105) Canel M, Serrels A, Miller D, Timpson P, Serrels B, Frame MC, et al. Quantitative in vivo imaging of the effects of inhibiting integrin signaling via Src and FAK on cancer cell movement: effects on E-cadherin dynamics. Cancer Res 2010;70(22):9413-22.

(106) Arpitha P, Gao CY, Tripathi BK, Saravanamuthu S, Zelenka P. Cyclin-dependent kinase 5 promotes the stability of corneal epithelial cell junctions. Mol Vis 2013;19:319-32.

(107) Kenny HA, Chiang CY, White EA, Schryver EM, Habis M, Romero IL, et al. Mesothelial cells promote early ovarian cancer metastasis through fibronectin secretion. J Clin Invest 2014;124(10):4614-28.

(108) Kenny HA, Lengyel E. MMP-2 functions as an early response protein in ovarian cancer metastasis. Cell Cycle 2009;8(5):683-8.

(109) Kalluri R, Weinberg RA. The basics of epithelial-mesenchymal transition. J Clin Invest 2009;119(6):1420-8.

(110) Lee CH, Liu SY, Chou KC, Yeh CT, Shiah SG, Huang RY, et al. Tumor-associated macrophages promote oral cancer progression through activation of the Axl signaling pathway. Ann Surg Oncol 2014;21(3):1031-7.

(111) Valverde P, Obin MS, Taylor A. Role of Gas6/Axl signaling in lens epithelial cell proliferation and survival. Exp Eye Res 2004;78(1):27-37.

(112) Sainaghi PP, Castello L, Bergamasco L, Galletti M, Bellosta P, Avanzi GC. Gas6 induces proliferation in prostate carcinoma cell lines expressing the Axl receptor. J Cell Physiol 2005;204(1):36-44.

(113) Dunne PD, McArt DG, Blayney JK, Kalimutho M, Greer S, Wang T, et al. AXL is a key regulator of inherent and chemotherapy-induced invasion and predicts a poor clinical outcome in early-stage colon cancer. Clin Cancer Res 2014;20(1):164-75.

(114) Defilippi P, Di SP, Cabodi S. p130Cas: a versatile scaffold in signaling networks. Trends Cell Biol 2006;16(5):257-63.

(115) Nick AM, Stone RL, rmaiz-Pena G, Ozpolat B, Tekedereli I, Graybill WS, et al. Silencing of p130cas in ovarian carcinoma: a novel mechanism for tumor cell death. J Natl Cancer Inst 2011;103(21):1596-612.

(116) Van SS, Grijelmo C, De WO, Bruyneel E, Emami S, Gespach C, et al. Activation of the FAK-src molecular scaffolds and p130Cas-JNK signaling cascades by alpha1-integrins during colon cancer cell invasion. Int J Oncol 2007;31(6):1501-8.

Acknowledgements

I would like to express my gratitude to my supervisor, Dr. Antonella Tomassetti, for her expertise, understanding and huge support during my PhD project. I would like to thank Dr. Silvana Canevari for her helpful scientific suggestions. Many thanks to Anna Granata and Alessandro Satta for their friendship and support during these three years of PhD school. I would like to thank Alessandro Satta and Francesco Caroli for their valuable technical helps. I'm sincerely grateful to all my colleagues for their constructive suggestions and friendly help during these years. I would like to thank Chiara Alberti who has been a valuable colleague in the past and now a wonderful friend. Lastly and most importantly, I would like to thank my family for their loving encouragements. In particular I thank my little son, Samuel, who has pleased my days with his beautiful smile. To him I dedicate my thesis.

PART II-PUBLISHED PAPER

OPEN

Citation: Cell Death and Disease (2013) 4, e815; doi:10.1038/cddis.2013.353

www.nature.com/cddis

EGFR/MEK/ERK/CDK5-dependent integrin-independent FAK phosphorylated on serine 732 contributes to microtubule depolymerization and mitosis in tumor cells

K Rea[1], M Sensi[2], A Anichini[2], S Canevari*[,1] and A Tomassetti*[,1]

FAK is a non-receptor tyrosine kinase contributing to migration and proliferation downstream of integrin and/or growth factor receptor signaling of normal and malignant cells. In addition to well-characterized tyrosine phosphorylations, FAK is phosphorylated on several serines, whose role is not yet clarified. We observed that phosphorylated FAK on serine 732 (P-FAKSer732) is present at variable levels *in vitro*, in several melanoma, ovarian and thyroid tumor cell lines and *in vivo*, in tumor cells present in fresh ovarian cancer ascites. *In vitro* P-FAKSer732 was barely detectable during interphase while its levels strongly increased in mitotic cells upon activation of the EGFR/MEK/ERK axis in an integrin-independent manner. P-FAKSer732 presence was crucial for the maintenance of the proliferation rate and its levels were inversely related to the levels of acetylated α-tubulin. P-FAKSer732 localized at the microtubules (MTs) of the spindle, biochemically associated with MTs and contributed to MT depolymerization. The lack of the phosphorylation on Ser732 as well as the inhibition of CDK5 activity by roscovitine impaired mitotic spindle assembly and correct chromosome alignment during mitosis. We also identified, for the first time, that the EGF-dependent EGFR activation led to increased P-FAKSer732 and polymerized MTs. Our data shed light on the multifunctional roles of FAK in neoplastic cells, being involved not only in integrin-dependent migratory signaling but also in integrin-independent MT dynamics and mitosis control. These findings provide a new potential target for inhibiting the growth of tumor cells in which the EGFR/MEK/ERK/CDK5 pathway is active.

Cell Death and Disease (2013) **4,** e815; doi:10.1038/cddis.2013.353; published online 3 October 2013
Subject Category: Cancer

FAK, a ubiquitously expressed non-receptor tyrosine protein kinase, has a key role in regulating signals at sites of cell extracellular matrix adhesion through integrins and at activated growth factor receptors.[1] Integrin-dependent activated FAK is recruited to focal adhesions (FAs) and promotes dynamic actin and adhesion changes at the membrane and signaling to proliferation and to survival pathways. FAK expression is required for many normal cellular functions in development and angiogenesis,[2,3] and its expression is upregulated in a variety of late-stage cancers.[4] Through different molecular connections, FAK can influence cell movement regulating cytoskeleton remodeling, FA turnover and membrane protrusions.[1] FAK also seems to affect cell proliferation by regulating cell cycle progression from G1 to S phases by increasing the expression of cyclin D1.[5,6] For all these reasons, FAK expression and activation has been linked to cell transformation and metastasis.

The overall molecular structure of FAK is also consistent with its function as a protein scaffold. The amino-terminal tyrosine (Tyr) 397 residue of FAK, whose autophosphorylation leads to full FAK activation, creates a high-affinity binding site recognized by the SH2 domain of the Src family.[7] Src binding promotes FAK phosphorylation within the kinase domain activation loop at Tyr576 and Tyr577, which are necessary for maximal FAK-associated activity.[1] The carboxyl-terminal domain FAK-related non-kinase (FRNK) is a truncated isoform of FAK expressed in selected cellular types.[8] FRNK lacks the Tyr397, thus acting as a dominant negative isoform of FAK. FRNK inhibits both integrin- and growth factor-induced FAK activation and blocks FAK-mediated cell migration and proliferation.[9]

The COOH-terminal domain of FAK undergoes several serine (Ser) phosphorylation events whose role is not well understood. In neocortical neurons, phosphorylation of FAK at Ser732 (P-FAKSer732), by the post-mitotic

[1]Unit of Molecular Therapies, Department of Experimental Oncology and Molecular Medicine, Fondazione IRCCS Istituto Nazionale dei Tumori, 20133 Milan, Italy and [2]Unit of Immunobiology of Human Tumors, Department of Experimental Oncology and Molecular Medicine, Fondazione IRCCS Istituto Nazionale dei Tumori, 20133 Milan, Italy
*Corresponding authors: S Canevari or A Tomassetti, Unit of Molecular Therapies, Fondazione IRCCS Istituto Nazionale dei Tumori, Via Amadeo, 42, 20133 Milan, Italy. Tel: +39 022 390 2567; Fax: +39 022 390 3073; E-mail: silvana.canevari@istitutotumori.mi.it or Tel: +39 022 390 2568; Fax: +39 022 390 3073; E-mail: antonella.tomassetti@istitutotumori.mi.it
Keywords: FAK; microtubules; mitosis; EGFR; CDK5
Abbreviations: Ab, antibody; ac-α-tubulin, acetylated α-tubulin; CDK, cyclin-dependent kinase; EC, endothelial cell; FA, focal adhesion; FRNK, FAK-related non kinase; IF, immunofluorescence; IP, immunoprecipitation; MAb, monoclonal antibody; MT, microtubule; Mut, mutated; o.n., overnight; ROCK, Rho-associated protein kinase; Ser, serine; Tyr, tyrosine; wt, wild type
Received 15.5.13; revised 06.8.13; accepted 09.8.13; Edited by G Raschellá

cyclin-dependent kinase (CDK) 5, regulates microtubule (MT) stability and migration by pulling the proximal region of the nucleus into the leading process, likely in the direction of the centrosome.[10,11] In endothelial cells (ECs), P-FAKSer732, phosphorylated by Rho-associated protein kinase (ROCK),[12] has been found co-localized with γ-tubulin at the centrosomes; deletion of FAK in primary ECs causes an increase in centrosome numbers, and multipolar and disorganized spindles.[13]

P-FAKSer732 has been characterized mainly in normal cells.[10,12,13] Here, we aimed to analyze in detail the presence and the role of P-FAKSer732 in tumor cells.

Results

P-FAKSer732 is detected in tumor cells and is not localized at the FAs during migration. The presence of P-FAKSer732 was analyzed together with that of -Tyr576, the site responsible for maximal FAK activity, in melanoma, ovarian and thyroid cancer cells. Basically, in all cell lines the expression of FAK was also associated with the presence of P-FAKSer732 and -Tyr576, although at variable levels (Figure 1a). FAK was mainly phosphorylated on Ser732 in Me#21 and #25. High expression of FAK, P-FAKSer732 and -Tyr576 was also observed in Me#20, a primary tumor

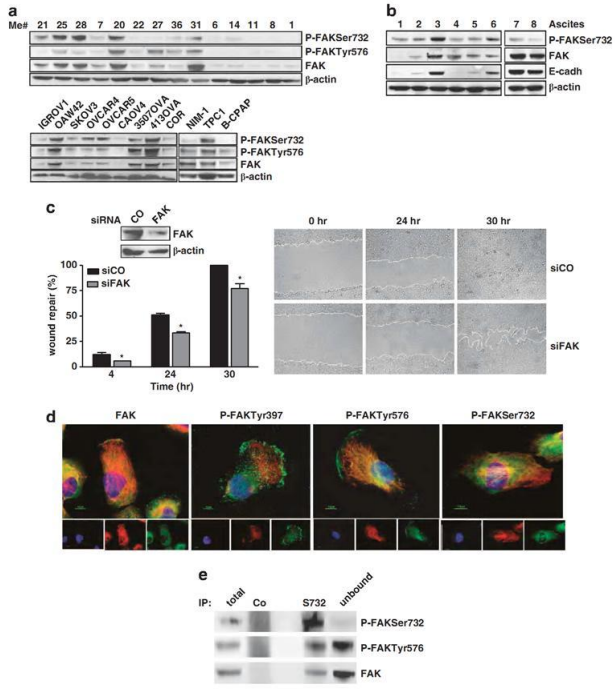

Figure 1 P-FAKSer732 is detected in tumor cells and is not localized at the FAs during migration. (**a**) Western blot analysis on total cell lysates from melanoma ($n=14$), ovarian ($n=9$) and thyroid ($n=3$) cancer cell lines. (**b**) Western blot analysis on total cell lysates from cells of ovarian cancer ascites ($n=8$). The presence in the ascites of tumor cells was evaluated by using the epithelial adhesion marker e-cadherin (cadh). (**c**) Wound-healing assay performed on control- (CO) or FAK- (FAK) silenced (Me)#28 cells. Left panel: western blotting showing the level of FAK silencing and the wound-healing repair capability at 4, 24 and 30 h from the scratch. Asterisks indicate statistically significant values ($P\leq 0.01$). Error bar, S.D. Right panel: representative images showing the wounds at the starting point ($t=0$ h), after 24 h and the wounds closure at the end of the experiment ($t=30$ h). Immunoblottings were performed with Abs against the proteins reported on the right. β-actin was used as control of gel loading. (**d**) IF performed on starved Me#28 cells induced to migrate though a wound. Cells were stained for P-FAKSer732, -Tyr 397, -Tyr 576, FAK (green) and α-tubulin (red). Nuclei were stained with DAPI (blue). Merged images are reported on the upper panels. (**e**) IP on Me#28 lysates with normal rabbit serum (CO) or anti-P-FAKSer732 (S732). Immunoprecipitated samples were analyzed by western blotting. Immunoblottings were performed with Abs against the proteins reported on the right

and in Me#31, a visceral metastases. All these melanoma cell lines, which also express the highest levels of FAK, belong to a subset of melanomas lacking the melanocyte transcription factor MITF and melanoma differentiation antigens.[14] Three out of eight ovarian carcinomas and one out of three thyroid cell lines expressed FAK, P-FAKSer732 and -Tyr576 at high levels. In the lysates from tumor cells contained in fresh ascites from advanced stage ovarian cancer (Supplementary Table S1), FAK was also found phosphorylated on Ser732 (Figure 1b), indicating that this phosphorylation is not restricted to cells cultured *in vitro*.

The melanoma Me#28 cell line was further characterized, and, for selected experiments, the ovarian carcinoma OAW42 and the thyroid carcinoma NIM-1 cell lines were also analyzed.

In tumor cells, FAK regulates cell motility by directing cell migration. During migration, phosphorylated FAK at tyrosine residues localizes at the FAs and/or at the front and the rear of the cells.[1] Indeed, transient knockdown of FAK through specific siRNA in Me#28 cells induced a statistically significant decrease of wound repair compared with cells transfected with a non-silencing siRNA both at 24 h and at 30 h (Figure 1c), when the latter had completely repaired the wound. Immunofluorescence (IF) was used to analyze the localization of FAK phosphorylated isoforms in Me#28 cells migrating into the wound. P-FAKSer732 localized in the cytoplasm and in a perinuclear region but not at FAs (Figure 1d), whereas both P-FAKTyr397 and -Tyr576 were detected in the cytoplasm and at FAs of the leading edge. In addition, western blot analysis of Me#28 samples following immunoprecipitation (IP) with anti-P-FAKSer732 antibody (Ab) indicated that the principal form in the immunoprecipitate consisted of FAK phosphorylated on Ser732 (Figure 1e), whereas the dominant form in the unbound fraction contained mainly P-FAKTyr576.

These results demonstrate that FAK exists as two distinct pools: the first associated with FAs and the second, phosphorylated on Ser732, localized in the cytoplasm in a perinuclear region.

FAK is phosphorylated at Ser732 independently from integrin engagement. To investigate whether the Ser732 phosphorylation was consequent to that at Tyr397, Me#28 cells were stably transfected with FRNK construct and the FRNK-expressing clone F6 was selected by western blotting (Figure 2a). Fetal calf serum (FCS) stimulation of Me#28

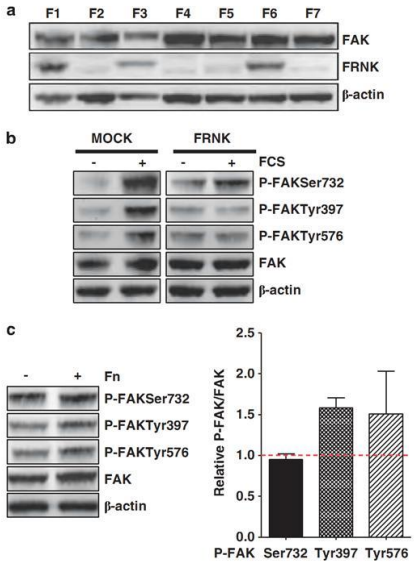

Figure 2 FAK is phosphorylated at Ser732 independently from integrin engagement. (**a**) Western blot analysis on total cell lysates of the clones obtained from FRNK-transfected (Me)#28. The clone F6, expressing the highest levels of FRNK protein, was selected for the experiment reported on panel b. (**b**) Western blotting on total lysates from Mock- or FRNK-transfected (clone F6) Me#28 cells. β-actin was used as control of gel loading. (**c**) Left panel: western blotting performed on lysates from starved Me#28 cells grown on plastic ($-$) or fibronectin (Fn) ($+$). β-actin was used as control of gel loading. Right panel: densitometric analysis reporting the levels of FAK phosphorylated isoforms respect to total FAK expression of cells grown on Fn. The mean values of five experiments are reported

cells transfected with FRNK construct (clone F6) led to increased phosphorylation of FAK only at Ser732, whereas mock-transfected cells showed also increased P-FAKTyr397 and -Tyr576 (Figure 2b).

To assess whether the phosphorylation at Ser732 was dependent on integrin engagement and activation, Me#28 cells were grown in absence of FCS for 24 h on plastic or fibronectin. Western blotting on cell lysates showed that P-FAKSer732 was not increased in cells grown onto fibronectin (Figure 2c), while P-FAKTyr397 and -Tyr576 increased, as expected, in cells grown on fibronectin indicating that P-FAKSer732 is not a downstream effector of integrin activation.

These results indicate that phosphorylation at Ser732 is independent of FAK autophosphorylation at Tyr397, while the latter is necessary for phosphorylation at Tyr576 upon integrin engagement, as already demonstrated.[15]

P-FAKSer732 accumulates in mitotic cells and co-localizes with MTs of the mitotic spindle. Then, we asked whether proliferative stimuli could induce P-FAKSer732. Indeed, FCS stimulation of starved Me#28, OAW42 and NIM-1 cell lines, induced, in all of them, increased levels of P-FAKSer732 (Figure 3a) that highly accumulated, as shown by IF in Figure 3b, in mitotic cells. In cells in interphase, P-FAKSer732 did not accumulate and was located in the cytoplasm, as already shown in Figure 1e.

Confocal IF was performed to better investigate on P-FAKSer732 localization in dividing Me#28 cells. P-FAKSer732 co-localized with α-tubulin at the mitotic spindle during metaphase (Figure 3c, left panel). During late anaphase, P-FAKSer732 co-localized with α-tubulin at the spindle, likely at the sites where MTs elongate and shrink (Figure 3c, middle panel), and accumulated in the middle of the spindle, indicating an interaction with the cortical actin.

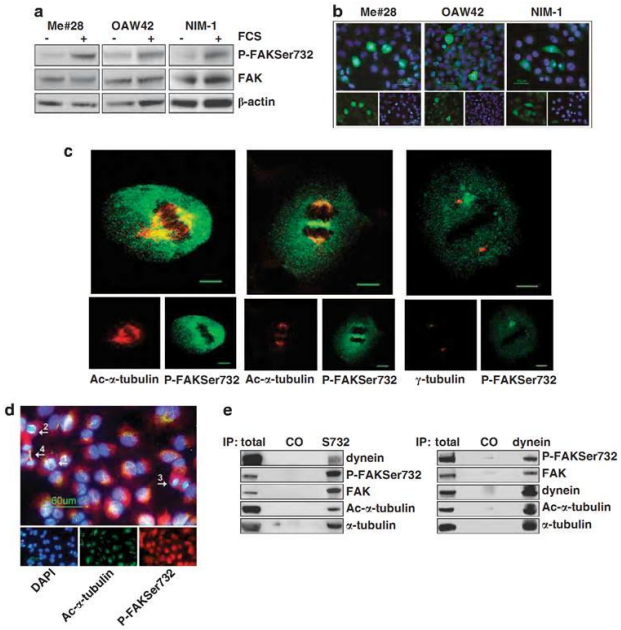

Figure 3 P-FAKSer732 accumulates in mitotic cells and co-localizes with MTs of the mitotic spindle. (**a**) Western blotting on total lysates from starved or FCS-stimulated cells. (**b**) IF performed on fixed cells upon FCS stimulation with anti-P-FAKSer732 Ab (green). Nuclei were stained with DAPI (blue). (**c**) Confocal IF performed on fixed Me#28 cells with anti-P-FAKSer732 and ac-α- (left and middle panels) or γ-tubulin Abs (right panel). Images of metaphases (left and right panels, section 14 and 12, respectively) and late anaphase (section 11, middle panel) are shown. Bars, 10 μm. (**d**) IF performed on Me#28 cells upon extraction of free tubulin with PEM buffer (see Materials and Methods). The white arrows indicate the mitotic phases: 1, prophase; 2 anaphase; 3, telophase; 4, cytokinesis. The immunostaining was performed with anti-P-FAKSer732 (red) and ac-α-tubulin (green). Nuclei were stained with DAPI (blue). Bars, 60 μm. (**e**) IP on lysates from Me#28 cells with anti-P-FAKSer732 (S732) and -dynein intermediate chain Abs. Immunoprecipitated fractions were analyzed by western blotting. Normal rabbit or mouse sera were used as negative control (CO). For immunoblottings, Abs are reported on the right

Anti-P-FAKSer732 also diffusely stained the cell cytoplasm, but no co-localization with γ-tubulin at the centrosome was observed (Figure 3c, right panel).

Furthermore, P-FAKSer732 co-localized with ac-α-tubulin of the spindle in all mitotic phases upon extraction of soluble tubulin (Figure 3d).

The MT motor protein dynein regulates MT dynamics and cortical pulling forces at the spindle poles.[16] To biochemically analyze the possible association between FAK, observed mainly at the MTs of the spindle, and dynein, an IP was performed on Me#28 lysates with anti-P-FAKSer732 and -dynein intermediate light chain Abs. Anti-P-FAKSer732 co-immunoprecipitated with both ac-α-tubulin and dynein (Figure 3e, left panel). Accordingly, anti-dynein Ab co-immunoprecipitated with FAK phosphorylated on Ser732 as well as with ac-α-tubulin (Figure 3e, right panel).

Therefore, P-FAKSer732 associates with polymerized MTs of the spindle during all mitotic stages and is biochemically linked to dynein arguing for the notion of a role during mitosis.

FAK contributes to cell proliferation when it is phosphorylated at Ser732. To assess a role of P-FAKSer732 in proliferation, Me#28 cells were treated with a specific siRNA against FAK and growth capability was assayed. The growth rate of melanoma cells decreased 25% after 48 h and up to 40% after 72 h (Figure 4a). Furthermore, phosphorylation on Ser10 of Histone H3 (herein named PHH3), a marker of mitosis,[17] was 30% lower in FAK-silenced cells in comparison with cells transfected with a control siRNA (Figure 4b), suggesting a role of FAK in the control of the mitosis.

To specifically assess a role of P-FAKSer732 in cell proliferation, we transiently transfected, in control or FAK-silenced Me#28 cells, a GFP construct alone, or containing the wild-type (wt) GFP-FAK or a mutated FAK on Ser732→Ala[10] (herein named Mut GFP-FAK). Control silenced cells transfected with Mut GFP-FAK displayed a 53% growth rate reduction in comparison with those transfected with wt GFP-FAK (Figure 4c). Growth reduction reached 70% when Mut GFP-FAK was transfected into FAK-silenced cells. The re-expression of wt GFP-FAK in FAK-silenced cells was not able to return proliferation to that observed in control-siRNA-treated cells although a 30% increase was observed respect to siFAK-treated cells transfected with GFP only. These data argue for the hypothesis that a delicate balance between total FAK and P-FAKSer732 is necessary to maintain the correct growth rate.

The above reported results were further confirmed by western blotting of cell lysates from the transfectants described above. Both wt and Mut GFP-FAK-transfected cells showed a decrease of PHH3 (Figure 4d), indicating a role in the entry in mitosis. Conversely, expression of the Mut GFP-FAK increased the amount of polymerized MTs, evaluated with anti-acetylated α-tubulin (ac-α-tubulin) Ab.

These data strongly indicate that P-FAKSer732 is associated to an increased growth potential and, together with the results shown above, also argue for the hypothesis of

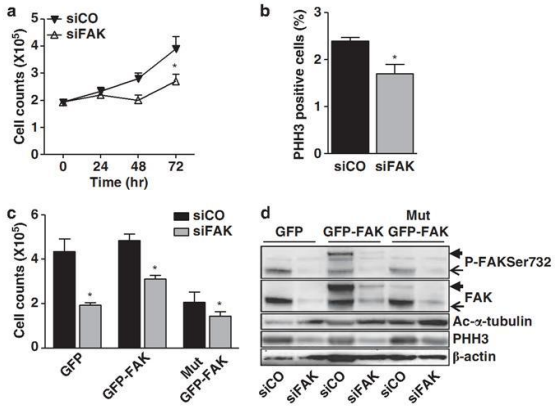

Figure 4 FAK contributes to cell proliferation when is phosphorylated at Ser732. (**a**) Proliferation assay performed on cells silenced with control- (siCO) or FAK- (siFAK) siRNA. Representative growth curves of one of three independent experiments are shown; each point represents the mean of three replicates. Error bars, S.D. Asterisks indicate statistical significant values ($P<0.0001$). (**b**) Mitotic index performed on control- (siCO) or FAK- (siFAK) silenced (Me)#28 cell. The level of mitosis is reported as the percentage of PHH3-positive cells measured by FACS. Asterisk, $P\leq 0.05$. (**c**) Proliferation rate of control- (siCO)- or FAK- (siFAK)-silenced Me#28 cells transfected with GFP alone, wt GFP- or Mut GFP-FAK vectors. The experiment was done in triplicate. Asterisks indicate statistical significant values ($P<0.001$). Error bars, S.D. (**d**) Western blotting on cell lysates of the transfectants described above, treated with control (siCO) or FAK (siFAK) siRNA. Endogenous FAK, thin arrow, ectopic FAK, thick arrow. For immunoblottings, Abs are reported on the right. β-actin was used as control of gel loading

its involvement in the regulation of the MT dynamics and in the mitotic spindle assembly.

P-FAKSer732 contributes to MT depolymerization. To investigate whether the effect on MTs, analyzed as ac-α-tubulin, could only be due to P-FAKSer732, NIM-1 cells, that express low levels of FAK (Figure 1a), were transfected with the construct expressing wt and Mut GFP-FAK. Western blot analysis of cell lysates showed that cells transfected with Mut GFP-FAK contained about 2.5-fold more ac-α-tubulin compared with cells transfected with wt GFP-FAK (Figure 5a). Conversely, iper-expression of FAK, as in wt GFP-FAK-transfected cells, was associated to 50% decrease of ac-α-tubulin respect to GFP-transfected cells.

The fact that the amount of polymerized MTs was inversely related to the amount of P-FAKSer732 argues for the hypothesis that FAK can modulate MT dynamics. To test this possibility, we performed a MT re-growth assay on Me#28 and OAW42 cells upon FAK silencing. Silenced cells were treated overnight (o.n.) with nocodazole to force MT depolymerization, evaluated as the absence of ac-α-tubulin, and then MT re-growth was analyzed after nocodazole washout. FAK-silenced cells showed a higher amount of ac-α-tubulin indicating higher levels of polymerized MTs and, after nocodazole treatment, ac-α-tubulin was slightly detected. Of note, the knockdown of FAK induced a better rescue of MT re-growth after nocodazole removal compared with cells transfected with control siRNA (Figure 5b).

These data strongly indicate that FAK phosphorylated at Ser732 has a role in MT depolymerization.

Lack of Ser732 phosphorylation impairs spindle assembly and mitosis. To specifically evaluate the role of P-FAKSer732 during mitosis, wt and Mut GFP-FAK were transiently transfected in Me#28 and NIM-1 cells. In interphase, wt (Figure 6a, left panel) and Mut GFP-FAK (Figure 6b, left panel) were mainly localized at the sites of the FAs, and no differences were observed between the two transfectants. In mitotic cells, Mut GFP-FAK localized in randomly positioned spindle showing a diffused staining along the entire spindle and the chromosomes appeared significantly unaligned (Figure 6b, right panel). wt GFP-FAK-transfected cells showed a regular spindle with wt GFP-FAK mainly localized on polar MTs (Figure 6a, right panel). In agreement with these results, the number of mitosis was six- and threefold lower in Mut GFP-FAK-transfected Me#28 and NIM-1 cells (Figure 6c).

The MEK/ERK pathway is involved in the phosphorylation at Ser732 associated with polymerized MTs. Several solid tumors have a hyper-activated MEK/ERK pathway and ERK was already proposed to be a regulator of MT dynamics and mitosis.[18,19] Thus, a possible involvement of MEK/ERK and Rho/ROCK pathways, which generates P-FAKSer732 in ECs,[12] was analyzed upon treatment with UO126 and Y27632, which are inhibitors of MEK and ROCK, respectively. In FCS-stimulated Me#28 cells, UO126 inhibited P-FAKSer732 nearly 90% and Y27632 reduced P-FAKSer732 up to 30% (Figure 7a). As FAK can be an up- and a downstream effector of both MEK/ERK and Rho/ROCK pathways,[20] the effects of FAK expression on these pathways was analyzed. Transient FAK silencing in Me#28 cells induced 35% reduction of ERK phosphorylation (Figure 7b),

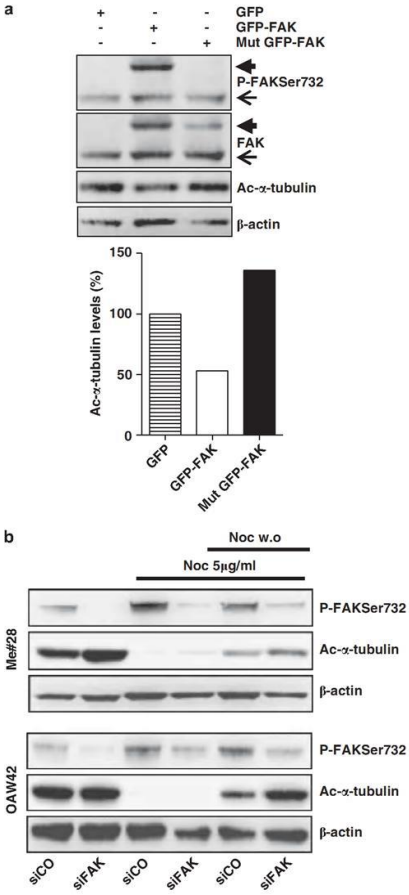

Figure 5 P-FAKSer732 contributes to MT depolymerization. (**a**) Upper panel: western blotting on cell lysates from NIM-1 cells transfected with GFP alone, wt or Mut GFP-FAK vectors. Endogenous FAK, thin arrow, ectopic FAK, thick arrow. Lower panel: densitometric analysis performed on the western blotting shown in the upper panel. The results of an experiment of three performed are shown. (**b**) MT re-growth assay was performed on Me#28 and OAW42 cells transfected with control (siCO) or FAK- (siFAK) siRNA. For immunoblottings, Abs are reported on the right. β-actin was used as control of gel loading

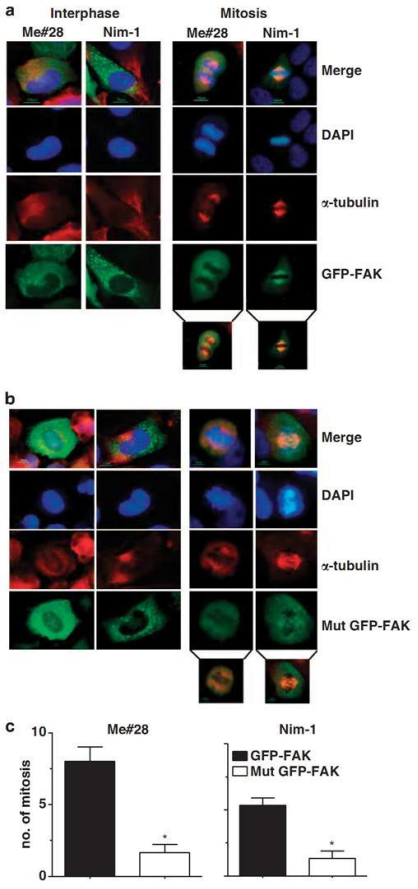

Figure 6 Lack of Ser732 phosphorylation impairs spindle assembly and mitosis. Me#28 and NIM-1 cells transiently transfected with wt (**a**) or Mut GFP-FAK (**b**) vectors. IF was performed with anti-α-tubulin (red) Ab on fixed cells. Nuclei were stained with DAPI (blue). Inserts on the bottom report green/red merge showing the localization in the spindle of the exogenous wt or Mut GFP-FAK. Bars, 10 μm. (**c**) Number of mitosis in transfected cells. Error bars, S.D. Asterisks indicate $P \leq 0.05$

confirming that FAK expression and/or activation could regulate ERK phosphorylation. Y27632 treatment in control siRNA-transfected cells slightly decreased ERK phosphorylation and reached a 70% decrease in FAK-silenced cells arguing for the notion that ROCK further induced the decrease of ERK phosphorylation when FAK decreased. As shown above, UO126 completely inhibited P-FAKSer732. These results strongly indicate that MEK/ERK pathway is responsible for P-FAKSer732.

Observing the relationship among P-FAKSer732, MEK/ERK activation and polymerized tubulin (Figures 4 and 5), we assessed whether MEK/ERK inhibitor was able to modulate the amount of polymerized tubulin. UO126 treatment on Me#28 and OAW42 cells increased the amount of ac-α-tubulin and decreased the amount of P-FAKSer732 in a dose-dependent manner, indicating an inverse correlation between FAK, phosphorylated on Ser732 by MEK/ERK and MT polymerization (Figure 7c).

The biochemical association of P-FAKSer732 with polymerized MTs was then investigated by western blotting on cell extracts upon separation of soluble and polymerized α-tubulin fractions. P-FAKSer732 was found in both soluble and MT fractions, but UO126 treatment decreased the levels of P-FASer732 in the MT fraction only (Figure 7d), indicating that a part of P-FAKSer732 is associated with ac-α-tubulin and that *de novo* phosphorylation on Ser732 of FAK occurs at the level of MTs. Ac-α-tubulin of MT fraction increased in UO126-treated cells.

EGF-dependent EGFR/MEK/ERK/CDK5 pathway induces P-FAKSer732, thus contributing to mitosis. MEK/ERK pathway is one of the downstream effector of EGFR[21] and CDK5 phosphorylates FAK on Ser732 in neural cells.[11] To test the hypothesis that P-FAKSer732 is induced by EGFR/CDK5 pathway activation, starved Me#28, NIM-1 and OAW42 cells were stimulated with EGF. In all the three cell lines, EGF stimulation increased P-ERK together with P-FAKSer732 and P-CDK5Tyr15, the active kinase isoform (Figure 8a). To test whether CDK5 was downstream of EGFR/MEK/ERK signaling cascade, ERK2 siRNA-treated Me#28 cells were stimulated with EGF. EGF stimulation strongly decreased P-FAKSer732 and P-CDK5Tyr15 of ERK2-silenced cells but not of control siRNA-treated cells (Figure 8b). To confirm the presence of the axis MEK/ERK/CDK5/P-FAKSer732, starved Me#28, OAW42 and NIM-1 cells were treated with increasing concentrations of roscovitine, a potent CDK5 inhibitor.[22] Roscovitine treatment decreased the amount of P-FAKSer732 in a dose-dependent manner in all cell lines (Figure 8c), but did not affect the level of P-FAKTyr397 and of P-ERK. Moreover, roscovitine treatment increased the amount of ac-α-tubulin in a dose-dependent manner.

IF on roscovitine-treated NIM-1 cells showed impaired spindle (Figure 8d), according to the data reported in Figure 6. P-FAKSer732 staining was lower and diffused with respect to that observed on FCS-treated cells, and no co-localization with acetylated α-tubulin was observed.

These data strongly indicate that EGFR/MEK/ERK/CDK5 pathway induces the phosphorylation of FAK at Ser732 independently from the FAK autophosphorylation, thus contributing to spindle formation and mitosis of tumor cells.

Discussion

We present here a deep analysis on the role of FAK phosphorylated on Ser 732 in tumor cells. We have found

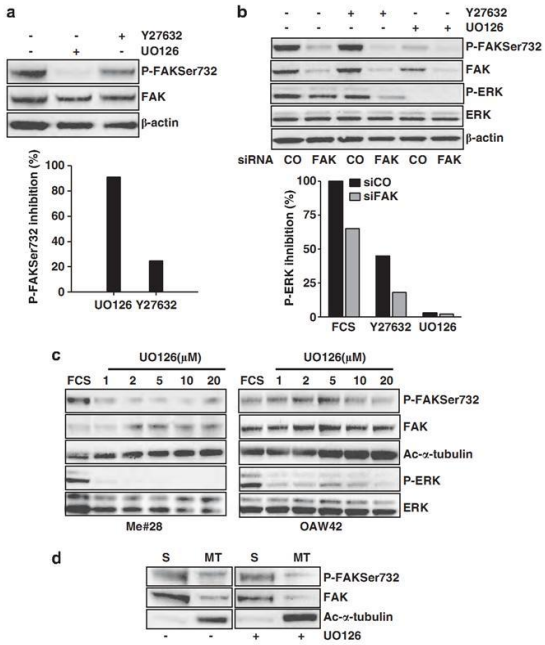

Figure 7 The MEK/ERK pathway is involved in the phosphorylation at Ser732 associated with polymerized MTs. (**a**) Me#28 cells treated with UO126 or Y27632 inhibitors for 24 h. Upper panel: western blotting performed on lysates from untreated or treated cells. Bottom panel: densitometric analysis of the western blotting shown in the upper panel, reporting the percentage of P-FAKSer732 respect to total FAK upon inhibitor treatments. Error bars, S.D. (**b**) Upper panel: western blotting performed on lysates from Me#28 cells transfected with control- (CO) or FAK- (FAK) siRNA. Bottom panel: densitometric analysis of the western blotting shown in the upper panel, reporting the percentage of P-ERK respect to total ERK upon inhibitor treatments. β-Actin was used as control of gel loading. (**c**) Western blotting on lysates from starved Me#28 and OAW42 cells stimulated with FCS and treated with increasing concentration of UO126 (1–20 μM). Total ERK was used as control of gel loading. (**d**) Western blotting of soluble (S) or polymerized MT (MT) fractions (see Materials and Methods) from Me#28 cells left untreated or treated with UO126 (20 μM)

that the phosphorylation of FAK at Ser732 occurs independently from integrin activation, is not localized at the sites of FAs and accumulates in mitotic cells strongly suggesting that, regardless of FAK involvement in migration, P-FAKSer732 has a role in mitosis, thus regulating the proliferation of tumor cells. P-FAKSer732 appears to control mitotic spindle assembly and correct chromosome segregation. Hence, FAK can exert in tumor cells a dual role: one, fully described elsewhere, integrin-dependent associated to phosphorylation of Tyr397 and -576 with a role in migration, and the other, characterized here for the first time, integrin-independent associated to phosphorylation on Ser732 upon activation of the EGFR/MEK/ERK/CDK5 pathway, regulating MT dynamics.

Although P-FAKSer732 was already observed in neural and in few non-neural cells, that is, Cos, HeLa cells and ECs, phosphorylated by CDK5,[10,13] our results clearly increase the knowledge about the role of FAK phosphorylated on Ser732 focusing in tumor cells. While in migrating neural cells P-FAKSer732 was shown to be responsible for the MT assembly to generate forces for nuclear movement, in ECs P-FAKSer732 associated to the centrosomes was related to centrosome function during mitosis. On the contrary, we found P-FAKSer732 localized at the mitotic spindle and not at the centrosomes indicating that P-FAKSer732 exerts, in the analyzed tumor cells, a role at the level of the spindle MTs. Indeed, we also gave evidences of an inverse relationship between P-FAKSer732 and ac-α-tubulin, and the MT re-growth assay clearly showed that the lack of FAK expression delayed MT polymerization, strongly indicating for the first time a role of FAK in MT dynamics.

Dynein is a minus-end MT motor protein that contribute to the generation of forces necessary to keep the spindle pole at the correct distance from the equator.[23] On the other hand, different actin structures and actin-associated proteins contribute to spindle orientation through the anchorage of

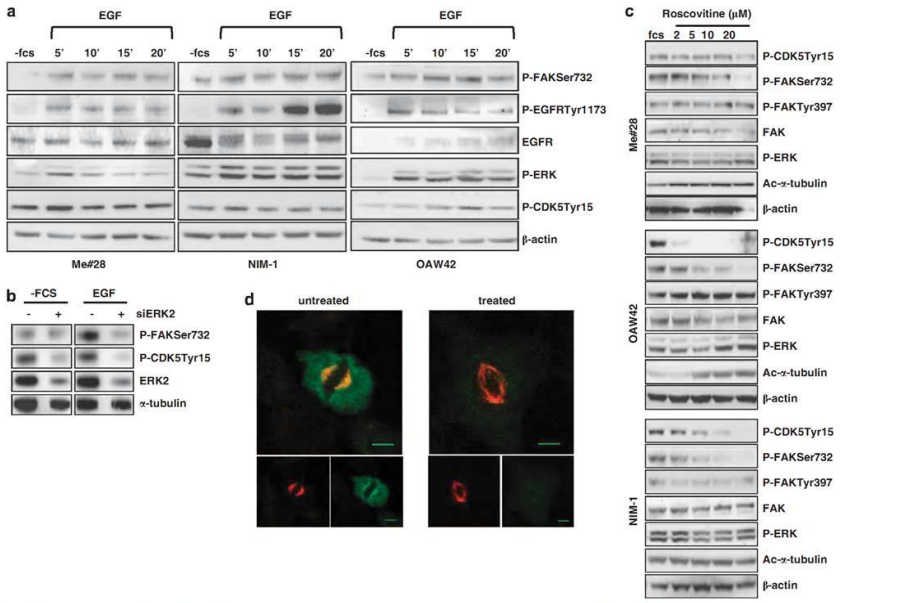

Figure 8 EGF-dependent EGFR/MEK/ERK/CDK5 pathway induces P-FAKSer732, thus contributing to mitosis. (**a**) Western blotting on lysates from starved Me#28, NIM-1 and OAW42 cells stimulated with EGF (20 ng/ml) for up to 20 min. For immunoblottings, Abs are reported on the right. β-Actin was used as control of gel loading. (**b**) Western blotting on cell lysates from Me#28 cells silenced with control (−) or ERK2 (+) siRNA, starved and then stimulated with EGF (20 ng/ml) for 15 min. Abs are reported on the right. α-Tubulin was used as control of gel loading. (**c**) Western blotting on lysates from starved Me#28, OAW42 and NIM-1 cells untreated or treated with roscovitive (2–20 μM) and stimulated with FCS. Abs are reported on the right. β-Actin was used as control of gel loading. (**d**) Confocal IF performed on fixed NIM-1 cells untreated or treated with roscovitive (10 μM) and stained with anti-P-FAKSer732 (green) and α-tubulin (red) Abs. Scale bars, 20 μm

astral MTs.[24] The localization of P- FAKSer732 at both MTs of the spindle and cortical ring as well as the association with dynein suggest a role of P-FAKSer732 as molecular cue for correct MT dynamics, spindle assembly and/or correct chromosome segregation. Further studies will be required to elucidate the involvement of FAK during mitotic spindle assembly and positioning.

In solid tumors, one of the hallmarks is the chromosome instability caused by wrong chromosome segregation. The alteration of MT dynamics is one of the causes of the chromosomal instability.[25] In this context, P-FAKSer732 seems to participate to MT depolymerization, thus maintaining normal spindle assembly and function. However, as already observed for MCAK, the mitotic centromere-associated kinesin,[26] the phosphorylation of FAK at the Ser732 could be finely orchestrated by kinases and phosphatases specifically activated in tumor cells. Therefore, future attention should be paid to analyze, in a wide panel of tumor biopsies, as well as in their normal counterparts, the relationship between the presence of P-FAKSer732 and the clinical outcome or sensitivity to conventional therapies. In addition, our data also suggests that the activation of the identified signaling pathway could be preferentially activated in different tumor subsets. Indeed, melanoma cell lines displaying the highest levels of P-FAKSer732 belong to a tumor subgroup lacking MITF and melanoma differentiation antigens such as MART-1 and gp100.[14] The presence of P-FAKSer732 in ovarian carcinoma cells from ascites further supports a correlation between this particular FAK phosphorylation and malignant cells with high proliferative capability *in vivo*. These data indicate that the analysis of the involvement of FAK in the mitotic spindle assembly and function in tumor cells appear to be instrumental for developing specific inhibitors to this particular FAK function in malignant cells.

We also showed that P-FAKSer732 was generated by the activation of the EGFR/MEK//ERK/CDK5 signaling. In neural cells, CDK5 is considered a post-mitotic kinase whose activation is dependent on the expression of CDK activators p35 and p39.[27] In tumors, p35-dependent activation of CDK5 appeared to occur following ERK activation, which in turn led

to increased Egr1 transcriptional activity and upregulation of p35 expression.[28] In pancreatic cancer, inhibition of CDK5 kinase activity was found to suppress ras signaling,[29] indicating a possible relationship between MEK/ERK and CDK5 activations. As we have clearly shown here that the MEK/ERK pathway activation and the activated P-CDK5Tyr15 are associated with the generation of P-FAK-Ser732, at least in the analyzed tumor cells, the induction of p35 or p39 expression can be hypothesized. Several years ago, Harrison and Turley[18] showed in H-ras-transformed cells that ERK associated with the MTs of the mitotic spindle, thus regulating their stability. Based on our results, we hypothesize that those observations were not due to ERK itself, but due to FAK upon phosphorylation at Ser732 caused likely by CDK5. Analysis of CDK5 expression and activation as well as p35 and p39 expression await further investigation in tumor cells especially when the ras/RAF/MEK/ERK is constitutively activated by mutations.

Although ROCK does not appear to phosphorylate FAK on Ser732, as suggested previously,[12] we cannot exclude involvement of Rho/ROCK pathway in the activation of the signaling circuit MEK/ERK/FAK/ERK. This hypothesis is not weird, as the Rho/ROCK pathway regulates actin dynamics through cofillin[30] and spindle orientation is regulated by cortical actin.[24] Experiments are ongoing to better clarify the mechanism that links Rho/ROCK pathway and P-FAKSer732.

The link between EGFR activation and P-FAKSer732, never demonstrated before for tumor cells, might be considered an important step forward in understanding EGFR function in tumors. Further knowledge may be useful to design alternative therapeutic approach, especially in tumors that become resistant to anti-EGFR compounds.

Materials and Methods

Antibodies and reagents. Abs against P-FAKSer732, -Tyr576 and -Tyr 397 (rabbit) were from Biosource (Invitrogen, San Francisco, CA, USA); anti-FAK (rabbit); anti-MAP kinase (ERK1/2; rabbit); anti-P-EGFRTyr1173 (mouse), anti-EGFR (rabbit), anti-carboxyl-terminal domain of FAK from Santa Cruz Biotechnology (Santa Cruz, CA, USA); anti-α-tubulin (mouse) from Thermo Scientific (Fremont, CA, USA); anti-ac-α-tubulin (mouse) from Promega (Promega, Madison, WI, USA); anti-β-actin (rabbit), anti-dynein intermediate chain (mouse) from Sigma-Aldrich (St. Louis, MO, USA); anti-phosphorylated ERK1/2 kinase (rabbit), anti-P-histone H3 (Ser10) (rabbit) from Cell Signaling Technology (New England BioLabs, Beverly, MA, USA); anti-CDK5Tyr15 (rabbit) from Abcam (Abcam, Cambridge, UK) Fluorochrome-conjugated Alexa Fluor 488 and 546 secondary Abs were from Molecular Probes (Invitrogen). UO126 was from Promega; Y27632, nocodazole and roscovitine were from Sigma-Aldrich. Human recombinant EGF was from PeproTech, Inc. (Rocky Hill, NJ, USA). G418 and Lipofectamine 2000 were purchased from Invitrogen.

Cells. Human melanoma cell lines were obtained from surgical specimens of patients admitted to INT. These cells have been extensively characterized as reported elsewhere.[14] Nine human ovarian cancer cell lines were used in this study: IGROV-1 kindly provided by Dr. Bénard (Paris, France);[31] SKOV3 and CAOV4 from ATCC; OVCAR4 and OVCAR5 provided by Dr. Camalier (NCI-NIH, USA); 3507OVA and 413OVA by Dr. van den Berg-Bakker (Leiden, the Netherlands);[32] COR by Dr. Balconi (M Negri, Milan, Italy). They were maintained in RPMI 1640 medium (Sigma, St. Louis, MO, USA) supplemented with 10% FCS (Hyclone, Logan, UT, USA), 1% L-glutamine at 37 °C in a humidified atmosphere of 5% CO_2 in air. OAW42 was provided by Dr. A. Ullrich, (Max Planck Institute of Biochemistry, Martinsried, Germany)[33] and maintained in DMEM supplemented with 10% FCS and 1% L-glutamine in a humidified atmosphere of 5% CO_2. The human thyroid cell lines NIM-1,[34] TPC1 and BCPAP[35] were maintained in DMEM supplemented with 10% FCS and 1% L-glutamine in a humidified atmosphere of 5% CO_2 in air. Ascites from patients with stage III ovarian cancer were collected at the time of debulking surgery. Cytological analysis confirmed that the ascites mainly contained tumor cells, as also demonstrated by the expression of the epithelial marker E-cadherin. The features of ovarian carcinoma specimens are listed in Supplementary Table S1. UO126, Y27632 and roscovitine treatment were performed o.n. on starved cells before the relevant stimulation.

Stable transfection. Me#28 cells were placed on 96-well dishes and transfected after 24 h with 0.2 μg per well of the FRNK-containing vector (kindly provided by Dr. Ungefrorer, Hamburg) and pcDNA3.1 (Invitrogen), as mock-transfected vector, using Lipofectamine 2000 reagent following the manufacturer's protocol. At 48 h after the transfection, G418-containing media was added and changed every 48–72 h thereafter to generate stable transfectants. After 2 weeks, isolated colonies were analyzed by western blotting for the presence of FRNK (41 kDa) in total cell lysates using the anti-carboxyl-terminal domain of FAK.

Cell growth on fibronectin. Fibronectin-coated 12-well coated plate was prepared with a 2 μg/ml fibronectin solution in RPMI and incubated (o.n.) at 37 °C. The next day, cells (0.8×10^5/well) were plated in serum-free condition on plastic or fibronectin for 20 min. Western blotting was performed on total lysates as described below.

Western blotting and IP. Cells were washed with ice-cold PBS containing Na_3VO_4 (0.1 mM) and lysated with NuPAGE LDS sample buffer (1 ×) (Invitrogen) under reducing conditions. Proteins were separated on precast 4–12% SDS-polyacrylamide gels (Invitrogen). Western blot was performed as described[36] and analyzed using ChemiDoc XRS System and the Quantity One software (Bio-Rad, Hercules, CA, USA). The relevant values were always normalized with the values of the protein used as control of gel loading.

The separation of soluble and polymerized tubulin has been described elsewhere.[37] In some experiments, cells were grown in standard medium o.n., washed twice in PEM buffer (100 mM PIPES pH 6.9, 1 mM EGTA, 2 mM $MgCl_2$) and then cells were incubated in PEM buffer containing 0.2% Triton X-100 for 1 min at 37 °C and then rinsed and incubated in PEM buffer at 37 °C for 5 min. Cells were lysed as described above.

IP was performed essentially as described.[36] Briefly, cells were lysed in cold lysis buffer (150 mM NaCl, 50 mM Tris-HCl, pH 7.4, 0.25% NaDoc, 1 mM EDTA pH 8, 1 mM Na_3VO_4, 1% PMSF, 1% NP-40 and protease inhibitors) for 30 min on ice. Cellular debris and nuclei were removed by centrifugation at 13 000 r.p.m./min for 30 min at 4 °C. Normal rabbit or mouse sera were used as negative control. Primary Ab was bound to beads conjugated with goat anti-mouse or -rabbit Ab (Dynabeads; Dynal ASA, Oslo, Norway) and incubated with cell extracts o.n. at 4 °C with rotation. Beads were washed once with cold lysis buffer, twice with PBS plus BSA and protease inhibitors, and once with PBS plus inhibitor (10 min/wash). Immuno-precitated proteins were separated on 4–12% SDS-PAGE under reducing conditions.

siRNA treatment and transient transfection. siRNA transfections were performed using Lipofectamine 2000 according to the manufacturer's protocol. For FAK silencing, 40 pmol/ml small-interfering RNA (siRNA) duplex specific for FAK (Smart Pool, Thermo Scientific, Dharmacon, Inc. Chicago, IL, USA) or control siRNA (Qiagen-Xeragon, Germantown, MD, USA) were applied. Total cell lysates were prepared 48 h after transfection. Otherwise, 24 h after siRNAs treatment, transfected cells were placed on six-well dishes and transfected with 2 μg of GFP, wt GFP- and Mut GFP-FAK vectors[10] using Lipofectamine 2000 reagent (Invitrogen), following the manufacturer's protocol. In some experiments, cells were transfected with wt and Mut GFP-FAK vectors without FAK silencing.

For ERK2 silencing, 40 pmol/ml siRNA duplex specific for MAPK1(Smart Pool, Thermo Scientific, Dharmacon, Inc.) or control siRNA (Qiagen-Xeragon) were applied. Treatment with EGF (20 ng/ml) was carried out 24 h after transfection in a serum-free medium. Total cell lysates were prepared 48 h after transfection.

Wound-healing assay. Confluent cultures of Me#28 transfected with FAK siRNA or control siRNA were wounded using a sterile 200-μl pipette tip. Wound closure was assessed 4, 24 and 30 h later with an inverted microscope with a × 10, 0.75 NA PanFluor objective (Nikon, Tokyo, Japan). Images were acquired with ACT-1 software (Nikon) at a resolution of 1280 × 1024 pixels. The wound closure was measured on 10 different micrographs captured in three wells for each condition. Data are expressed as percentage of wound closure of the original wound width.

Immunofluorescence. Cells (2×10^4) were seeded on 8-well glass chamber slides (Nalge Nunc International, Rochester, NY, USA). Before immunostaining, cells were washed with cold PBS, fixed with 2% paraformaldehyde for 20 min and permeabilized for 10 min in PBS/Tween 0.1%. To dilute out of the cell-free tubulin heterodimers cells grown on 8-well glass chamber slides were washed twice in PEM buffer.[37] Then cells were incubated in PEM buffer containing 0.2% Triton X-100 for 1 min at 37 °C and then rinsed and incubated in PEM buffer at 37 °C for 5 min. Cells were then fixed in methanol/acetone (1 : 1). Samples were mounted with Prolong Gold Antifade reagent with DAPI (Invitrogen) and analyzed using an Eclipse TE2000-S microscope with a × 40, 0.75 NA PanFluor objective (Nikon). Images were acquired with ACT-1 software (Nikon). Confocal microscopy was carried out using a Microradiance 2000 microscopy (Bio-Rad Laboratories, Hercules, CA, USA) equipped with Ar (488 nm) and HeNe (543 nm) lasers. Images were obtained using a × 40 oil immersion lens 1.4 NA and analyzed using Lasersharp 2000 software. z-stacks of 24 (metaphase) and 19 (anaphase) sections were acquired. Images were processed using ImageJ and Adobe Photoshop.

Cell proliferation and mitotic index. Cells (1×10^3 cells/well) were plated into 48-well plates. At 0, 24, 48 and 72 h, the number of cells was evaluated by Countess automated cell counter (Invitrogen).

For evaluation of the mitotic index, cells were transiently transfected with siRNA. After 48 h, trypsinized cells were fixed by adding 4.5 ml of ice-cold 70% ethanol and incubated at 4 °C. After two washes with PBS/0.03% BSA, cells were incubated with anti-PHH3 (1 : 40) diluted in PBS/0.03% BSA for 1 h at 37 °C followed by incubation with Alexa Fluor 488 goat-anti-rabbit Ab (1 : 1000) in PBS/0.03% BSA for 1 h at room temperature. The mitotic index was reported as the percentage of PHH3-positive cells determined by FACS using the FACSCalibur (Becton Dickinson, San Jose, CA, USA) with CELLQuest software.

MT re-growth assay. Cells (8×10^4/well) seeded on six-well plates, were transfected with FAK or control siRNA and grown for 24 h. MTs were depolymerized treating the cells with 5 μg/ml nocodazole in complete medium at 37 °C o.n. Cells were washed with complete medium once and incubated at 37 °C. For Me#28 and OAW42 cells, the MT re-growth was allowed for 30 min and 3 h, respectively. Total cell lysates were analyzed by western blotting.

Statistical analyses. GraphPad Prism software (GraphPad Software, San Diego, CA, USA) was used to analyze all data. Differences between mean values were determined by Student's *t*-test and 2way ANOVA test.

Conflict of Interest

The authors declare no conflict of interest.

Acknowledgements. We thank Ms. Gabriella Nicolini for her technical assistance. We also thank Dr. Ungefrorer for kindly providing FRNK construct, Professor Tsai for the wt and Mut GFP-FAK vector constructs, Dr. Paola Defilippi for her fruitful discussion, the gynecologic clinical staff and the biorepository personnel at the Fondazione IRCCS Istituto Nazionale dei Tumori for the ovarian carcinoma specimens and Dr. Marina Bagnoli for their management. This work was supported by Italian Ministry of Health, (grants 'Tumori Femminili' to SC and 'Programma integrato in Oncologia, to AT) and Associazione Italiana per la Ricerca sul Cancro (grant IG13055 to AT and grant IG11608 to AA). We thank Dr. Moore for the English editing of the manuscript.

Author Contributions

KR performed research, analyzed and interpreted data and wrote manuscript (including first draft). MS interpreted and discussed data; AA discussed data and obtained funding; SC interpreted and discussed data and obtained funding; AT designed study, interpreted data, wrote manuscript and obtained funding. All authors approved the final version of the manuscript.

1. Schaller MD. Cellular functions of FAK kinases: insight into molecular mechanisms and novel functions. *J Cell Sci* 2010; **123**: 1007–1013.
2. Corsi JM, Houbron C, Billuart P, Brunet I, Bouvree K, Eichmann A *et al.* Autophosphorylation-independent and -dependent functions of focal adhesion kinase during development. *J Biol Chem* 2009; **284**: 34769–34776.
3. Braren R, Hu H, Kim YH, Beggs HE, Reichardt LF, Wang R. Endothelial FAK is essential for vascular network stability, cell survival, and lamellipodial formation. *J Cell Biol* 2006; **172**: 151–162.
4. Gabarra-Niecko V, Schaller MD, Dunty JM. FAK regulates biological processes important for the pathogenesis of cancer. *Cancer Metastasis Rev* 2003; **22**: 359–374.
5. Zhao J, Pestell R, Guan JL. Transcriptional activation of cyclin D1 promoter by FAK contributes to cell cycle progression. *Mol Biol Cell* 2001; **12**: 4066–4077.
6. Wang X, Urvalek AM, Liu J, Zhao J. Activation of KLF8 transcription by focal adhesion kinase in human ovarian epithelial and cancer cells. *J Biol Chem* 2008; **283**: 13934–13942.
7. Calalb MB, Polte TR, Hanks SK. Tyrosine phosphorylation of focal adhesion kinase at sites in the catalytic domain regulates kinase activity: a role for Src family kinases. *Mol Cell Biol* 1995; **15**: 954–963.
8. Schaller MD, Borgman CA, Parsons JT. Autonomous expression of a noncatalytic domain of the focal adhesion-associated protein tyrosine kinase $pp125^{FAK}$. *Mol Cell Biol* 1993; **13**: 785–791.
9. Lietha D, Cai X, Ceccarelli DF, Li Y, Schaller MD, Eck MJ. Structural basis for the autoinhibition of focal adhesion kinase. *Cell* 2007; **129**: 1177–1187.
10. Xie Z, Sanada K, Samuels BA, Shih H, Tsai LH. Serine 732 phosphorylation of FAK by Cdk5 is important for microtubule organization, nuclear movement, and neuronal migration. *Cell* 2003; **114**: 469–482.
11. Xie Z, Tsai LH. Cdk5 phosphorylation of FAK regulates centrosome-associated miocrotubules and neuronal migration. *Cell Cycle* 2004; **3**: 108–110.
12. Le Boeuf F, Houle F, Sussman M, Huot J. Phosphorylation of focal adhesion kinase (FAK) on Ser732 is induced by rho-dependent kinase and is essential for proline-rich tyrosine kinase-2-mediated phosphorylation of FAK on Tyr407 in response to vascular endothelial growth factor. *Mol Biol Cell* 2006; **17**: 3508–3520.
13. Park AY, Shen TL, Chien S, Guan JL. Role of focal adhesion kinase Ser-732 phosphorylation in centrosome function during mitosis. *J Biol Chem* 2009; **284**: 9418–9425.
14. Sensi M, Catani M, Castellano G, Nicolini G, Alciato F, Tragni G *et al.* Human cutaneous melanomas lacking MITF and melanocyte differentiation antigens express a functional Axl receptor kinase. *J Invest Dermatol* 2011; **131**: 2448–2457.
15. Hanks SK, Calalb MB, Harper MC, Patel SK. Focal adhesion protein-tyrosine kinase phosphorylated in response to cell attachment to fibronectin. *Proc Natl Acad Sci USA* 1992; **89**: 8487–8491.
16. Laan L, Pavin N, Husson J, Romet-Lemonne G, van DM, Lopez MP *et al.* Cortical dynein controls microtubule dynamics to generate pulling forces that position microtubule asters. *Cell* 2012; **148**: 502–514.
17. Juan G, Traganos F, James WM, Ray JM, Roberge M, Sauve DM *et al.* Histone H3 phosphorylation and expression of cyclins A and B1 measured in individual cells during their progression through G2 and mitosis. *Cytometry* 1998; **32**: 71–77.
18. Harrison RE, Turley EA. Active erk regulates microtubule stability in H-ras-transformed cells. *Neoplasia* 2001; **3**: 385–394.
19. Roberts EC, Shapiro PS, Nahreini TS, Pages G, Pouyssegur J, Ahn NG. Distinct cell cycle timing requirements for extracellular signal-regulated kinase and phosphoinositide 3-kinase signaling pathways in somatic cell mitosis. *Mol Cell Biol* 2002; **22**: 7226–7241.
20. Mitra SK, Hanson DA, Schlaepfer DD. Focal adhesion kinase: in command and control of cell motility. *Nat Rev Mol Cell Biol* 2005; **6**: 56–68.
21. Tarcic G, Yarden Y. MAP Kinase activation by receptor tyrosine kinases: in control of cell migration. *Methods Mol Biol* 2010; **661**: 125–135.
22. Lopes JP, Agostinho P. Cdk5: multitasking between physiological and pathological conditions. *Prog Neurobiol* 2011; **94**: 49–63.
23. Kotak S, Busso C, Gonczy P. Cortical dynein is critical for proper spindle positioning in human cells. *J Cell Biol* 2012; **199**: 97–110.
24. Stevermann L, Liakopoulos D. Molecular mechanisms in spindle positioning: structures and new concepts. *Curr Opin Cell Biol* 2012; **24**: 816–824.
25. Thompson SL, Compton DA. Chromosome missegregation in human cells arises through specific types of kinetochore-microtubule attachment errors. *Proc Natl Acad Sci USA* 2011; **108**: 17974–17978.
26. Sanhaji M, Friel CT, Wordeman L, Louwen F, Yuan J. Mitotic centromere-associated kinesin (MCAK): a potential cancer drug target. *Oncotarget* 2011; **2**: 935–947.
27. Liebl J, Furst R, Vollmar AM, Zahler S. Twice switched at birth: cell cycle-independent roles of the 'neuron-specific' cyclin-dependent kinase 5 (Cdk5) in non-neuronal cells. *Cell Signal* 2011; **23**: 1698–1707.
28. Harada T, Morooka T, Ogawa S, Nishida E. ERK induces p35, a neuron-specific activator of Cdk5, through induction of Egr1. *Nat Cell Biol* 2001; **3**: 453–459.
29. Feldmann G, Mishra A, Hong SM, Bisht S, Strock CJ, Ball DW *et al.* Inhibiting the cyclin-dependent kinase CDK5 blocks pancreatic cancer formation and progression through the suppression of Ras-Ral signaling. *Cancer Res* 2010; **70**: 4460–4469.
30. Geneste O, Copeland JW, Treisman R. LIM kinase and Diaphanous cooperate to regulate serum response factor and actin dynamics. *J Cell Biol* 2002; **157**: 831–838.
31. Bénard J, De Silva J, De Blois MC, Boyer P, Duvilland P, Chiric E *et al.* Characterization of a human ovarian adenocarcinoma line, IGROV1, in tissue culture and in nude mice. *Cancer Res* 1985; **45**: 4970–4979.

32. van den Berg-Bakker CA, Hagemeijer A, Franken-Postma EM, Smit VT, Kuppen PJ, van Ravenswaay C *et al*. Establishment and characterization of 7 ovarian carcinoma cell lines and one granulosa tumor cell line: growth features and cytogenetics. *Int J Cancer* 1993; **53**: 613–620.
33. Ramakrishna V, Negri DRM, Brusic V, Fontanelli R, Canevari S, Bolis G *et al*. Generation and phenotypic characterization of new human ovarian cancer lines with the identification of antigens potentially recognizable by HLA-restricted cytotoxic T cells. *Int J Cancer* 1997; **73**: 143–150.
34. Tohyama K, Yoshida Y, Ohashi K, Sano E, Kobayashi H, Endo K *et al*. Production of multiple growth factors by a newly established human thyroid carcinoma cell line. *Jpn J Cancer Res* 1992; **83**: 153–158.
35. Schweppe RE, Klopper JP, Korch C, Pugazhenthi U, Benezra M, Knauf JA *et al*. Deoxyribonucleic acid profiling analysis of 40 human thyroid cancer cell lines reveals cross-contamination resulting in cell line redundancy and misidentification.. *J Clin Endocrinol Metab* 2008; **93**: 4331–4341.
36. De Santis G, Miotti S, Mazzi M, Canevari S, Tomassetti A. E-cadherin directly contributes to PI3K/AKT activation by engaging the PI3K-p85 regulatory subunit to adherens junctions of ovarian carcinoma cells. *Oncogene* 2009; **28**: 1206–1217.
37. Baldassarre G, Belletti B, Nicoloso MS, Schiappacassi M, Vecchione A, Spessotto P *et al*. p27(Kip1)-stathmin interaction influences sarcoma cell migration and invasion. *Cancer Cell* 2005; **7**: 51–63.

Supplementary Information accompanies this paper on Cell Death and Disease website (http://www.nature.com/cddis)